1976

A two-dimensional time-dependent numerical model investigation of the coastal sea circulation around the Chesapeake Bay entrance

Everett Michael Stanley
College of William and Mary - Virginia Institute of Marine Science

76-19,811

STANLEY, Everett Michael, 1938-
A TWO-DIMENSIONAL TIME-DEPENDENT NUMERICAL MODEL INVESTIGATION OF THE COASTAL SEA CIRCULATION AROUND THE CHESAPEAKE BAY ENTRANCE.

The College of William and Mary in Virginia, Ph.D., 1976
Physical Oceanography

Xerox University Microfilms, Ann Arbor, Michigan 48106

A TWO-DIMENSIONAL TIME-DEPENDENT NUMERICAL MODEL INVESTIGATION OF THE COASTAL SEA CIRCULATION AROUND THE CHESAPEAKE BAY ENTRANCE

A Dissertation

Presented to

The Virginia Institute of Marine Science

The College of William and Mary in Virginia

In Partial Fulfillment

Of the Requirements for the Degree of

Doctor of Philosophy

by

Everett Michael Stanley

1976

APPROVAL SHEET

This dissertation is submitted in partial fulfillment of

the requirements for the degree of

Doctor of Philosophy

E. M. Stanley

E. M. Stanley

Approved, May 1976

Albert Y. Kuo

Dr. Albert Y. Kuo

Christopher S. Welch

Dr. Christopher S. Wel~~che~~

Victor Goldsmith

Dr. Victor Goldsmith

W. G. MacIntyre

Dr. W. G. MacIntyre

Paul A. Haefner Jr.

Dr. Paul A. Haefner, Jr.

Jerrold S. Rosenbaum

Dr. Jerrold S. Rosenbaum (Assistant Professor of Mathematical Science, Virginia Commonwealth University)

TABLE OF CONTENTS

Page

ACKNOWLEDGMENTS

I wish to thank the David W. Taylor Naval Ship Research and Development Center for making this work possible by providing the necessary funds and sabbatical leave.

I am grateful to Dr. A. Kuo, whose patience, guidance, and continuous support during this work will always be remembered, and to the members of the committee who read and commented on this work.

I am also indebted to the people at the computing centers of the Virginia Institute of Marine Science and the David W. Taylor Naval Ship Research and Development Center for their time and support in helping me to interface with the complex computing machinery necessary to do this work.

I wish to thank the Graphics Department of the Virginia Institute of Marine Science for furnishing Figure 1 of this report and Dr. W. Boicourt of Johns Hopkins University for furnishing Figure 42.

To Dr. E. C. Fischer, who not only backed my efforts in this work but also remained a friend and loyal supporter, I give my thanks.

Finally, to my wife and family, who gave up many days and weekends together and cheerfully supported this effort, I am forever grateful.

LIST OF FIGURES

Figure		Page

Figure		Page

DEFINITION OF SYMBOLS

Symbol	Definition
	Lower Case
a_o	wave amplitude, cm
f	Coriolis parameter, $2\Omega\sin\theta$, sec^{-1}
g	gravitational constant, 980 cm sec^{-2}
h	water depth referenced to mean sea level, cm
$\bar{h}$	average water depth referenced to mean sea level, cm
k	wave number $(2\pi/L)$, cm^{-1}
m	subscripts in numerical notation indicating x direction
n	subscripts in numerical notation indicating y direction
n'	Manning coefficient
p	pressure, gm cm^{-1} sec^{-2}
s	real time variation of salinity, $s = \rho\tilde{S}$, gm cm^{-3}
s'	salinity deviation from average, gm cm^{-3}
t	time, sec

Symbol	Definition
u	velocity in x direction, cm sec^{-1}
u'	velocity deviation from average, x direction, cm sec^{-1}
v	velocity in y direction, cm sec^{-1}
v'	velocity deviation from average, y direction, cm sec^{-1}
w	velocity in z direction, cm sec^{-1}
x	direction in right-hand coordinate system, positive to east
y	direction in right-hand coordinate system, positive to north
z	direction in right-hand coordinate system, positive up

Upper Case

Symbol	Definition
A_i	turbulent eddy viscosity (i = x, y, or z), cm^2 sec^{-1}
C	Chezy coefficient, $cm^{1/2}$ sec^{-1}
D_i	dispersion (i = x or y), cm^2 sec^{-1}
E_i	turbulent eddy diffusion (i = x, y, or z), cm^2 sec^{-1}
H	total water depth $h + \delta$, cm

Symbol	Definition
H^{it}_{jB}, H^{it}_{jF}	shorthand notation for h + δ in finite difference notation, where j = x or y and it = t, 2t, etc. (See Chapter IV.)
L	distance x or y direction, cm
S	salinity averaged with respect to depth, gm kg^{-1}
$\tilde{S}$	real time variation of salinity, gm kg^{-1}
T	wave period, sec
U	velocity in x direction integrated with respect to depth, cm sec^{-1}
$\bar{U}$	average depth integrated velocity in x direction, cm sec^{-1}
V	velocity in y direction integrated with respect to depth, cm sec^{-1}
$\bar{V}$	average depth integrated velocity in y direction, cm sec^{-1}
W'	wind speed, cm sec^{-1}
Y	jet or Bay mouth width, cm
A_j A_j' B_j B_j' C_j C_j' D_j D_j' E_j E_j' F_j F_j'	constants in recursion equations, where j = m or n. (These constants are defined in Chapter IV; computer notation is given in Appendix A.)

Symbol	Definition
H_j	constants in recursion equations, where j = m
P_j Q_j	or n (cont)
R_j T_j	

Greek

α	constant in mixing length theory, dimensionless
δ	tidal height, cm
θ	angle, degree of latitude
ρ	density, gm cm^{-3}
ρ'	density deviation from average, gm cm^{-3}
ρ_a'	density of air, gm cm^{-3}
$\bar{\rho}$	density, average, with respect to depth, gm cm^{-3}
σ	wave angular frequency $(2\pi/T)$, cm sec^{-1}
τ_{ij}	general stress term, gm cm^{-1} sec^{-2}
τ_i^s τ_i^b	surface and bottom stress, gm cm^{-1} sec^{-2}
Ω	earth's angular velocity, 0.729211×10^{-4} sec^{-1}
ΔL	grid spacing, cm
ΔT	whole time step for numerical technique, sec
Δt	half time step for numerical technique ($\Delta T = 2\Delta t$), sec

A TWO-DIMENSIONAL TIME-DEPENDENT
NUMERICAL MODEL INVESTIGATION OF THE
COASTAL SEA CIRCULATION AROUND THE
CHESAPEAKE BAY ENTRANCE

ABSTRACT

A computer study was made of the resultant flow field arising from the discharge of a tidal estuary or river onto the continental shelf. The approach was to: (1) vertically integrate the continuity, momentum, and mass balance equations assuming incompressible flow and using the hydrostatic assumption and a Boussinesq approximation for density; (2) numerically model the vertically integrated equations; and (3) apply the equations to a simplified coastal geometry and determine the effects of different physical factors on the flow field. The numerical equations were written using a multi-operational computational technique which was found to be fast and stable. Velocity and/or tidal heights were found to be usable on open boundary conditions for the multi-operational computational scheme.

General conclusions from the study show that the outflow from an estuary can be divided into three types: dispersive, entraining, or a mixture of the two.

Specifically, results of the model study using a steady-state or oscillating jet to simulate the Chesapeake Bay time averaged (non-tidal) or tidal outflow show that for the cases studied: the longitudinal centerline velocity for both tidal and non-tidal flows decreases rapidly as a function of distance from the Bay mouth, the transverse U velocity profile for the non-tidal case (steady-state jet) is a hyperbolic secant squared function, the sea surface slope is important in modeling the flow and should be known to within 1-2 cm, the Coriolis force was not an important factor in the turning of the outflow due to the dominance of bottom friction, and the wind and ambient current were the most important factors in the turning of the outflow to the south. The model studies also showed the existence of a northern flow above the Bay entrance and a weak residual eddy motion above and below the Bay mouth for the tidal case.

EVERETT MICHAEL STANLEY

THE VIRGINIA INSTITUTE OF MARINE SCIENCE

THE COLLEGE OF WILLIAM AND MARY IN VIRGINIA

In chief, men marvel Nature renders not
Bigger and bigger the bulk of ocean, since
So vast the down-rush of the waters be,
And every river out of every realm
Cometh thereto; and add the random rains
And flying tempest, which spatter every sea
And every land bedew; add their own springs:
Yet all of these unto the ocean's sum
Shall be but as the increase of a drop.

Titus Lucretius Carus

A TWO-DIMENSIONAL TIME-DEPENDENT NUMERICAL MODEL INVESTIGATION OF THE COASTAL SEA CIRCULATION AROUND THE CHESAPEAKE BAY ENTRANCE

CHAPTER I

INTRODUCTION AND BACKGROUND

The Middle Atlantic Bight extends from Cape Hatteras, North Carolina, to Cape Cod, Massachusetts. It can be broken into two main sections: the New York Bight, extending from the tip of Long Island, New York, to Cape May, New Jersey, and the Chesapeake Bight (Figure 1), which covers the area from Cape May, New Jersey, to Cape Hatteras, North Carolina. The region of the Chesapeake Bight was first explored and described by Captain John Smith who called it the Virginia Sea. One of the chief characteristics of the 314-km coastline of the Chesapeake Bight is the Chesapeake Bay entrance. The effluence from this Bay, its interaction with the surrounding shelf waters, and the resultant circulation constitute the primary physical problem investigated in this thesis.

The first general oceanographic descriptions of the Chesapeake Bight region were given by Parr (1933), Bigelow (1933), and Bigelow and Sears (1935). The surface flow is generally southerly (Miller (1952), Howe (1962), Bumpus and

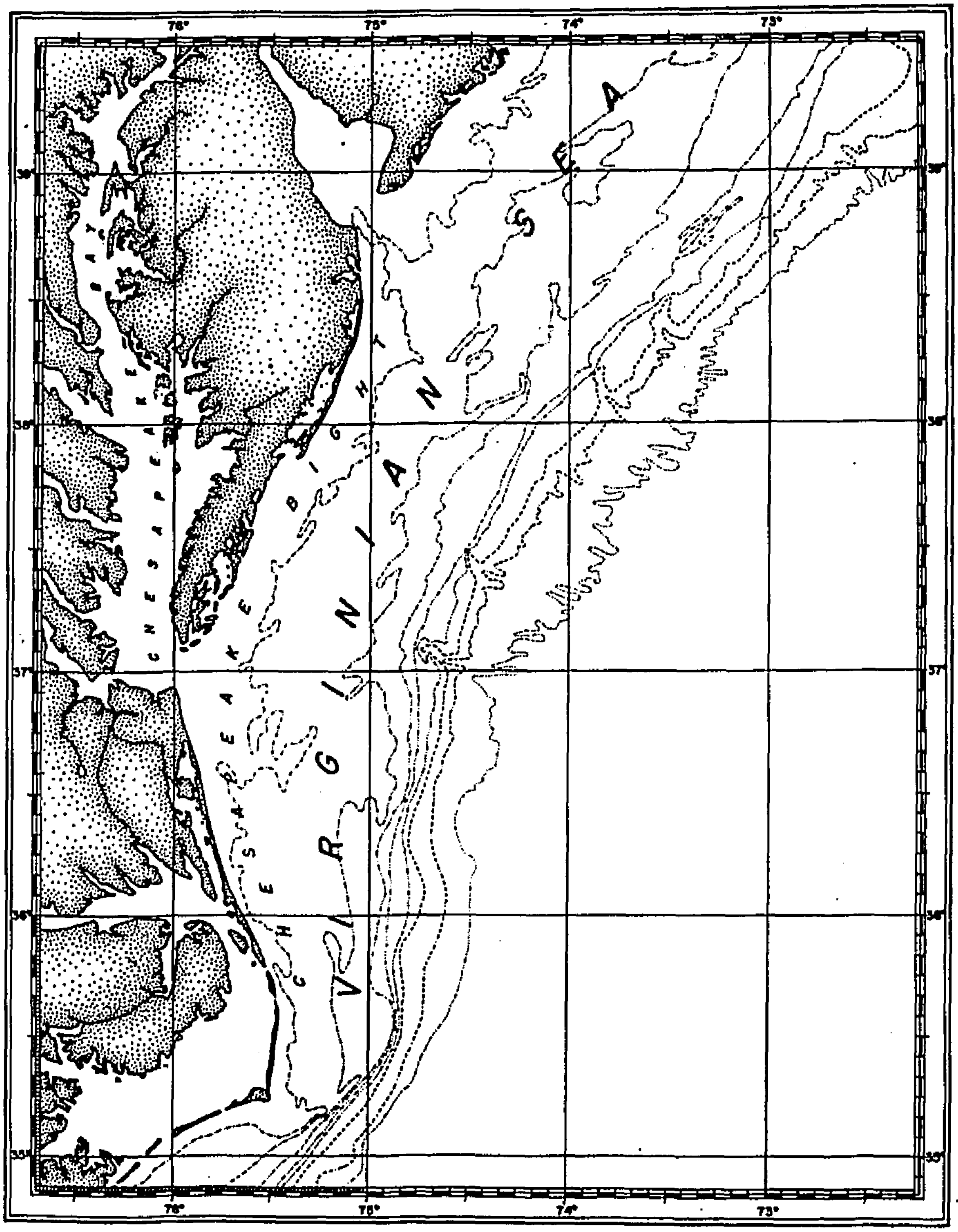

Figure 1
Location of Chesapeake Bight

Lauzier (1965), Harrison, Norcross, Pore, and Stanley (1967), Bumpus (1969)), but it is influenced by surface winds. The bottom drift is southerly in deep water and generally toward the Chesapeake Bay entrance in the shallow in-shore area (Bumpus (1965), Harrison et al (1967)), but it can vary with season, density stratification, and winds. The overall southerly surface flow is augmented by the discharge from the Chesapeake Bay and smaller coastal estuaries and lagoons, with the Chesapeake Bay being the largest contributor. This slow-moving southerly drift turns northward and is entrained in the Gulf Stream at Cape Hatteras (Ford and Miller (1952), Stommel (1965), Fisher (1972)). However, during periods of strong northerly winds, large segments of water from the Chesapeake Bight can be transported past Cape Hatteras into Raleigh Bay, and these have been documented by Harrison et al (1967), Bumpus and Pierce (1955), and Stefansson et al (1971).

Recently, work by Boicourt (1973) has shown that there may exist, during the summer, a return shoreward flow at mid-depths from the edge of the continental shelf. This return flow compensates for the off-shore drift of the Ekman layer caused by the predominately southerly winds at this time of year. Also, new current meter data (Boicourt (1973)) from the Bay mouth show great variability of the efflux of the Bay waters onto the continental shelf and the possibility of this movement of water onto the shelf being controlled to some extent by the wind.

Thus, while a large amount of field data has been accumulated since Bigelow's pioneering work in 1933 and a basic understanding of the movement of the shelf waters has been outlined, there have been few attempts to understand the interrelationship between the outflow from the Chesapeake Bay and the circulation of the shelf waters. How this interrelationship changes and what factors are affecting it are difficult questions to answer.

A logical starting point to eradicate this deficiency would be to consider the application of the extensive work on plane submerged jets discharging into an infinite medium. Many papers and several books (Abramovich (1963), Birkhoff and Zarantonello (1957)) have been written on this subject. However, when the theory and experimental results of a plane jet are compared with what occurs when a large river or estuary empties into a coastal sea, little correlation can be found between the two. The major discrepancy occurs because the plane jet is an entraining one and its angle of spread is small. An estuary or river outflow is generally divergent and can be affected by tide, winds, stratification, ambient currents, and rotation of the earth. This can be seen when comparing classical jet theory with the descriptive work of Stefansson and Richards (1963) and Park (1966) on the Columbia River, Ryther et al (1967) and Gibbs (1970) on the Amazon, Wright and Coleman (1971) on the south pass of the Mississippi, and Garvine (1974) on the Connecticut River. These investigations describe the circulation and distribution of salinity and nutrients which result from the discharge of the above rivers into the surrounding waters and discuss some of the physical factors affecting the circulation.

Recently, several investigators have tried to either apply the results of the theory of the classical jet (referenced above) to the natural environment or take a theoretical approach specifically formulated for the hydrodynamics of a river discharging into a larger body of water.

Bates (1953) suggested that the deceleration of river effluence discharging onto a continental shelf was in accordance with the theory of turbulent jet diffusion as described in Chapter VI. This reasoning was applied to the mouths of the Mississippi River to help understand the formation of deltas.

Iselin (1955) has given a physical description of factors which should affect the circulation in a coastal area and has outlined some rules which have been accepted almost without question.

A more rigorous theoretical approach has been attempted by Takano (1954a, 1954b, 1955), Borichansky and Midhailov (1966), and Bondar (1970). They consider variables, such as bottom and side friction, geometry of the channel entrance, bottom slope, Coriolis force, and density differences, to describe the resultant flow patterns. Their results will also be discussed in Chapter VI.

Finally, Gadgil (1971) has determined the effect of a simple rotating and non-rotating system on the shape and velocity distribution of a steady jet. She has shown that, if a simple laboratory jet is rotated strongly, bottom friction dominates and the jet will be dispersive; while for a non-rotating jet, side friction will dominate and the jet will entrain the surrounding fluid.

The theoretical investigations described above are very useful in gaining an understanding of the physical factors affecting the flow field caused by a river or estuary discharging onto a continental shelf. These results, however, have been derived from the momentum equations where some terms have been left out or simplified to render an analytical solution possible. In like manner, the purely descriptive studies of jet and shelf circulations have given a view where individual factors affecting the flow have been lumped together to give a mean, average, or seasonal pattern of flow, obliterating their individual contributions.

The intent of this investigation is to examine the characteristics of flow resulting from a tidal estuary (Chesapeake Bay) emptying onto a continental shelf using as many of the terms in the equations of motion and the mass balance equation as possible. No effort will be made to reproduce the physical geometry and dynamical situation of the shelf exactly because the extensive data needed for input into the model are not available. Instead the approach will be to vertically integrate the equations of continuity, momentum, and mass balance, assuming where applicable: (1) incompressible flow, (2) a Boussinesq-type approximation, (3) the hydrostatic assumption, and (4) that only the horizontal components of the rotational terms are important. The resultant equations will then be applied to a simplified geometry resembling that of the continental shelf and Chesapeake Bay entrance. Specifically, the effect of tidal flow, bottom and side frictions, force of Coriolis, bottom slope, wind, and ambient currents on the overall circulation patterns will be considered. Further, three circulation characteristics observed in field work of the area will be specifically looked for:

(1) deflection of the Bay effluent, (2) a northern flow above the Bay entrance, and (3) a clockwise eddy south of the Bay entrance.

CHAPTER II

DERIVATION OF TWO-DIMENSIONAL DIFFERENTIAL EQUATIONS

Basic Concepts

A right-hand corrdinate system is assumed with x being positive to the right or east and z being positive upward. The velocity components are the usual u, v, and w for the x, y, and z directions, respectively. The basic equations describing the conservation of mass and momentum in a water body are:

continuity equation

$$\frac{\partial \rho}{\partial t} + \frac{\partial}{\partial x}(\rho u) + \frac{\partial}{\partial y}(\rho v) + \frac{\partial}{\partial z}(\rho w) = 0; \qquad 2.1$$

momentum equation in the x direction

$$\frac{\partial}{\partial t}(\rho u) + \frac{\partial}{\partial x}(\rho u^2) + \frac{\partial}{\partial y}(\rho u v) + \frac{\partial}{\partial z}(\rho u w) =$$

$$-\frac{\partial p}{\partial x} + f\rho v + \frac{\partial}{\partial x}\tau_{xx} + \frac{\partial}{\partial y}\tau_{xy} + \frac{\partial}{\partial z}\tau_{xz}; \qquad 2.2$$

momentum equation in the y direction

$$\frac{\partial}{\partial t}(\rho v) + \frac{\partial}{\partial x}(\rho v u) + \frac{\partial}{\partial y}(\rho v^2) + \frac{\partial}{\partial z}(\rho v w) =$$

$$-\frac{\partial p}{\partial y} - f\rho u + \frac{\partial}{\partial x}\tau_{yx} + \frac{\partial}{\partial y}\tau_{yy} + \frac{\partial}{\partial z}\tau_{yz}; \qquad 2.3$$

momentum equation in the z direction

$$\frac{\partial}{\partial t}(\rho w) + \frac{\partial}{\partial x}(\rho w u) + \frac{\partial}{\partial y}(\rho w v) + \frac{\partial}{\partial z}(\rho w^2) =$$

$$-\frac{\partial p}{\partial z} - \rho g + \frac{\partial}{\partial x}\tau_{zx} + \frac{\partial}{\partial y}\tau_{zy} + \frac{\partial}{\partial z}\tau_{zz} ; \qquad 2.4$$

mass balance equation of salt

$$\frac{\partial s}{\partial t} + \frac{\partial}{\partial x}(us) + \frac{\partial}{\partial y}(vs) + \frac{\partial}{\partial z}(ws) =$$

$$\frac{\partial}{\partial x}\left(E_x \frac{\partial s}{\partial x}\right) + \frac{\partial}{\partial y}\left(E_y \frac{\partial s}{\partial y}\right) + \frac{\partial}{\partial z}\left(E_z \frac{\partial s}{\partial z}\right) ; \qquad 2.5$$

where t, ρ, p, f, g, s, and E_i represent time, density, pressure, Coriolis parameter, gravitational acceleration, real time variation of salinity, and turbulent diffusion coefficient in the i direction. τ_{ij} represents the shear stress, where the subscript i is the direction of the stress and the plane in which the stress acts is given by the normal to the plane j.

Integration of Equation of Continuity

As shown in Figure 2, let the depth of water be h (referenced to mean sea level), δ the tidal height, and H the total water depth ($H = h + \delta$).

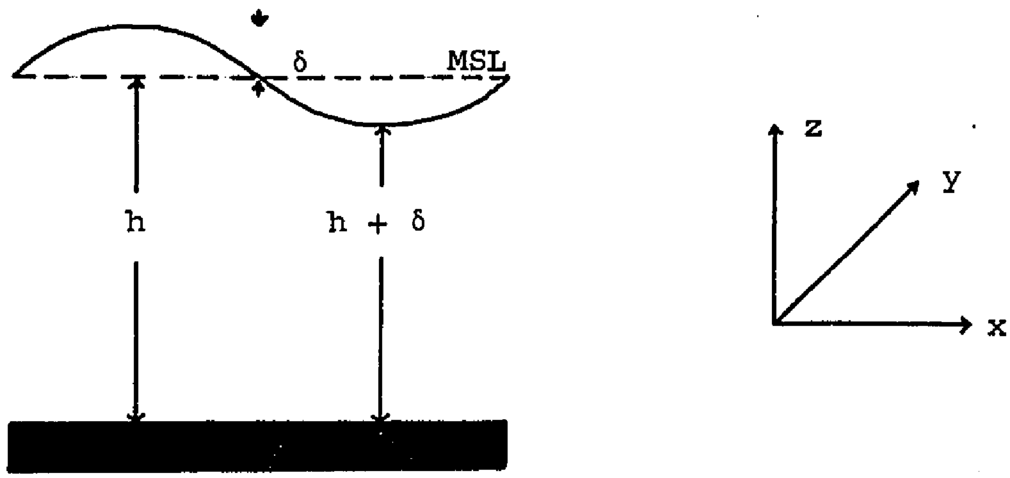

Figure 2

Coordinate notation

In an incompressible flow field, equation 2.1 may be simplified to give

$$\frac{\partial u}{\partial x} + \frac{\partial v}{\partial y} + \frac{\partial w}{\partial z} = 0. \qquad 2.6$$

Integrating with respect to z from -h to δ gives

$$\int_{-h}^{\delta} \frac{\partial u}{\partial x} dz + \int_{-h}^{\delta} \frac{\partial v}{\partial y} dz + \int_{-h}^{\delta} \frac{\partial w}{\partial z} dz = 0. \qquad 2.7$$

Applying Leibnitz's rule, the boundary conditions $w = \frac{\partial \delta}{\partial t} + u \frac{\partial \delta}{\partial x} + v \frac{\partial \delta}{\partial y}$ at the free surface and $u = v = w = 0$ at the bottom give for 2.7

$$\frac{\partial}{\partial t}(\delta) + \frac{\partial}{\partial x}\int_{-h}^{\delta} u\, dz + \frac{\partial}{\partial y}\int_{-h}^{\delta} v\, dz = 0. \qquad 2.8$$

Since the velocity in a natural environment is seldom constant with respect to depth, we set

$$u = u(z) = U + u'(z) \qquad 2.9$$

where U is the velocity averaged with respect to depth, and u'(z) is the variation of the velocity u from the average U.

By definition,

$$\int_{-h}^{\delta} u'(z)\,dz = 0 \qquad 2.10$$

and

$$\frac{1}{H}\int_{-h}^{\delta} u\,dz = U; \qquad 2.11$$

or, rearranging,

$$UH = \int_{-h}^{\delta} u\,dz.$$

Doing the same for the velocity v gives

$$v = v(z) = V + v'(z) \qquad 2.12$$

and

$$VH = \int_{-h}^{\delta} v\,dz. \qquad 2.13$$

Now, substitution of 2.11 and 2.13 into 2.8 gives

$$\frac{\partial \delta}{\partial t} + \frac{\partial}{\partial x}(UH) + \frac{\partial}{\partial y}(VH) = 0. \qquad 2.14$$

Integration of Momentum Equations

Now, applying equations 2.1 and 2.6 to 2.2 and 2.3 and integrating with respect to depth between the limits of -h and δ give for the equation in the x direction

$$\int_{-h}^{\delta}\frac{\partial}{\partial t}u\,dz + \int_{-h}^{\delta}\frac{\partial}{\partial x}(u^2)\,dz + \int_{-h}^{\delta}\frac{\partial}{\partial y}(uv)\,dz + \int_{-h}^{\delta}\frac{\partial}{\partial z}(uw)\,dz = -\int_{-h}^{\delta}\frac{1}{\rho}\frac{\partial p}{\partial x}\,dz +$$

$$\int_{-h}^{\delta} fv\,dz + \int_{-h}^{\delta}\frac{1}{\rho}\frac{\partial}{\partial x}\tau_{xx}\,dz + \int_{-h}^{\delta}\frac{1}{\rho}\frac{\partial}{\partial y}\tau_{xy}\,dz + \int_{-h}^{\delta}\frac{1}{\rho}\frac{\partial}{\partial z}\tau_{xz}\,dz\,; \qquad 2.15$$

and for the equation in the y direction

$$\int_{-h}^{\delta}\frac{\partial}{\partial t}v\,dz + \int_{-h}^{\delta}\frac{\partial}{\partial x}(uv)\,dz + \int_{-h}^{\delta}\frac{\partial}{\partial y}(v^2)\,dz + \int_{-h}^{\delta}\frac{\partial}{\partial z}(vw)\,dz = -\int_{-h}^{\delta}\frac{1}{\rho}\frac{\partial p}{\partial y}\,dz -$$

$$\int_{-h}^{\delta} fu\,dz + \int_{-h}^{\delta}\frac{1}{\rho}\frac{\partial}{\partial x}\tau_{yx}\,dz + \int_{-h}^{\delta}\frac{1}{\rho}\frac{\partial}{\partial y}\tau_{yy}\,dz + \int_{-h}^{\delta}\frac{1}{\rho}\frac{\partial}{\partial z}\tau_{yz}\,dz. \qquad 2.16$$

Using Leibnitz's rule, the boundary conditions for the surface and bottom (as in the equation of continuity) and equations 2.11 and 2.13 on 2.15 and 2.16 give for the equation in the x direction

$$\frac{\partial}{\partial t}(UH)+\frac{\partial}{\partial x}(U^2H)+\frac{\partial}{\partial y}(UVH)+\frac{\partial}{\partial x}\int_{-h}^{\delta}(u')^2 dz+\frac{\partial}{\partial y}\int_{-h}^{\delta}(u'v')\,dz=$$

$$-\int_{-h}^{\delta}\frac{1}{\rho}\frac{\partial p}{\partial x}dz+fVH+\int_{-h}^{\delta}\frac{1}{\rho}\frac{\partial}{\partial x}\tau_{xx}\,dz+\int_{-h}^{\delta}\frac{1}{\rho}\frac{\partial}{\partial y}\tau_{yx}\,dz+\int_{-h}^{\delta}\frac{1}{\rho}\frac{\partial}{\partial z}\tau_{xz} \qquad 2.17$$

and the equation in the y direction

$$\frac{\partial}{\partial t}(VH)+\frac{\partial}{\partial x}(UVH)+\frac{\partial}{\partial y}(V^2H)+\frac{\partial}{\partial x}\int_{-h}^{\delta}(u'v')\,dz+\frac{\partial}{\partial y}\int_{-h}^{\delta}(v')^2 dz=$$

$$-\int_{-h}^{\delta}\frac{1}{\rho}\frac{\partial p}{\partial y}-fUH+\int_{-h}^{\delta}\frac{1}{\rho}\frac{\partial}{\partial x}\tau_{yx}\,dz+\int_{-h}^{\delta}\frac{1}{\rho}\frac{\partial}{\partial y}\tau_{yy}\,dz+\int_{-h}^{\delta}\frac{1}{\rho}\frac{\partial}{\partial z}\tau_{yz}\,dz\,. \qquad 2.18$$

To further simplify the above two equations, several assumptions must be made. First is the hydrostatic assumption and the resultant equation

$$\frac{\partial p}{\partial z}=-\rho g \qquad 2.19$$

Second, a Boussinesq-type approximation is assumed in which the vertical variation of density ρ is ignored except in the gravitational term. Now, considering only the pressure gradient term in 2.17 for the time being, applying the above assumptions and Leibnitz's rule gives

$$-\int_{-h}^{\delta}\frac{1}{\rho}\frac{\partial p}{\partial x}dz=-\frac{1}{\bar\rho}\int_{-h}^{\delta}\frac{\partial p}{\partial x}dz=-\frac{1}{\bar\rho}\left[\frac{\partial}{\partial x}\int_{-h}^{\delta}p\,dz+p\Big|_{-h}\frac{\partial(-h)}{\partial x}-p\Big|_{\delta}\frac{\partial\delta}{\partial x}\right], \qquad 2.20$$

where $p|_\delta = 0$ is the pressure at the free surface or sea-air interface. If the same type of convention for the density variation as a function of depth is used as was for the velocity, i.e., the density consists of a depth averaged part plus a variation from this average,

$$\rho = \bar{\rho} + \rho'. \qquad 2.21$$

To expand 2.20 to a form which can be used, 2.21 is substituted into equation 2.19 and integrated from the surface $z = \delta$ to any depth z

$$p = \int_{\delta}^{z} -g(\bar{\rho} + \rho')\,dz$$

or

$$p = \bar{\rho} g(\delta - z) + g\int_{z}^{\delta} \rho'\,dz. \qquad 2.22$$

Integrating 2.22 over depth gives

$$\int_{-h}^{\delta} p\,dz = \bar{\rho} g \int_{-h}^{\delta} (\delta - z)\,dz + g\int_{-h}^{\delta}\left(\int_{z}^{\delta} \rho'\,dz\right)dz$$

$$= \bar{\rho} g \frac{(\delta + h)^2}{2} + g\int_{-h}^{\delta}\left(\int_{z}^{\delta} \rho'\,dz\right)dz.$$

2.23

Differentiating the above with respect to x yields

$$\frac{\partial}{\partial x}\int_{-h}^{\delta} p\,dz = \bar{\rho} g(\delta+h)\left(\frac{\partial \delta}{\partial x}+\frac{\partial h}{\partial x}\right)+g\,\frac{(\delta+h)^2}{2}\frac{\partial \bar{\rho}}{\partial x}+$$

$$g\,\frac{\partial}{\partial x}\int_{-h}^{\delta}\left(\int_{z}^{\delta}\rho' dz\right)dz.$$

2.24

The term $p|_{-h}$ can be evaluated from 2.22, giving

$$p|_{-h} = \bar{\rho} g H, \qquad 2.25$$

since

$$\int_{-h}^{\delta}\rho' dz = 0.$$

Substituting equations 2.24 and 2.25 into 2.20 and simplifying yields

$$-\int_{-h}^{\delta}\frac{1}{\rho}\frac{\partial p}{\partial x}dz = -g H\frac{\partial \delta}{\partial x} - \frac{g}{2}\frac{H^2}{\bar{\rho}}\frac{\partial \bar{\rho}}{\partial x} - \frac{g}{\bar{\rho}}\frac{\partial}{\partial x}\int_{-h}^{\delta}\left(\int_{z}^{\delta}\rho' dz\right)dz. \qquad 2.26$$

Likewise, for the y direction without repeating the derivation, the results using the same approach will be

$$-\int_{-h}^{\delta}\frac{1}{\rho}\frac{\partial p}{\partial y}dz = -g H\frac{\partial \delta}{\partial y} - \frac{g}{2}\frac{H^2}{\bar{\rho}}\frac{\partial \bar{\rho}}{\partial y} - \frac{g}{\bar{\rho}}\frac{\partial}{\partial y}\int_{-h}^{\delta}\left(\int_{z}^{\delta}\rho' dz\right)dz. \qquad 2.27$$

For homogeneous or weakly stratified water columns, as considered here, the last term in 2.26 and 2.27 can be dropped due to its small value (Appendix A).

The shear stress terms of 2.17 and 2.18 can also be simplified using the Boussinesq approximation to give

$$\int_{-h}^{\delta} \frac{1}{\rho}\frac{\partial}{\partial x}\tau_{xx}\,dz + \int_{-h}^{\delta} \frac{1}{\rho}\frac{\partial}{\partial y}\tau_{xy}\,dz + \int_{-h}^{\delta} \frac{1}{\rho}\frac{\partial}{\partial z}\tau_{xz}\,dz =$$

$$\frac{1}{\rho}\left[\frac{\partial}{\partial x}\int_{-h}^{\delta}\tau_{xx}\,dz + \frac{\partial}{\partial y}\int_{-h}^{\delta}\tau_{xy}\,dz + \tau_x^s - \tau_x^b\right] \qquad 2.28$$

and

$$\int_{-h}^{\delta} \frac{1}{\rho}\frac{\partial}{\partial x}\tau_{yx}\,dz + \int_{-h}^{\delta} \frac{1}{\rho}\frac{\partial}{\partial y}\tau_{yy}\,dz + \int_{-h}^{\delta} \frac{1}{\rho}\frac{\partial}{\partial z}\tau_{yz}\,dz =$$

$$\frac{1}{\rho}\left[\frac{\partial}{\partial x}\int_{-h}^{\delta}\tau_{yx}\,dz + \frac{\partial}{\partial y}\int_{-h}^{\delta}\tau_{yy}\,dz + \tau_y^s - \tau_y^b\right], \qquad 2.29$$

where τ_x^s, τ_x^b, τ_y^s, τ_y^b are the surface and bottom stresses in planes of the local surface and bottom in the x and y directions, respectively. Substituting 2.26 through 2.29 into the proper places in 2.17 and 2.18 results in

$$\frac{\partial}{\partial t}(UH) + \frac{\partial}{\partial x}(U^2H) + \frac{\partial}{\partial y}(UVH) + \frac{\partial}{\partial x}\int_{-h}^{\delta}(u')^2 dz + \frac{\partial}{\partial y}\int_{-h}^{\delta}(u'v')\,dz =$$

$$-gH\frac{\partial \delta}{\partial x} - \frac{gH^2}{2\bar{\rho}}\frac{\partial \bar{\rho}}{\partial x} + fVH + \frac{1}{\bar{\rho}}\frac{\partial}{\partial x}\int_{-h}^{\delta}\tau_{xx}\,dz + \frac{1}{\bar{\rho}}\frac{\partial}{\partial y}\int_{-h}^{\delta}\tau_{xy}\,dz +$$

$$\frac{1}{\bar{\rho}}\left(\tau_x^s - \tau_x^b\right) \qquad 2.30$$

and

$$\frac{\partial}{\partial t}(VH) + \frac{\partial}{\partial x}(VUH) + \frac{\partial}{\partial y}(V^2H) + \frac{\partial}{\partial x}\int_{-h}^{\delta}(u'v')\,dz + \frac{\partial}{\partial y}\int_{-h}^{\delta}(v')^2 dz =$$

$$-gH\frac{\partial \delta}{\partial x} - \frac{gH^2}{2\bar{\rho}}\frac{\partial \bar{\rho}}{\partial x} + fUH + \frac{1}{\bar{\rho}}\frac{\partial}{\partial x}\int_{-h}^{\delta}\tau_{yx}\,dz + \frac{1}{\bar{\rho}}\frac{\partial}{\partial y}\int_{-h}^{\delta}\tau_{yy}\,dz +$$

$$\frac{1}{\bar{\rho}}\left(\tau_y^s - \tau_y^b\right). \qquad 2.31$$

Further, the turbulent velocity fluctuation and the shear stress terms in 2.30 can be combined and approximated (Leendertse et al (1973)) by

$$\frac{\partial}{\partial x}\int_{-h}^{\delta}\left(\frac{\tau_{xx}}{\rho} - u'^2\right)dz = \frac{\partial}{\partial x} A_x H \frac{\partial U}{\partial x} = \frac{\partial}{\partial x}\alpha H^2 U \frac{\partial U}{\partial x}$$

$$\frac{\partial}{\partial y}\int_{-h}^{\delta}\left(\frac{\tau_{xy}}{\rho} - u'v'\right)dz = \frac{\partial}{\partial y} A_y H \frac{\partial U}{\partial y} = \frac{\partial}{\partial y}\alpha H^2 V \frac{\partial U}{\partial y}.$$

side friction terms 2.32

Following the lead of Dronkers (1964), the bottom stress term can also be approximated by

$$-\frac{\tau_x^b}{\rho} = -\frac{gU[U^2+V^2]^{1/2}}{C^2}.$$

bottom friction term 2.33

For the y direction the approximations for equation 2.31 give

$$\frac{\partial}{\partial x}\int_{-h}^{\delta}\left(\frac{\tau_{yx}}{\rho} - u'v'\right)dz = \frac{\partial}{\partial x} A_x H \frac{\partial V}{\partial x} = \frac{\partial}{\partial x}\alpha H^2 U \frac{\partial V}{\partial x}$$

$$\frac{\partial}{\partial y}\int_{-h}^{\delta}\left(\frac{\tau_{yy}}{\rho} - v'^2\right)dz = \frac{\partial}{\partial y} A_y H \frac{\partial V}{\partial y} = \frac{\partial}{\partial y}\alpha H^2 V \frac{\partial V}{\partial y}$$

side friction terms 2.34

and

$$-\frac{\tau_y^b}{\rho} = -\frac{gV[U^2+V^2]^{1/2}}{C^2}.$$

bottom friction term 2.35

In equations 2.32 through 2.35, C is the Chézy coefficient and A the turbulent eddy viscosity. The Chézy coefficient can be related (Henderson (1966)) to depth by the equation

$$C = \frac{h^{1/6}}{n'} \tag{2.36}$$

where h is the depth in meters and n' is the Manning coefficient. The turbulent eddy viscosities were simplified by relating them to the mixing length theory, giving

$$A_x = \alpha H U \tag{2.37}$$

$$A_y = \alpha H V \tag{2.38}$$

where α is a constant. Substituting the terms in 2.32 through 2.35 into 2.30 and 2.31 and applying equation 2.13 gives the final momentum equations of

$$\frac{\partial U}{\partial t} + U\frac{\partial U}{\partial x} + V\frac{\partial U}{\partial y} = fV - g\frac{\partial \delta}{\partial x} - \frac{gH}{2\bar{\rho}}\frac{\partial \bar{\rho}}{\partial x} - \frac{gU[U^2+V^2]^{1/2}}{HC^2} +$$

$$\frac{\tau_x^s}{\bar{\rho}H} + \frac{1}{H}\left[\frac{\partial}{\partial x}\alpha H^2 U\frac{\partial U}{\partial x}\right] + \frac{1}{H}\left[\frac{\partial}{\partial y}\alpha H^2 V\frac{\partial U}{\partial y}\right] \tag{2.39}$$

and

$$\frac{\partial V}{\partial t} + U\frac{\partial V}{\partial x} + V\frac{\partial V}{\partial y} = -fU - g\frac{\partial \delta}{\partial y} - \frac{gH}{2\bar{\rho}}\frac{\partial \bar{\rho}}{\partial y} - \frac{gV[U^2+V^2]^{1/2}}{HC^2}$$

$$\frac{\tau_y^s}{\bar{\rho}H} + \frac{1}{H}\left[\frac{\partial}{\partial x}\alpha H^2 U\frac{\partial V}{\partial x}\right] + \frac{1}{H}\left[\frac{\partial}{\partial y}\alpha H^2 V\frac{\partial V}{\partial y}\right]. \tag{2.40}$$

Integration of Mass Balance Equation

Lastly, the two-dimensional mass balance equation is derived by starting with 2.5, integrating with respect to z between the limits of δ and $-h$, and applying Leibnitz's rule, giving

$$\frac{\partial}{\partial t}\int_{-h}^{\delta} s\,dz + \frac{\partial}{\partial x}\int_{-h}^{\delta}(us)\,dz + \frac{\partial}{\partial y}\int_{-h}^{\delta}(vs)\,dz - \left[s\left(\frac{\partial\delta}{\partial t} + u\frac{\partial\delta}{\partial x} + v\frac{\partial\delta}{\partial y} - w\right)\right]_{\delta} +$$

$$\left[s\left(-\frac{\partial h}{\partial t} - u\frac{\partial h}{\partial x} - v\frac{\partial h}{\partial y} - w\right)\right]_{-h} - \frac{\partial}{\partial x}\int_{-h}^{\delta} E_x\frac{\partial s}{\partial x}\,dz - \frac{\partial}{\partial y}\int_{-h}^{\delta} E_y\frac{\partial s}{\partial y}\,dz +$$

$$\left[\left(E_x\frac{\partial s}{\partial x}\right)\frac{\partial\delta}{\partial x} + \left(E_y\frac{\partial s}{\partial y}\right)\frac{\partial\delta}{\partial y} - E_z\frac{\partial s}{\partial z}\right]_{\delta} + \left[\left(E_x\frac{\partial s}{\partial x}\right)\frac{\partial h}{\partial x} + \left(E_y\frac{\partial s}{\partial y}\right)\frac{\partial h}{\partial y} +\right.$$

$$\left. E_z\frac{\partial s}{\partial z}\right]_{-h} = 0, \qquad 2.41$$

where $[\ ]_{\delta}$ and $[\ ]_{-h}$ designate the quantities in the brackets being evaluated at $z = \delta$ and $z = -h$, respectively.

Again, using the same technique for representing the variation of s as a function of depth as was done previously for the velocity and density, i.e.,

$$s = S + s'(z) \qquad 2.42$$

and

$$\frac{1}{H}\int_{-h}^{\delta} s'\,dz = 0, \qquad 2.43$$

gives upon integration of 2.42 with respect to depth

$$\int_{-h}^{\delta} s\, dz = HS' . \qquad 2.44$$

Substitution of 2.44 into 2.41, setting the boundary conditions that the salt flux through the surface and bottom is 0, and using the results of 2.11 and 2.12 give

$$\frac{\partial}{\partial t}(HS') + \frac{\partial}{\partial x}(HUS') + \frac{\partial}{\partial y}(HVS') = -\frac{\partial}{\partial x}\int_{-h}^{\delta}(u's')\,dz - \frac{\partial}{\partial y}\int_{-h}^{\delta}(v's')\,dz +$$

$$\frac{\partial}{\partial x}\int_{-h}^{\delta} E_x \frac{\partial S'}{\partial x}\,dz + \frac{\partial}{\partial y}\int_{-h}^{\delta} E_y \frac{\partial S'}{\partial y}\,dz . \qquad 2.45$$

Finally, letting the turbulent diffusion terms be replaced by a dispersion term D_i such that

$$D_x H \frac{\partial S'}{\partial x} = \int_{-h}^{\delta}\left(E_x \frac{\partial S'}{\partial x} - u's'\right) dz \qquad 2.46$$

and

$$D_y H \frac{\partial S'}{\partial y} = \int_{-h}^{\delta}\left(E_y \frac{\partial S'}{\partial y} - v's'\right) dz \qquad 2.47$$

gives

$$\frac{\partial}{\partial t}(HS') + \frac{\partial}{\partial x}(HUS') + \frac{\partial}{\partial y}(HVS') = \frac{\partial}{\partial x}\left[D_x H \frac{\partial S'}{\partial x}\right] + \frac{\partial}{\partial y}\left[D_y H \frac{\partial S'}{\partial y}\right] . \qquad 2.48$$

Expanding the left-hand side and applying the equation of continuity (2.14) gives

$$\frac{\partial S'}{\partial t} + \frac{\partial}{\partial x}(US') + \frac{\partial}{\partial y}(VS') = \frac{1}{H}\left[\frac{\partial}{\partial x} D_x H \frac{\partial S'}{\partial x}\right] + \frac{1}{H}\left[\frac{\partial}{\partial y} D_y H \frac{\partial S'}{\partial y}\right]. \qquad 2.49$$

CHAPTER III

FORMULATION OF FINITE DIFFERENCE EQUATIONS

Basic Concepts

The final equations in the previous chapter (2.14, 2.39, 2.40, and 2.49) form a set of partial differential equations which together and without further assumptions have no known analytical solution. For these equations to be applied, as outlined in the Introduction, it will be necessary to use numerical techniques to approximate their exact solution.

The approach in forming a numerical approximation was: first, choosing a finite difference technique and computational scheme for the equations; second, formulating a computational grid for the equations; third, writing the analytical equations in finite difference form with the computational scheme and grid governing the formulation of the equations; fourth, solving the numerical equations for the unknown parameters; and fifth, programming the finite difference solution derived from step four for machine computation of the unknown parameters.

Finite Difference Equations and Computational Scheme - For the final equations of Chapter II, several computational schemes were possible. As an example, Gordon and Spaulding (1974) recently referenced over 160 different numerical models for tidal rivers, estuaries, and coastal rivers. Because of the need to include non-linear terms and the desire to have a fast stable finite difference scheme, the formulations of Leendertse (1970) were chosen for the hyperbolic equations of flow and the ADI (Alternating Direction Implicit) technique of Peaceman and Rachford (1955) and Douglas and Gunn (1964) was chosen for the parabolic equations of transport.

The computational scheme requires a set of finite difference equations (consisting of one each of the continuity, momentum, and mass balance equations) for both the x and y directions. The first set of equations are written implicitly for the unknowns of δ, U, and S in the x direction for the first half of the forward time step (details of the time step will be explained shortly), while δ, V, and S (known from a previous time step) are written explicitly for the y direction in the same equations. For the second half of the forward time step, δ, V, and S for the y direction are written implicitly and δ, U, and S for the x direction are written explicitly. This results in a solution scheme which has better stability than a purely explicit set of equations and requires fewer simultaneous equations to solve than a straight implicit formulation. This is important since the computational effort increases as the cube of the number of simultaneous equations.

A detailed description of how to solve the finite difference equations for U, V, δ, and S will be given in Chapter IV. However, some idea of the approach to be used in solving these equations after they are written in finite difference form will be necessary in order to write them in their proper format.

In brief, the solution technique will consist of first solving simultaneously for the unknowns of tidal height δ and velocity U for the x direction at the first half of the forward time step. This technique requires the simultaneous solution of the continuity and momentum equations whose value of δ and U when determined are then used to solve for S in the mass balance equations for the same time step. Next, δ and V are determined simultaneously in the y direction for the last half of the forward time step, and their values are used to calculate S for this half time step. This procedure eliminates the need of the solution of four simultaneous equations (for U, V, δ, and S) and makes computation easier.

<u>Grid</u> - The grid of points to be used in writing the equations is similar to that used by Leendertse (1967, 1970)

and is illustrated in Figure 3. Grid points for tidal height δ, density ρ, and salinity S are located at the + points; while values for mean water depth h, velocity U and V are located at the points O, -, and |, respectively. All like points are separated by a distance Δx or Δy. The grid points are grouped into squares as shown in Figure 3, with a +, O, -, and | forming the corner of each square.

The squares are numbered with integer values of m and n for the x and y directions. The values of m for the x direction increase from right to left, and the values of n increase from top to bottom. The grid is set up so that the predominantly southern flow of water in the area enters the grid at the top (i.e., northern edge) and leaves at the bottom and in the negative y direction. Formulation of the finite difference equations should present no difficulty because of this notation and can be handled by a sign reversal for the first order derivative terms of the y direction.

Stability - The stability of explicit numerical equations is a function of the grid size and time step, and expressions, such as the Courant-Friedrichs-Lewy criterion, are available to predict the maximum allowable time step for a specific grid size. For a multi-operational method as described above, no such formula exists. Leendertse (1970)

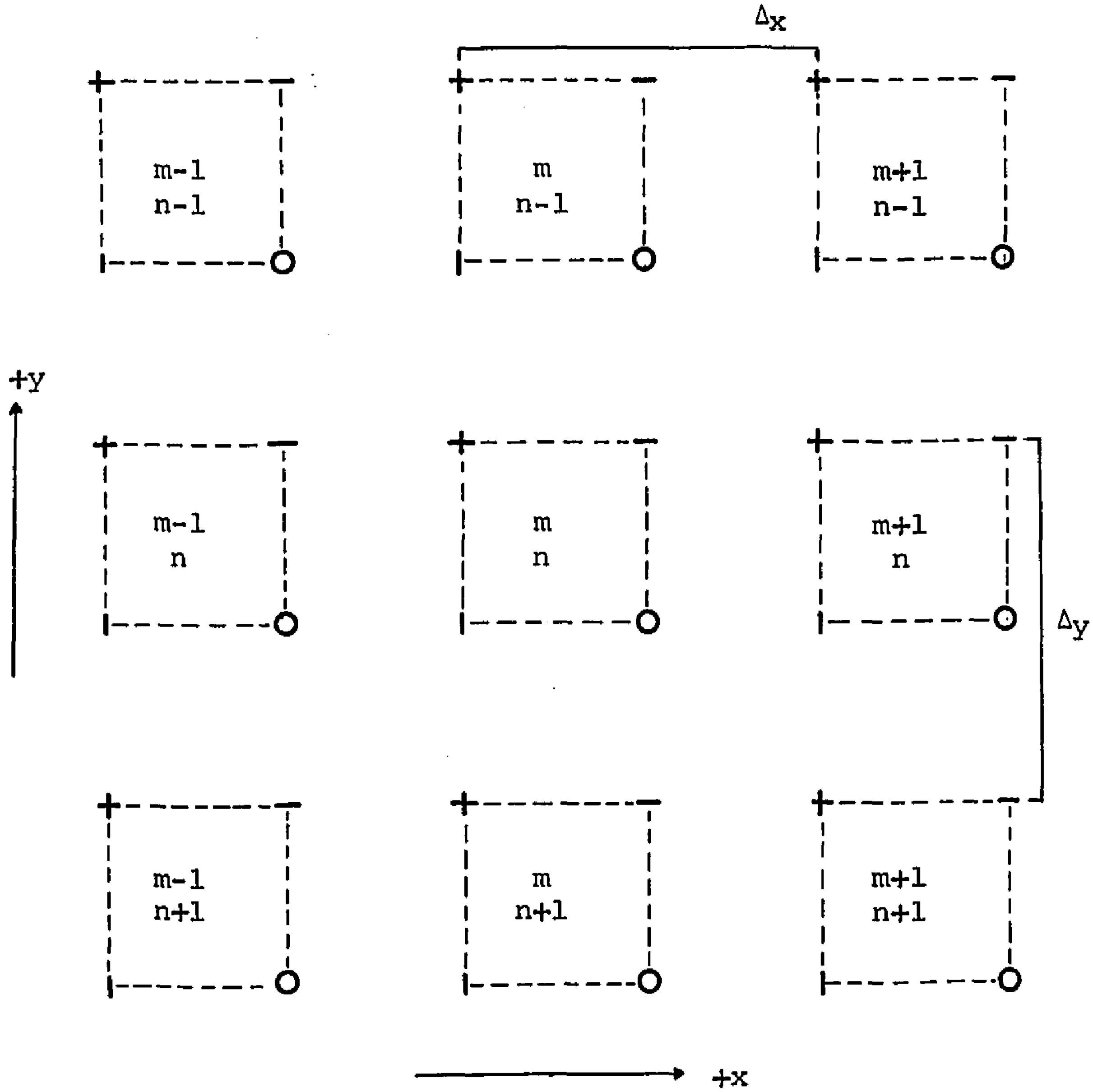

Legend

— grid points for velocity U in x direction

| grid points for velocity V in y direction

O grid points for water depth, -h

+ grid points for salinity S, density ρ, tidal height δ

Figure 3
Grid point arrangement

has taken a simplified approach in evaluating the stability and some of the factors affecting a multi-operational scheme. He used a linear analysis on a one-dimensional transport equation to study the effects of grid size and time step. He found that, for a time centered multi-operational method, the dispersion of the solution will be independent of the grid size if a sufficient representation of the concentration field is present.

In the discussion to come, the Courant-Friedrichs-Lewy criterion will be quoted to give an indication of how the time step chosen for the multi-operational technique compares with that of a pure explicit scheme.

Convention - For the equations to follow, the time step ΔT consists of two halves, one each for the x and y directions such that $\Delta T = 2\Delta t$. The time notations below will be used to conserve space in writing the numerical equations.

Time x direction, calculation of δ, U, and S

$$(2k-1)\Delta t = t = \text{past time}$$

$$2k\Delta t = 2t = \text{present time}$$

$$(2k+1)\Delta t = 3t = \text{future time}$$

Time y direction, calculation of δ, V, and S

$$2k\Delta t = 2t = \text{past time}$$

$$(2k+1) = 3t = \text{present time}$$

$$(2k+2) = 4t = \text{future time,}$$

where $k = 1,2,\ldots k_{max}$. The above notation t, 2t, 3t, and 4t will appear as a superscript of the variables.

The location of the variable in the grid will be given by subscripts m and n. Wind stress was assumed to be constant over the grid, although it could be made to vary, and no subscripts were used. Depth below mean sea level h was not allowed to vary with time; therefore, no time superscript will be used.

The finite difference equations are to be written so that they are centered in both space (centered differences tend to be more stable) and time. The centering in space (on the grid) is around the local derivative (time derivative) variable, i.e., either δ, U, V, or S of the equation being written.

Equation of Continuity

The finite difference form of the equation of continuity, upon applying the previously described operations and conditions for time $(2k+1)\Delta t$ (stepping in time from the present time $2k\Delta t$ to $(2k+1)\Delta t$), is

$$\left(\zeta^{3t}_{m,n}-\zeta^{2t}_{m,n}\right)\frac{1}{\Delta t}+\Big[\left(h_{m,n}+h_{m,n-1}+\zeta^{2t}_{m+1,n}+\zeta^{2t}_{m,n}\right)U^{3t}_{m,n}-$$

$$\left(h_{m-1,n}+h_{m-1,n-1}+\zeta^{2t}_{m-1,n}+\zeta^{2t}_{m,n}\right)U^{3t}_{m-1,n}\Big]\frac{1}{2\Delta x}+$$

$$\Big[\left(h_{m,n-1}+h_{m-1,n-1}+\zeta^{2t}_{m,n}+\zeta^{2t}_{m,n-1}\right)V^{2t}_{m,n-1}-$$

$$\Big[h_{m,n}+h_{m-1,n}+\zeta^{2t}_{m,n+1}+\zeta^{2t}_{m,n}\Big)V^{2t}_{m,n}\Big]\frac{1}{2\Delta y}=0.$$

3.1

Likewise, for time (2k+2), stepping from (2k+1) Δt above to (2k+2) Δt, the equation of continuity is

$$\left(\zeta^{4t}_{m,n}-\zeta^{3t}_{m,n}\right)\frac{1}{\Delta t}+\Big[\left(h_{m,n}+h_{m,n-1}+\zeta^{3t}_{m+1,n}+\zeta^{3t}_{m,n}\right)U^{3t}_{m,n}-$$

$$\left(h_{m-1,n}+h_{m-1,n-1}+\zeta^{3t}_{m-1,n}+\zeta^{3t}_{m,n}\right)U^{3t}_{m-1,n}\Big]\frac{1}{2\Delta x}+$$

$$\Big[\left(h_{m,n-1}+h_{m-1,n-1}+\zeta^{3t}_{m,n}+\zeta^{3t}_{m,n-1}\right)V^{4t}_{m,n-1}-$$

$$\left(h_{m,n}+h_{m-1,n}+\zeta^{3t}_{m,n+1}+\zeta^{3t}_{m,n}\right)V^{4t}_{m,n}\Big]\frac{1}{2\Delta y}=0.$$

3.2

Momentum Equations

Using the same techniques for the momentum equation in the x direction yields

$$\left(U^{3t}_{m,n}-U^{t}_{m,n}\right)\frac{1}{2\Delta t}+\left(U^{t}_{m+1,n}-U^{t}_{m-1,n}\right)\left(U^{3t}_{m,n}\right)\left(\frac{1}{2\Delta x}\right)+$$

$$\left(U^{t}_{m,n-1}-U^{t}_{m,n+1}\right)\left(V^{2t}_{m+1,n}+V^{2t}_{m+1,n-1}+V^{2t}_{m,n-1}+V^{2t}_{m,n}\right)\left(\frac{1}{8\Delta y}\right)+$$

$$\left(\delta^{3t}_{m+1,n}-\delta^{3t}_{m,n}+\delta^{t}_{m+1,n}+\delta^{t}_{m,n}\right)\left(\frac{g}{2\Delta x}\right)+\left(\bar{\rho}^{2t}_{m+1,n}-\bar{\rho}^{2t}_{m,n}\right)\left(h_{m,n}+\right.$$

$$\left.h_{m,n-1}+\delta^{2t}_{m+1,n}+\delta^{2t}_{m,n}\right)\left(\frac{g}{2\Delta x}\right)\left(1/\left(\bar{\rho}^{2t}_{m+1,n}+\bar{\rho}^{2t}_{m,n}\right)\right)-$$

$$(f/4)\left(V^{2t}_{m+1,n}+V^{2t}_{m+1,n-1}+V^{2t}_{m,n-1}+V^{2t}_{m,n}\right)+$$

$$\frac{(g)\left(U^{3t}_{m,n}+U^{t}_{m,n}\right)\left[\left(U^{t}_{m,n}\right)^2+(1/16)\left(V^{2t}_{m+1,n}+V^{2t}_{m+1,n-1}+V^{2t}_{m,n-1}+V^{2t}_{m,n}\right)^2\right]^{1/2}}{\left(h_{m,n}+h_{m,n-1}+\delta^{2t}_{m+1,n}+\delta^{2t}_{m,n}\right)\left[\left(C^{2t}_{m+1,n}+C^{2t}_{m,n}\right)/2\right]^2}-$$

$$\left(4\tau^{s}_{x}/\left(\bar{\rho}^{2t}_{m+1,n}+\bar{\rho}^{2t}_{m,n}\right)\left(h_{m,n}+h_{m,n-1}+\delta^{2t}_{m+1,n}+\delta^{2t}_{m,n}\right)\right)-$$

$$\left(2/\left(h_{m,n}+h_{m,n-1}+\delta^{2t}_{m,n}+\delta^{2t}_{m+1,n}\right)\right)\left[\left(\left(\left(h_{m+1,n}+h_{m,n-1}+h_{m,n}+h_{m+1,n}\right)/4\right)+\right.\right.$$

$$\left.\delta^{2t}_{m+1,n}\right)^2\alpha\left(U^{t}_{m,n}+U^{t}_{m+1,n}\right)\left(U^{t}_{m+1,n}-U^{t}_{m,n}\right)-\left(\left(\left(h_{m,n}+h_{m,n-1}+h_{m-1,n-1}+\right.\right.\right.$$

$$\left.\left.h_{m-1,n}\right)/4\right)+\delta^{2t}_{m,n}\right)^2\alpha\left(U^{t}_{m,n}+U^{t}_{m-1,n}\right)\left(U^{t}_{m,n}-U^{t}_{m-1,n}\right)\left.\right]\frac{1}{2(\Delta x)^2}-$$

$$\left(2/\left(h_{m,n}+h_{m,n-1}+\delta^{2t}_{m,n}+\delta^{2t}_{m+1,n-1}\right)\right)\left[\left(\left(\left(\delta^{2t}_{m,n-1}+\delta^{2t}_{m+1,n}+\delta^{2t}_{m,n}+\delta^{2t}_{m+1,n-1}\right)/4\right)+\right.\right.$$

$$\left.h_{m,n-1}\right)^2\alpha\left(V^{2t}_{m,n-1}+V^{2t}_{m+1,n-1}\right)\left(U^{t}_{m,n-1}-U^{t}_{m,n}\right)-\left(\left(\left(\delta^{2t}_{m,n}+\delta^{2t}_{m+1,n}+\delta^{2t}_{m,n+1}+\right.\right.\right.$$

$$\left.\left.\delta^{2t}_{m+1,n+1}\right)/4\right)+h_{m,n}\right)^2\alpha\left(V^{2t}_{m,n}+V^{2t}_{m+1,n}\right)\left(U^{t}_{m,n}-U^{t}_{m,n+1}\right)\left.\right]\frac{1}{2(\Delta y)^2}=0. \qquad 3.3$$

The resultant equation in the y direction is

$$\left(V^{4t}_{m,n} - V^{2t}_{m,n}\right)\frac{1}{2\Delta t} + \left(U^{3t}_{m,n} + U^{3t}_{m-1,n+1} + U^{3t}_{m,n+1} + U^{3t}_{m-1,n}\right)\left(V^{2t}_{m+1,n} -\right.$$

$$\left.V^{2t}_{m-1,n}\right)\left(\frac{1}{8\Delta x}\right) + \left(V^{4t}_{m,n}\right)\left(V^{2t}_{m,n-1} - V^{2t}_{m,n+1}\right)\left(\frac{1}{2\Delta y}\right) +$$

$$\left(\delta^{4t}_{m,n} - \delta^{4t}_{m,n+1} + \delta^{2t}_{m,n} - \delta^{2t}_{m,n+1}\right)\left(\frac{g}{2\Delta y}\right) + \left(\bar{\rho}^{3t}_{m,n} - \bar{\rho}^{3t}_{m,n+1}\right)\left(h_{m,n} +\right.$$

$$\left.h_{m-1,n} + \delta^{3t}_{m,n+1} + \delta^{3t}_{m,n}\right)\left(\frac{g}{2\Delta y}\right)\left(1/\left(\bar{\rho}^{3t}_{m,n+1} + \bar{\rho}^{3t}_{m,n}\right)\right) +$$

$$(f/4)\left(U^{3t}_{m,n+1} + U^{3t}_{m,n} + U^{3t}_{m-1,n+1} + U^{3t}_{m-1,n}\right) +$$

$$\frac{(g)\left(V^{4t}_{m,n} + V^{2t}_{m,n}\right)\left[\left(V^{2t}_{m,n}\right)^2 + (1/16)\left(U^{3t}_{m,n+1} + U^{3t}_{m,n} + U^{3t}_{m-1,n+1} + U^{3t}_{m-1,n}\right)^2\right]^{1/2}}{\left(h_{m,n} + h_{m-1,n} + \delta^{3t}_{m,n+1} + \delta^{3t}_{m,n}\right)\left[\left(C^{3t}_{m,n+1} + C^{3t}_{m,n}\right)/2\right]^2} -$$

$$\left(4\tau^{s}_{y}/\left(\bar{\rho}^{3t}_{m,n+1} + \bar{\rho}^{3t}_{m,n}\right)\left(h_{m,n} + h_{m-1,n} + \delta^{3t}_{m,n+1} + \delta^{3t}_{m,n}\right)\right) -$$

$$\left(2/\left(h_{m,n} + h_{m-1,n} + \delta^{3t}_{m,n} + \delta^{3t}_{m,n+1}\right)\right)\left[\left(\left(\left(\delta^{3t}_{m,n} + \delta^{3t}_{m+1,n} + \delta^{3t}_{m,n+1} + \delta^{3t}_{m+1,n+1}\right)/4\right) +\right.\right.$$

$$\left.h_{m,n}\right)^2 \alpha \left(U^{3t}_{m,n} + U^{3t}_{m,n+1}\right)\left(V^{2t}_{m+1,n} - V^{2t}_{m,n}\right) - \left(\left(\left(\delta^{3t}_{m,n} + \delta^{3t}_{m,n+1} + \delta^{3t}_{m-1,n+1} +\right.\right.\right.$$

$$\left.\left.\left.\delta^{3t}_{m-1,n}\right)/4\right) + h_{m-1,n}\right)^2 \alpha \left(U^{3t}_{m-1,n} + U^{3t}_{m-1,n+1}\right)\left(V^{2t}_{m,n} - V^{2t}_{m-1,n}\right)\Big]\frac{1}{2(\Delta x)^2} -$$

$$\left(2/\left(h_{m,n} + h_{m-1,n} + \delta^{3t}_{m,n} + \delta^{3t}_{m,n+1}\right)\right)\left[\left(\left(\left(h_{m,n} + h_{m-1,n} + h_{m-1,n-1} + h_{m,n-1}\right)/4\right) +\right.\right.$$

$$\left.\delta^{3t}_{m,n}\right)^2 \alpha \left(V^{2t}_{m,n-1} + V^{2t}_{m,n}\right)\left(V^{2t}_{m,n-1} - V^{2t}_{m,n}\right) - \left(\left(\left(h_{m-1,n} + h_{m,n} + h_{m-1,n+1} +\right.\right.\right.$$

$$\left.\left.\left.h_{m,n+1}\right)/4\right) + \delta^{3t}_{m,n+1}\right)^2 \alpha \left(V^{2t}_{m,n} + V^{2t}_{m,n+1}\right)\left(V^{2t}_{m,n} - V^{2t}_{m,n+1}\right)\Big]\frac{1}{2(\Delta y)^2} = 0.$$

3.4

Mass Balance Equation

Remembering that U and δ for the x direction at time $(2k+1)\Delta t$ are known before S is calculated, the following results for the mass balance equation in the x direction are derived

$$
\begin{aligned}
&\Big[S'^{3t}_{m,n}\big((h_{m,n}+h_{m,n-1}+h_{m-1,n-1}+h_{m-1,n})/4\big)+\delta^{3t}_{m,n}\Big) - \\
&\quad S'^{2t}_{m,n}\big((h_{m,n}+h_{m,n-1}+h_{m-1,n-1}+h_{m-1,n})/4\big)+\delta^{2t}_{m,n}\Big)\Big]\frac{1}{\Delta t} + \\
&\Big[(h_{m,n}+h_{m,n-1}+\delta^{2t}_{m+1,n}+\delta^{2t}_{m,n})\, U^{3t}_{m,n}\,(S'^{3t}_{m+1,n}+S'^{3t}_{m,n}) - \\
&\quad (h_{m-1,n}+h_{m-1,n-1}+\delta^{2t}_{m-1,n}+\delta^{2t}_{m,n})\, U^{3t}_{m-1,n}\,(S'^{3t}_{m,n}+S'^{3t}_{m-1,n})\Big]\frac{1}{4\Delta x} + \\
&\Big[(h_{m,n-1}+h_{m-1,n-1}+\delta^{2t}_{m,n}+\delta^{2t}_{m,n-1})\, V^{2t}_{m,n-1}\,(S'^{2t}_{m,n}+S'^{2t}_{m,n-1}) - \\
&\quad (h_{m,n}+h_{m-1,n}+\delta^{2t}_{m,n}+\delta^{2t}_{m,n+1})\, V^{2t}_{m,n}\,(S'^{2t}_{m,n+1}+S'^{2t}_{m,n})\Big]\frac{1}{4\Delta y} - \\
&\Big[(h_{m,n}+h_{m,n-1}+\delta^{3t}_{m+1,n}+\delta^{3t}_{m,n})\, D^{3t}_{x_{m,n}}\,(S'^{3t}_{m+1,n}-S'^{3t}_{m,n}) - \\
&\quad (h_{m-1,n}+h_{m-1,n-1}+\delta^{3t}_{m-1,n}+\delta^{3t}_{m,n})\, D^{3t}_{x_{m-1,n}}\,(S'^{3t}_{m,n}-S'^{3t}_{m-1,n})\Big]\frac{1}{2(\Delta x)^2} - \\
&\Big[(h_{m-1,n-1}+h_{m,n-1}+\delta^{2t}_{m,n}+\delta^{2t}_{m,n-1})\, D^{2t}_{y_{m,n-1}}\,(S'^{2t}_{m,n-1}-S'^{2t}_{m,n}) - \\
&\quad (h_{m,n}+h_{m-1,n}+\delta^{2t}_{m,n+1}+\delta^{2t}_{m,n})\, D^{2t}_{y_{m,n}}\,(S'^{2t}_{m,n}-S'^{2t}_{m,n+1})\Big]\frac{1}{2(\Delta y)^2} = 0.
\end{aligned}
\tag{3.5}
$$

Likewise, the mass balance equation in the y direction becomes

$$
\begin{aligned}
&\Big[S^{4t}_{m,n} \big(\big(h_{m,n} + h_{m,n-1} + h_{m-1,n-1} + h_{m-1,n} \big) / 4 \big) + \delta^{4t}_{m,n} \big) - \\
&S^{3t}_{m,n} \big(\big(h_{m,n} + h_{m,n-1} + h_{m-1,n-1} + h_{m-1,n} \big) / 4 \big) + \delta^{3t}_{m,n} \big) \Big] \frac{1}{\Delta t} + \\
&\Big[\big(h_{m,n} + h_{m,n-1} + \delta^{3t}_{m+1,n} + \delta^{3t}_{m,n} \big) U^{3t}_{m,n} \big(S^{3t}_{m+1,n} + S^{3t}_{m,n} \big) - \\
&\big(h_{m-1,n} + h_{m-1,n-1} + \delta^{3t}_{m-1,n} + \delta^{3t}_{m,n} \big) U^{3t}_{m-1,n} \big(S^{3t}_{m,n} + S^{3t}_{m-1,n} \big) \Big] \frac{1}{4\Delta x} + \\
&\Big[\big(h_{m,n-1} + h_{m-1,n-1} + \delta^{3t}_{m,n} + \delta^{3t}_{m,n-1} \big) V^{4t}_{m,n-1} \big(S^{4t}_{m,n} + S^{4t}_{m,n-1} \big) - \\
&\big(h_{m,n} + h_{m-1,n} + \delta^{3t}_{m,n} + \delta^{3t}_{m,n+1} \big) V^{4t}_{m,n} \big(S^{4t}_{m,n+1} + S^{4t}_{m,n} \big) \Big] \frac{1}{4\Delta y} - \\
&\Big[\big(h_{m,n} + h_{m,n-1} + \delta^{3t}_{m+1,n} + \delta^{3t}_{m,n} \big) D^{3t}_{x_{m,n}} \big(S^{3t}_{m+1,n} - S^{3t}_{m,n} \big) - \\
&\big(h_{m-1,n} + h_{m-1,n-1} + \delta^{3t}_{m,n} + \delta^{3t}_{m-1,n} \big) D^{3t}_{x_{m-1,n}} \big(S^{3t}_{m,n} - S^{3t}_{m-1,n} \big) \frac{1}{2(\Delta x)^2} - \\
&\Big[\big(h_{m,n-1} + h_{m-1,n-2} + \delta^{4t}_{m,n} + \delta^{4t}_{m,n-1} \big) D^{4t}_{y_{m,n-1}} \big(S^{4t}_{m,n-1} - S^{4t}_{m,n} \big) - \\
&\big(h_{m,n} + h_{m-1,n} + \delta^{4t}_{m,n+1} + \delta^{4t}_{m,n} \big) D^{4t}_{y_{m,n}} \big(S^{4t}_{m,n} - S^{4t}_{m,n+1} \big) \Big] \frac{1}{2(\Delta y)^2} = 0. \qquad 3.6
\end{aligned}
$$

CHAPTER IV

METHOD OF SOLUTION FOR THE UNKNOWNS OF U, V, δ, AND S

Basic Concepts

Starting Values - Values of velocity, tidal height, and salinity must be specified at all computational points on the grid at time t = 0 (initial conditions). Thereafter, at the advanced time step the values of U, V, δ, and S need only be specified on the boundaries of the grid when needed to predict their values in the interior at the same time step. These boundary values can be specified on either an open or closed boundary and can be grouped as described below.

Boundaries - Closed boundaries are the easiest to work with from a computational standpoint because here velocities and mass fluxes become zero, requiring no field data, and the only dynamic variable, tidal height, can be easily measured with tide gauges or calculated from tables. Open boundaries present more serious difficulties in the sense that more detailed data, particularly if time-dependent models are used, are needed, requiring more complex numerical and computational techniques. Thus, it is desirable to have all closed boundaries; but, for a coastal situation, this is impossible, and the physical layout sometimes requires as many as three open boundaries.

To show how boundaries are used in this thesis, Figure 4 was drawn to illustrate a simple coastal situation of an estuary or river emptying onto a continental shelf. The closed boundaries are drawn through points that include the depth data points (0) and always one of the velocity data points (| or -).

The open boundary can be drawn through points representing either tidal height (+) or velocity (| or -) so that one of these variables must be defined on the boundary in order to calculate tidal heights and velocities in the interior of the grid (boundary value problem). If salinity is being calculated, it must be defined on all four boundaries (+) in order to calculate values in the interior of the grid at the advanced time step. If two open boundaries in the same direction exist, then a combination of boundary conditions can be used, i.e., tidal height or velocity on both boundaries or a combination of each. For the situation in this thesis, two of the above combinations were tried: tidal height at both boundaries and tidal height and velocity, one on each boundary.

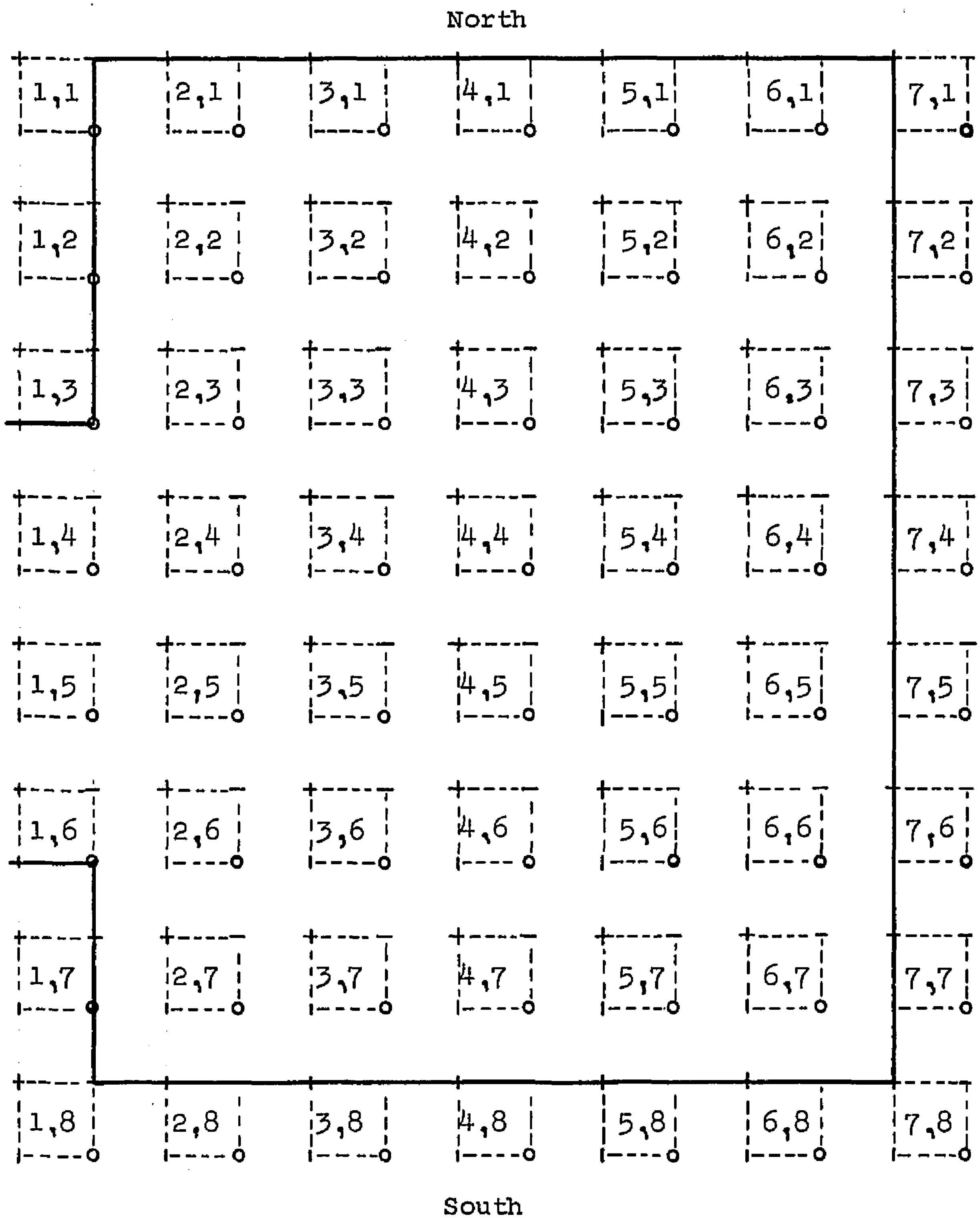

Figure 4

Illustration of
grid and boundary conditions

The reason for this choice was dictated by the availability of historical data for use with the model at a future date. The boundary condition chosen on the western side of the computational area was velocity since data were available from continuous current meter records at the Bay entrance and the realization that the investigation was to study the effect of fresh water runoff from the Bay. The boundary on the eastern side was chosen to be tidal height, since it was felt that this could be calculated accurately (Redfield (1958)). The northern boundary condition was chosen as either velocity, because of the availability of data and the weak southern flow, or tidal height. It was felt in the beginning that, if either of these boundaries were placed well above the Bay entrance, any error caused by the data would not affect the overall results and, more importantly, the boundary conditions would not be affected by the flux from the Bay mouth (this point will be discussed in the results). The southern boundary was chosen as tidal height because of the lack of good velocity data across the shelf in this region and the ease of estimating tidal height.

Upon the choice of the boundary conditions as stated above, the final finite difference equations must be solved so that the input of the boundary conditions will result in their solution giving values of U, V, δ, and S.

Recursion Equations

Grouping of Terms - The first step in solving for the unknown values of U, V, δ, and S in equations 3.1 through 3.6 is to group the resultant equation around the unknown values of δ, U, V, and S. In order to simplify the results of this step, the following shorthand notations common to all equations will be used:

$$\bar{h} = (h_{m,n} + h_{m,n-1} + h_{m-1,n-1} + h_{m-1,n})/4$$

$$H^{it}_{XF} = h_{m,n} + h_{m,n-1} + \delta^{it}_{m+1,n} + \delta^{it}_{m,n}$$

$$H^{it}_{XB} = h_{m-1,n} + h_{m-1,n-1} + \delta^{it}_{m-1,n} + \delta^{it}_{m,n}$$

$$H^{it}_{YF} = h_{m,n-1} + h_{m-1,n-1} + \delta^{it}_{m,n} + \delta^{it}_{m,n-1}$$

$$H^{it}_{YB} = h_{m,n} + h_{m-1,n} + \delta^{it}_{m,n} + \delta^{it}_{m,n+1}$$

$$\bar{U}^{it} = (U^{it}_{m,n+1} + U^{it}_{m,n} + U^{it}_{m-1,n+1} + U^{it}_{m-1,n})/4$$

$$\bar{V}^{it} = (V_{m+1,n} + V_{m+1,n-1} + V^{it}_{m,n-1} + V^{it}_{m,n})/4,$$

where it is the general notation for the time t, 2t, 3t, or 4t.

Using the notation in the continuity equation for the x direction (equation 3.1) yields the simplified form

$$A_m \delta^{3t}_{m,n} + B_m U^{3t}_{m,n} + C_m U^{3t}_{m-1,n} = D_m. \qquad 4.1$$

Since all unknowns are at the same time 3t and on the same row n, these notations can be dropped, giving

$$A_m \delta_m + B_m U_m + C_m U_{m-1} = D_m, \qquad 4.2$$

where

$$A_m = 1/\Delta t$$

$$B_m = (1/2\Delta L)\, H^{2t}_{XF}$$

$$C_m = -(1/2\Delta L)\, H^{2t}_{XB}$$

and

$$D_m = -\left[\left(-\delta^{2t}_{m,n}\right)\frac{1}{\Delta t} + \frac{1}{2\Delta L}\left(H^{2t}_{YF} V^{2t}_{m,n-1} - H^{2t}_{YB} V^{2t}_{m,n}\right)\right]$$

are constants which can be calculated from known information. ΔL is a general notation devoting grid spacing Δx and Δy (for this study $\Delta x = \Delta y$).

Using the same procedure for the momentum equation 3.3 yields

$$E_m U^{3t}_{m,n} + F_m \delta^{3t}_{m+1,n} - F_m \delta^{3t}_{m,n} = H_m. \qquad 4.3$$

Dropping the time and row notation as before, 4.3 becomes

$$E_m U_m + F_m \delta_{m+1} - F_m \delta_m = H_m \qquad 4.4$$

where

$$E_m = \frac{1}{2\Delta t} + \left(U^t_{m+1,n} - U^t_{m-1,n}\right)\frac{1}{2\Delta L} + \frac{g\left[\left(U^t_{m,n}\right)^2 + \left(\overline{V}^{2t}\right)^2\right]^{1/2}}{H^{2t}_{XF}\left[\left(C^{2t}_{m+1,n} + C^{2t}_{m,n}\right)/2\right]^2}$$

$$F_m = (g/2\Delta L)$$

and

$$H_m = -\Big\{(-1/2\Delta t)\,U^t_{m,n} + \left(U^t_{m,n-1} - U^t_{m,n+1}\right)\overline{V}^{2t}(1/2\Delta L) +$$

$$\left(\delta^t_{m+1,n} - \delta^t_{m,n}\right)(g/2\Delta L) + \left(\overline{\rho}^{2t}_{m+1,n} - \overline{\rho}^{2t}_{m,n}\right)\left(1/(\overline{\rho}^{2t}_{m+1,n} + \overline{\rho}^{2t}_{m,n})\right)H^{2t}_{XF}(g/2\Delta L) -$$

$$f\overline{V}^{2t} + \frac{g\,U^t_{m,n}\left[(U^t_{m,n})^2 + (\overline{V}^{2t})^2\right]^{1/2}}{H^{2t}_{XF}\left[(C^{2t}_{m+1,n} + C^{2t}_{m,n})/2\right]^2} - \left(4\,\tau^s_y/(\overline{\rho}^{2t}_{m+1,n} + \overline{\rho}^{2t}_{m,n})\,H^{2t}_{XF}\right) -$$

$$(2/H^{2t}_{XF})\Big[\Big(\Big(\Big(h_{m,n-1} + h_{m+1,n-1} + h_{m,n} + h_{m+1,n}\Big)/4\Big) + \delta^{2t}_{m+1,n}\Big)^2$$

$$\alpha\left(U^t_{m,n} + U^t_{m+1,n}\right)\left(U^t_{m+1,n} - U^t_{m,n}\right) - \left(\overline{h} + \delta^{2t}_{m,n}\right)^2\alpha\Big(U^t_{m,n} +$$

$$U^t_{m-1,n}\Big)\left(U^t_{m,n} - U^t_{m-1,n}\right)\Big]\left(1/2(\Delta L)^2\right) - (2/H^{2t}_{XF})\Big[\Big(\Big(\Big(\delta^{2t}_{m,n-1} + \delta^{2t}_{m+1,n} +$$

$$\delta^{2t}_{m,n} + \delta^{2t}_{m+1,n-1}\Big)/4\Big) + h_{m,n-1}\Big)^2\alpha\left(V^{2t}_{m,n-1} + V^{2t}_{m+1,n-1}\right)\Big(U^t_{m,n-1} -$$

$$U^t_{m,n}\Big) - \Big(\Big(\Big(\delta^{2t}_{m,n} + \delta^{2t}_{m+1,n} + \delta^{2t}_{m,n+1} + \delta^{2t}_{m+1,n+1}\Big)/4\Big) + h_{m,n}\Big)^2$$

$$\alpha\left(V^{2t}_{m,n} + V^{2t}_{m+1,n}\right)\left(U^t_{m,n} - U^t_{m,n+1}\right)\Big]\left(1/2(\Delta L)^2\right)\Big\}$$

are constants which can be calculated from known information.

Likewise, for the mass balance equation 3.5, simplifying and grouping terms yields

$$A'_m \delta_{m-1} + B'_m \delta_m + C'_m \delta_{m+1} = D'_m \,, \qquad 4.5$$

where

$$A'_m = -\left[\left(H^{2t}_{XB} \; U^{3t}_{m-1,n} \right) \left(1/4\Delta L \right) + \left(H^{3t}_{XB} \; D^{3t}_{X_{m-1,n}} \right) \left(1/2(\Delta L)^2 \right) \right]$$

$$B'_m = (1/\Delta t)\left(\bar{h} + \delta^{3t}_{m,n} \right) + \left(H^{2t}_{XF} \, U^{3t}_{m,n} - H^{2t}_{XB} \, U^{3t}_{m-1,n} \right)\left(1/4\Delta L \right) +$$

$$\left(H^{3t}_{XF} \, D^{3t}_{X_{m,n}} + H^{3t}_{XB} \, D^{3t}_{X_{m-1,n}} \right)\left(1/2(\Delta L)^2 \right)$$

$$C'_m = \left(H^{2t}_{XF} \; U^{3t}_{m,n} \right)\left(1/4\Delta L \right) - \left(H^{3t}_{XF} \; D^{3t}_{X_{m,n}} \right)\left(1/2(\Delta L)^2 \right)$$

and

$$D'_m = -\left\{ -\left(\bar{h} + \delta^{2t}_{m,n} \right) \delta'^{2t}_{m,n} \left(1/\Delta t \right) + \left[H^{2t}_{YF} \, V^{2t}_{m,n-1} \left(\delta'^{2t}_{m,n-1} + \delta'^{2t}_{m,n} \right) - \right. \right.$$

$$\left. H^{2t}_{YB} \, V^{2t}_{m,n} \left(\delta'^{2t}_{m,n} + \delta'^{2t}_{m,n+1} \right) \right] \left(1/4\Delta L \right) - \left[H^{2t}_{YF} \, D^{2t}_{Y_{m,n-1}} \left(\delta'^{2t}_{m,n-1} - \delta'^{2t}_{m,n} \right) - \right.$$

$$\left. \left. H^{2t}_{YB} \, D^{2t}_{Y_{m,n}} \left(\delta'^{2t}_{m,n} - \delta'^{2t}_{m,n+1} \right) \right] \left(1/2(\Delta L)^2 \right) \right\}$$

are also constants which can be calculated.

Duplicating the same procedure for the y direction gives for the continuity equation

$$A_n \delta_n + B_n V_{n-1} + C_n V_n = D_n \,, \qquad 4.6$$

where

$$A_n = A_m = (1/\Delta t)$$

$$B_n = (1/2\Delta L)\, H_{YF}^{3t}$$

$$C_n = -(1/2\Delta L)\, H_{YB}^{3t}$$

and

$$D_n = -\left\{ (1/\Delta t)(-\delta_{m,n}^{3t}) + (1/2\Delta L)(H_{XF}^{3t}\, U_{m,n}^{3t} - H_{XB}^{3t}\, U_{m-1,n}^{3t}) \right\}$$

are constants as for the y direction. The momentum equation 3.4 becomes

$$E_n V_n + F_n \delta_n - F_n \delta_{n+1} = H_n , \qquad 4.7$$

where

$$E_n = (1/2\Delta t) + (V_{m,n-1} - V_{m,n+1})(1/2\Delta L) + \frac{g\left[(V_{m,n}^{2t})^2 + (U^{3t})^2\right]^{1/2}}{H_{YB}^{3t}\left[(C_{m,n+1}^{3t} + C_{m,n}^{3t})/2\right]^2}$$

$$F_n = F_m = (g/2\Delta L)$$

and

$$H_n = -\{(1/2\Delta t)(-V^{2t}_{m,n}) + (\overline{U}^{3t})(V^{2t}_{m+1,n} - V^{2t}_{m-1,n})(1/2\Delta L) +$$

$$(\delta^{2t}_{m,n} - \delta^{2t}_{m,n+1})(g/2\Delta L) + (\overline{\rho}^{3t}_{m,n} - \overline{\rho}^{3t}_{m,n+1})(1/(\overline{\rho}^{3t}_{m,n+1} + \overline{\rho}^{3t}_{m,n}))\, H^{3t}_{YF}(g/2\Delta L) +$$

$$f(\overline{U}^{3t}) + \frac{g\, V^{2t}_{m,n}\left[(V^{2t}_{m,n})^2 + (\overline{U}^{3t})^2\right]^{1/2}}{H^{3t}_{YB}\left[(C^{3t}_{m,n+1} + C^{3t}_{m,n})/2\right]^2} - (4\, \tau^s_y/(\overline{\rho}^{3t}_{m,n+1} + \overline{\rho}^{3t}_{m,n})\, H^{3t}_{YB}) -$$

$$(2/H^{3t}_{YB})[(((\delta^{3t}_{m,n} + \delta^{3t}_{m+1,n} + \delta^{3t}_{m,n+1} + \delta^{3t}_{m+1,n+1})/4) + h_{m,n})^2 \alpha (U^{3t}_{m,n} +$$

$$U^{3t}_{m,n+1})(V^{2t}_{m+1,n} - V^{2t}_{m,n}) - (((\delta^{3t}_{m,n} + \delta^{3t}_{m,n+1} + \delta^{3t}_{m-1,n+1} + \delta^{3t}_{m-1,n})/4) +$$

$$h_{m-1,n})^2 \alpha (U^{3t}_{m-1,n} + U^{3t}_{m-1,n+1})(V^{2t}_{m,n} - V^{2t}_{m-1,n})](1/2(\Delta L)^2) - (2/H^{3t}_{YB})[(\overline{h} +$$

$$\delta^{3t}_{m,n})^2 \alpha (V^{2t}_{m,n-1} + V^{2t}_{m,n})(V^{2t}_{m,n-1} - V^{2t}_{m,n}) - (((h_{m-1,n} + h_{m,n} + h_{m-1,n+1} +$$

$$h_{m,n+1})/4) + \delta^{3t}_{m,n+1})^2 \alpha (V^{2t}_{m,n} + V^{2t}_{m,n+1})(V^{2t}_{m,n} - V^{2t}_{m,n+1})](1/2(\Delta L)^2)\}$$

are constants as for the y direction.

Finally, the mass balance equation for the y direction yields

$$A'_n \delta_{n-1} + B'_n \delta_n + C'_n \delta_{n+1} = D'_n , \qquad 4.8$$

where

$$A_n' = (H^{3t}_{YF}\, V^{4t}_{m,n-1})(1/4\Delta L) - (H^{4t}_{YF}\, D^{4t}_{Y_{m,n-1}})(1/2(\Delta L)^2)$$

$$B'_m = (1/\Delta t)(\bar{h} + \delta^{4t}_{m,m}) + (H^{3t}_{YF} V^{4t}_{m,m-1} - H^{3t}_{YB} V^{4t}_{m,m})(1/4\Delta L) +$$

$$(H^{4t}_{YF} D^{4t}_{Y_{m,m-1}} - H^{4t}_{YB} D^{4t}_{Y_{m,m}})(1/2(\Delta L)^2)$$

$$C'_m = -(H^{3t}_{YB} V^{4t}_{m,m})(1/4\Delta L) - (H^{4t}_{YB} D^{4t}_{Y_{m,m}})(1/2(\Delta L)^2)$$

and

$$D'_m = -\{-(\bar{h} + \delta^{3t}_{m,m})(1/\Delta t) + [H^{3t}_{XF} U^{3t}_{m,m}(\mathcal{S}'^{3t}_{m+1,m} + \mathcal{S}'^{3t}_{m,m}) -$$

$$H^{3t}_{XB} U^{3t}_{m-1,m}(\mathcal{S}'^{3t}_{m,m} + \mathcal{S}'^{3t}_{m-1,m})](1/4\Delta L) - [H^{3t}_{XF} D^{3t}_{X_{m,m}}(\mathcal{S}'^{3t}_{m+1,m} -$$

$$\mathcal{S}'^{3t}_{m,m}) - H^{3t}_{XB} D^{3t}_{X_{m-1,m}}(\mathcal{S}'^{3t}_{m,m} - \mathcal{S}'^{3t}_{m-1,m})](1/2(\Delta L)^2)\}$$

are constants as for the y direction.

Solution - The solution of the recursion equations 4.2, 4.4, and 4.5 through 4.8 is accomplished in the following manner: Starting with the continuity and momentum equations in the x direction (4.2 and 4.4), it can be seen that a total of four unknowns exist between these two equations, requiring two boundary conditions in order to be able to solve this set (A_m, B_m, C_m, D_m, E_m, F_m, and H_m are constants which can be calculated from known information). Recalling the previous discussion on boundary conditions, solutions of these equations are derived assuming a solution of the form

$$\delta_m + P_m U_m = Q_m \tag{4.9}$$

and

$$U_m + R_m \delta_{m+1} = T_m , \tag{4.10}$$

where P_m, Q_m, R_m, and T_m are constants to be defined.

Backstepping on 4.10 gives

$$U_{m-1} + R_{m-1} \delta_m = T_{m-1}$$

or

$$U_{m-1} = T_{m-1} - R_{m-1} \delta_m . \tag{4.11}$$

Substitution of 4.11 into 4.2 and grouping terms to come up with an equation like 4.9 gives the constants

$$P_m = \frac{B_m}{A_m - C_m R_{m-1}} \tag{4.12}$$

and

$$Q_m = \frac{D_m - C_m T_{m-1}}{A_m - C_m R_{m-1}} . \tag{4.13}$$

Rearranging 4.9 and substituting into 4.4 for δ_m and grouping terms to acquire an equation like 4.10 gives the constants

$$R_m = \frac{F_m}{E_m + P_m F_m} \tag{4.14}$$

and

$$T_m = \frac{H_m + F_m Q_m}{E_m + P_m F_m} . \tag{4.15}$$

Equations 4.12 through 4.15 are the four constants that are needed for use with 4.9 and 4.10 to calculate δ and U. To use these new constants at point m, values of the constants at the previous point m-1 are needed (4.12 and 4.13). Thus, some starting values are necessary before these equations can be used. If 4.2 is arranged in the form of 4.9, then the constants, for m = 2 only, are

$$P_m = \frac{B_m}{A_m} \qquad 4.16$$

and

$$Q_m = \frac{D_m - C_m U_{m-1}}{A_m}. \qquad 4.17$$

Since the boundary conditions are specified with velocity U (Figure 4) given for all time, 4.16 and 4.17 may be used to calculate P_2 and Q_2.

The procedure to calculate U and δ is as follows: Using the boundary conditions given at m = 1 for the velocity, Q_2 is calculated by 4.17 and P_2 by 4.16. Proceeding across the row (for the first half time step), the rest of the constants are calculated by 4.12 through 4.15. At $m = m_{max}-1$ calculations are terminated for the constants. The boundary conditions at the end of the row (δ in our case here) are used along with the constants at $m = m_{max}-1$ and 4.10 to calculate U at $m = m_{max}-1$. This value of U is then substituted into 4.9 to calculate δ at $m = m_{max}-1$. This value of δ along with the constants at $m = m_{max}-2$ is used to calculate U at $m = m_{max}-2$, etc until U is calculated at m = 2. Values of δ at m = 1 and U at m = m_{max} are then obtained by extrapolation, if needed, and all values for the row are completed and the next row is then ready to be calculated.

After U and δ have been calculated for all rows for time $(2k+1)\Delta t$, the value of S for all rows at the same time step must be calculated. Recalling the recursion equation 4.5, a solution of the type

$$S_m' + E_m' S_{m+1} = F_m' \qquad 4.18$$

is desired. Rearranging 4.5 in the form of 4.18 gives the constants (for m = 2 only)

$$E_m' = \frac{C_m'}{B_m'} \qquad 4.19$$

and

$$F_m' = D_m' - \frac{A_m' S_{m-1}'}{B_m'}, \qquad 4.20$$

which are the starting values for E_m' and F_m'. Since S_1 is given as a boundary condition, backstepping one space in 4.18, substituting in 4.15 for S_m-1, and grouping terms to come up with an equation like 4.18 gives the constants

$$E_m' = \frac{C_m'}{B_m' - A_m' E_{m-1}'} \qquad 4.21$$

and

$$F_m' = \frac{D_{m+1}' - A_{m+1} F_m'}{B_m' - A_m' E_{m-1}'}. \qquad 4.22$$

Since salinity is to be specified as a boundary condition on all four sides, the following procedure is used: Equations 4.19 and 4.20 are used for m = 2, using the values of salinity at m = 1 as a starting value. The results of this step are then used to start calculating the constants E_m' and F_m' (4.21 and 4.22) which are then calculated progressively until $m = m_{max}-1$ is reached. Then equation 4.18 is used along with these constants and boundary conditions to calculate the salinity in the reverse order as was done for δ and U.

The same procedure can be used to derive the recursion equations in the y direction (for either velocity or tidal height as a northern boundary condition), but it will not be repeated here. The results of the derivation of this type for V, δ and S are given below. The technique for calculation of V, δ and S with these equations is essentially the same as has been previously described.

Recursion equations for V and δ, y direction, are:

Starting equations for northern boundary

Velocity as a Boundary Condition	Tidal Height as a Boundary Condition
$P_2 = \dfrac{C_2}{A_2}$	$R_1 = -\dfrac{F_1}{E_1}$
$Q_2 = \dfrac{D_2 - B_2V_1}{A_2}$	$T_1 = \dfrac{H_1 - F_1\delta_1}{E_1}$

Constant equations

$$P_m = \frac{C_m}{A_m - B_m R_{m-1}}$$

$$Q_m = \frac{D_m - B_m T_{m-1}}{A_m - B_m R_{m-1}}$$

$$R_m = -\frac{F_m}{E_m - P_m F_m}$$

$$T_m = \frac{H_m - F_m Q_m}{E_m - P_m F_m} .$$

Recursion equations for S, y direction, are:

Starting equations

$$E_2' = \frac{C_2'}{B_2'}$$

$$F_2' = \frac{D_2' - A_2' S_1'}{B_2'} .$$

Constant equations

$$E_{m+1}' = \frac{C_{m+1}'}{B_{m+1}' - A_{m+1}' E_m'}$$

$$F_{m+1}' = \frac{D_{m+1}' - A_{m+1}' F_m'}{B_{m+1}' - A_{m+1}' E_m'} .$$

CHAPTER V

COMPUTER PROGRAM

General

The computer program for the computational scheme outlined in Chapter IV is called COASTAL MODEL and is written in Fortran IV for use on the Control Data Corporation (CDC) Model 6600 or 6700 computer. Both of CDC's scope 3.3 and 3.4 operating systems are compatible with the program. A core size of 75,000 octal is required, and a computation time of about 10 min is necessary for a 30 x 50 grid with 156 iterations covering two 12-hr tidal cycles. A table of equivalent notations between that used in the program and Chapters II through IV is given in Appendix B. Appendix C is a copy of the basic program which is not optimized and was used for Case I of the oscillating jet.

Main and Sub-programs

A general overall flow diagram of the program is given in Figure 5a with a more detailed illustration given in Figures 5b and 5c. It consists of a main driver program and five sub-programs. The main program handles input of

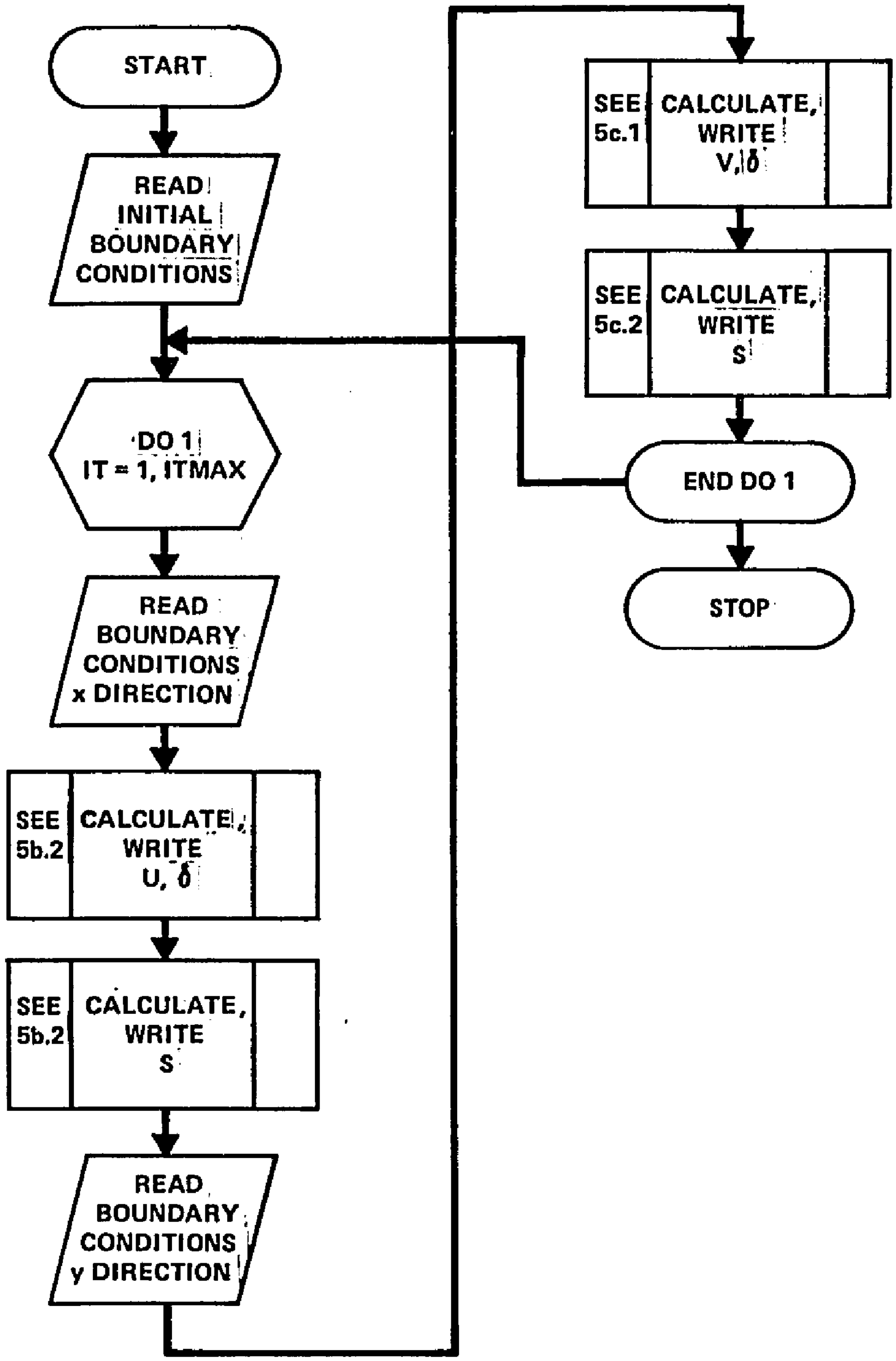

Figure 5a

Figure 5
Computer flow diagram for program COASTAL MODEL

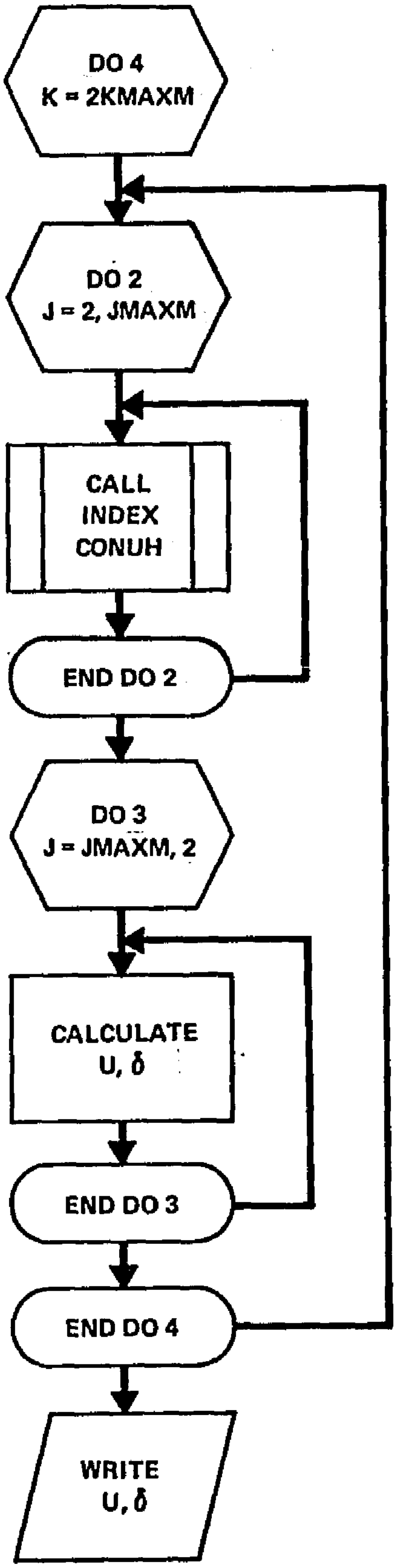

5b.1

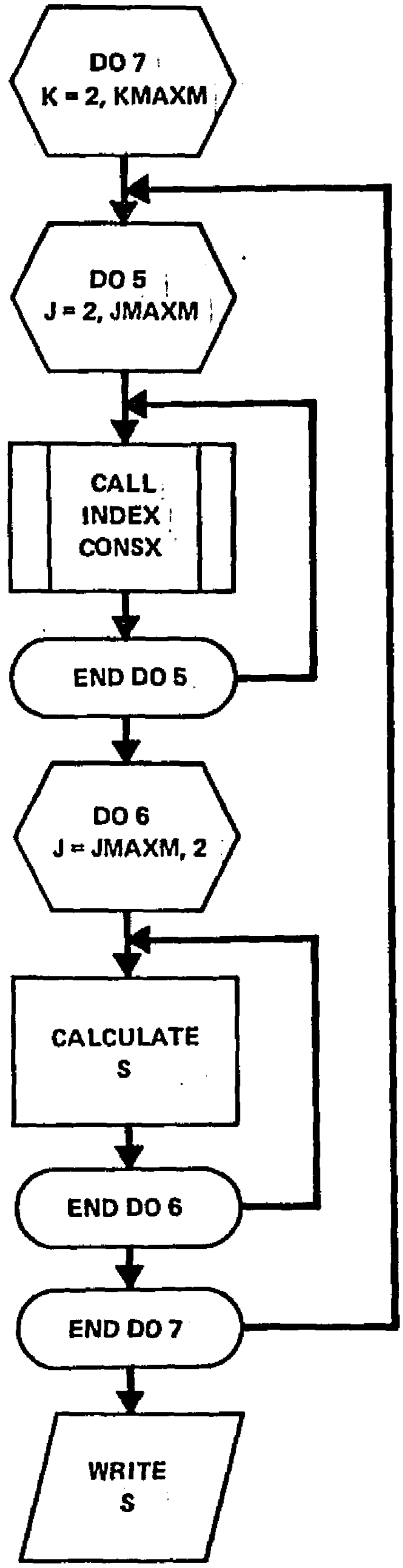

5b.2

Figure 5b

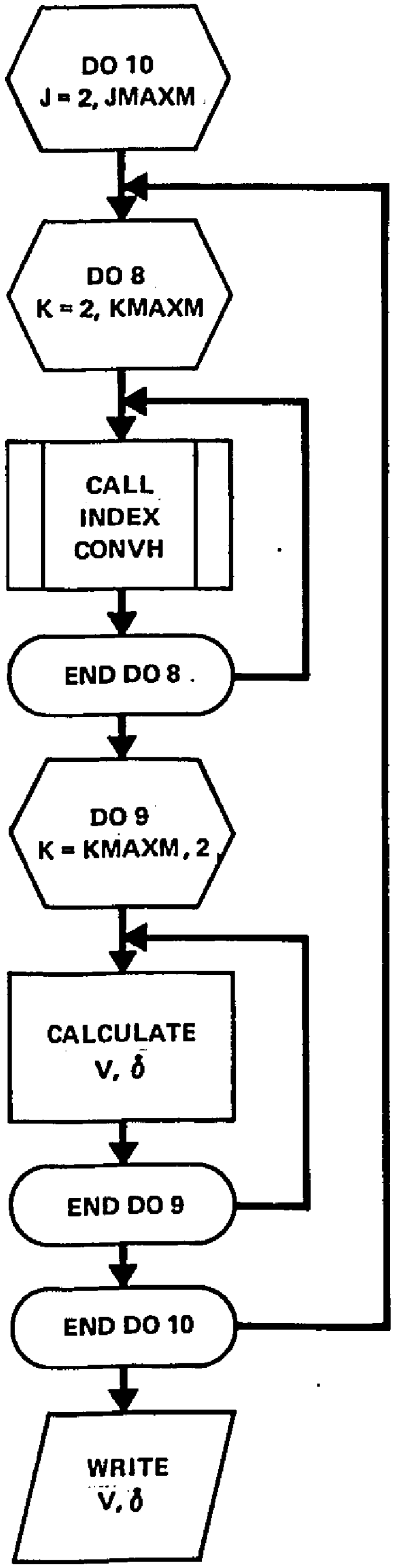

5c.1

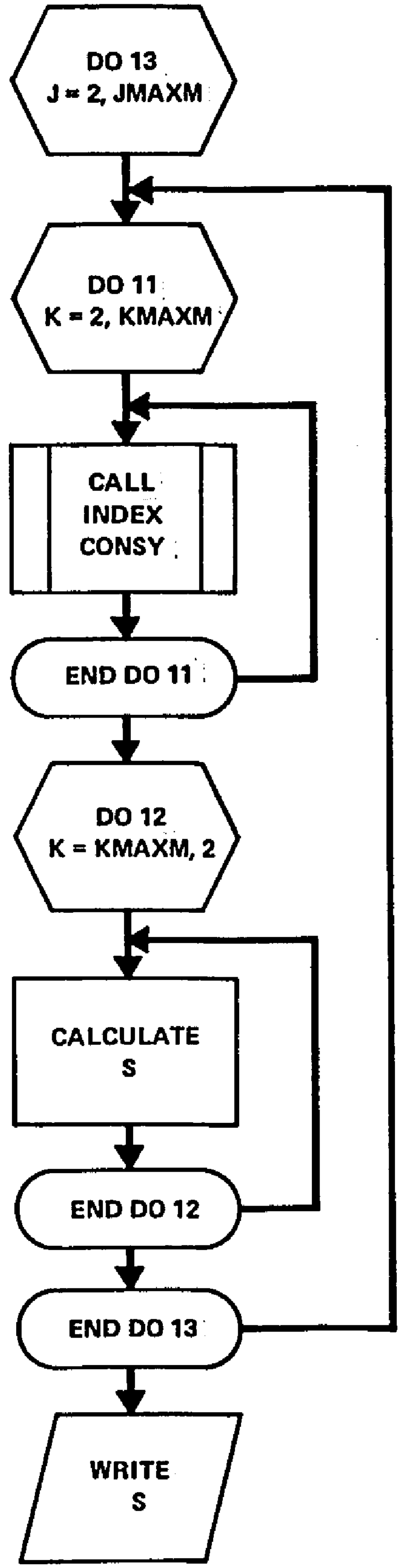

5c.2

Figure 5c

initial and boundary conditions, print and write statements, and controls the calculations through the proper sequence. The sub-programs and their functions are:

INDEX - calculates common parameters which are used repeatedly in the other sub-programs.

CONUH - calculates constants which are used to determine U and δ for the advanced time step from $2k\Delta t$ to $(2k+1)\Delta t$. Calculations are along x axis.

CONSX - calculates constants which are used to determine S for the advance time step from $2k\Delta t$ to $(2k+1)\Delta t$. Calculations are along x axis.

CONVH - calculates constants which are used to determine V and δ for the advanced time step from $(2k+1)\Delta t$ to $(2k+2)\Delta t$. Calculations are along y axis.

CONSY - calculates constants which are used to determine S for the advanced time step from $(2k+1)\Delta t$ to $(2k+2)\Delta t$. Calculations are along y axis.

Calculations were initiated by calling up the basic programs from disk, correcting, and compiling using CDC's optimum compiler. In executing the main program, data that were required but never changed, such as water depth h and gravitational acceleration g, were stored in the main program. Other information needed, such as grid spacing time step, wind stress, number of grid points in the x and y directions, and number of iterations, was read in from cards. Before starting the calculations of U and δ, initial and boundary conditions were either read in or calculated from the program.

Next, the sub-routines for INDEX and CONUH were called and executed, calculating along and m or x axis (J in computer notation) from $m = 2$ to $m = m_{max}-1$. U and δ were then calculated, moving from $m = m_{max}-1$ to $m = 2$.

This procedure was used for each row from $n = 2$ to $n_{max}-1$. Finally, values of U and δ were extrapolated linearly where needed to fill in the grid. Linear extrapolation was used because it was more accurate and provided less fluctuation at the boundary. The same procedure was followed for S, where the previously determined values of U and δ were used to calculate the constants in CONSX.

Calculations of V, δ, and S were performed in the same manner as described above, except that the time step was at $(2k+2)\Delta t$ and the constants were calculated along each column from $n = 2$ to $n_{max}-1$ using CONVH or CONSY. V and δ were then calculated in decreasing order until $n = 2$. This was repeated for each column from $m = 2$ to $m = m_{max}-1$. The salinity calculation was then performed in the same manner as described above.

Plot

The data resulting from COASTAL MODEL were stored as a printed format and on magnetic tape. Since the velocity data were not a vector but components of a vector, a program was devised to read U, V, and δ from the magnetic tape, compute a current vector, plot the vector, and contour the tidal height data. This was done by a program called MODPLOT on the CDC 6600 or 6700 computer. MODPLOT read the tape data generated by COASTAL MODEL, called up the proper Calcomp sub-routines, performed the calculations, and put all information on a separate tape which was then run on a Calcomp 936 plotted to generate the displays desired. The program MODPLOT is not in Appendix C.

The vector part of MODPLOT did not plot all the data available, only those from m = 1 to 15 and n = 15 to 37, i.e., the area centered around the Bay mouth. The program read the data desired, plotted a coastline, and calculated the vector centered at the + point of the computation grid. The technique of calculation consisted of taking the U and V components on either side of the + point, averaging to get a U and V at this point, and then calculating a vector.

Next, the tidal heights desired were read from the magnetic tape, and an in-house developed algorithm was used to contour the data. All tidal data points for the grid were used in this program.

CHAPTER VI

RESULTS AND DISCUSSION

Basic Concepts

Three physical situations were studied. The first was a tidal or long period wave reflecting from a wall. This situation was used to verify the accuracy and completeness of the finite difference formulations previously described and to correct any program problems.

The steady-state jet was used as an intermediate step between the wave reflection from a wall and an oscillating jet. This case was run to better understand the computational stability problem, determine techniques to handle open boundary conditions, compute data which could be directly compared to the steady-state jet data in the literature, and determine if there would be anything unique about this case which corresponds to time averaged flow for a river or estuary emptying onto a continental shelf.

The final situation represented a tidal estuary discharging onto a continental shelf. An oscillating jet was used to drive the flow and simulate a tide rather than having a tidal wave progressing shoreward and reacting with a steady jet. This allowed a simplification of boundary conditions by eliminating the need to try to determine the interrelationship between tidal and jet velocity at the Bay entrance.

The inputs and boundary conditions for each case are summarized in Table 1, and Figure 6 gives a physical picture of the computational domain and grid setup.

TABLE 1

EXPERIMENTAL PARAMETERS

	Reflection	Steady-State Jet	Oscillating Jet
Number of Grid Points			
x-direction	30	30	30
y-direction	50	50	50
Grid Spacing (ΔL), cm	179,640	359,280	359,280
Time Step (Δt), sec	150	300	300
Initial Conditions at t=0	U=0	U=0	U=0
	V=0	V=0	V=0
	δ=f(x)	δ=0	δ=f(y), or 0
Boundary Conditions for Grid			
Left Side	U=0, S=30.0	U=f(y)	U=f(t,y)
Right Side	δ=f(t), S=30.0	δ=0	δ=0,f(y)
Top	V=0, S=30.0	V=0,-4	δ=0,5,10
Bottom	δ=f(x,t), S=30.0	δ=0	δ=0
Chézy Coefficient, $cm^{1/2}$ sec^{-1}	0	400	400
Turbulent Eddy Viscosity Coefficient, cm^2 sec^{-1} (horizontal)	0	10^8	0
Coriolis Parameter (f), sec^{-1}	0	$8x10^{-5}$	$8x10^{-5}$
Bottom Slope	0	0	1/1354
Wind Stress (τ), gm cm^{-1} sec^{-2}	0	0	0,1.9
Depth, cm	1000	1000	f(x) 1000

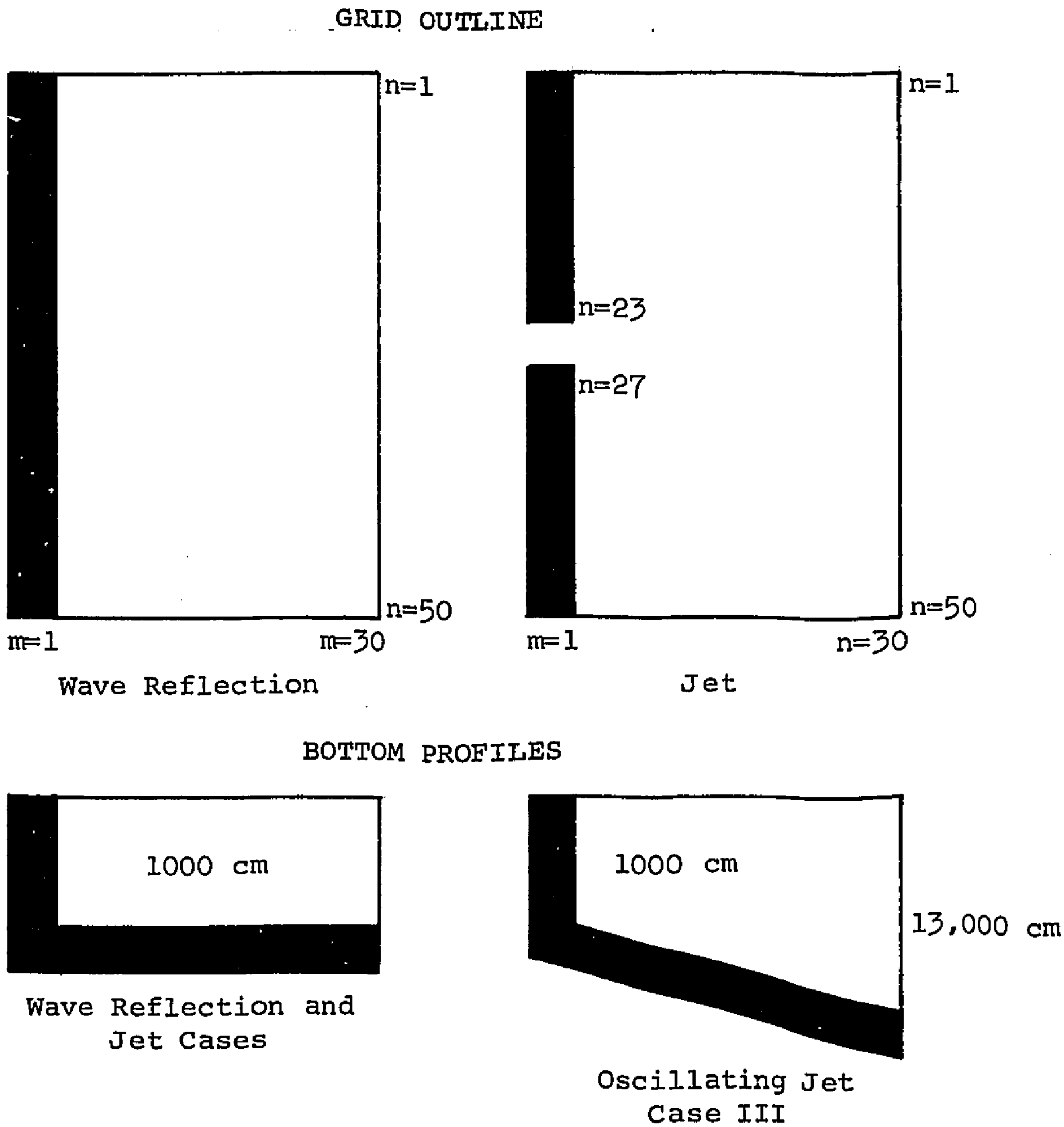

Figure 6

Grid outline and bottom profiles

Wave Reflection from a Wall

For this case a 30 x 50 point grid (30 points in the x direction, 50 points in the y direction) with a spacing $\Delta x = \Delta y = 179,640$ cm (0.97 nm) and a time step $\Delta t = 150$ sec was chosen. Water depth was 1000 cm, and no bottom friction, side friction, force of Coriolis, or wind stress was used. Initial conditions for time t = 0 were $U = V = 0$ and $\delta = f(x)$ or δ = constant. For the initial boundary condition δ, two cases were run: $\delta = 50$ cm (δ uniform over the grid) and $\delta = a_o \cos kx$ (tidal height decreasing as a function of distance from the coast). Results from all cases were the same, the only difference being the time required for the solution to reach a steady state. Results from the case $\delta = a_o \cos kx$ are discussed below. The wall was established on the left or western side of the grid, and the open sea constituted the northern, southern, and eastern boundaries, Figure 6. Boundary conditions for the x direction were velocity at the wall, $U = 0$, and tidal height in the open sea, $\delta = a_o \cos \sigma t \cos kx$, where $k = 2\pi/L$, $\sigma = 2\pi/T$, a_o = wave amplitude, and x is some fixed value. For the y direction velocity, $V = 0$ was used on the northern edge and tidal height, $\delta = a_o \cos \sigma t \cos kx$, on the southern edge. Salinity values of 30‰ were used on all boundaries. The value of 0.97 nm for the grid spacing was chosen so that the width of the Bay mouth (about 9.7 nm) would contain 10 grid points for the x velocity to be used later. A wave period of 12.42 hours (semi-diurnal tide) was used which gave a wave length of 4.4×10^7 cm for a depth of water of 1000 cm. The grid spacing was therefore adequate (Leendertse (1970)) to describe the wave and not generate stability problems. All runs were for a wave propagating in a direction normal to the wall.

Results of the computation are given in Figures 7, 8, and 9. Figure 7 is a plot of tidal height and velocity versus time for a point in the middle of the grid (m = 15, n = 25, Figure 6). Data from the calculations were plotted for only a half tidal cycle in order to amplify the results. The results of the computation are compared with the classical solution of a wave reflected from a wall (solid line, Figure 7) using equations from Ippen (1966) to calculate the data at the same point. It can be seen from this figure that there is good agreement between the theoretical and computed data.

Figure 8 is a plot of the theoretical and computed velocity profiles along the center of the computational grid (in an east-west direction, n = 25, m = 1,2,...,30) at maximum flood velocity. Agreement here is also good. Figure 9 is a plot of the theoretical and computed tidal

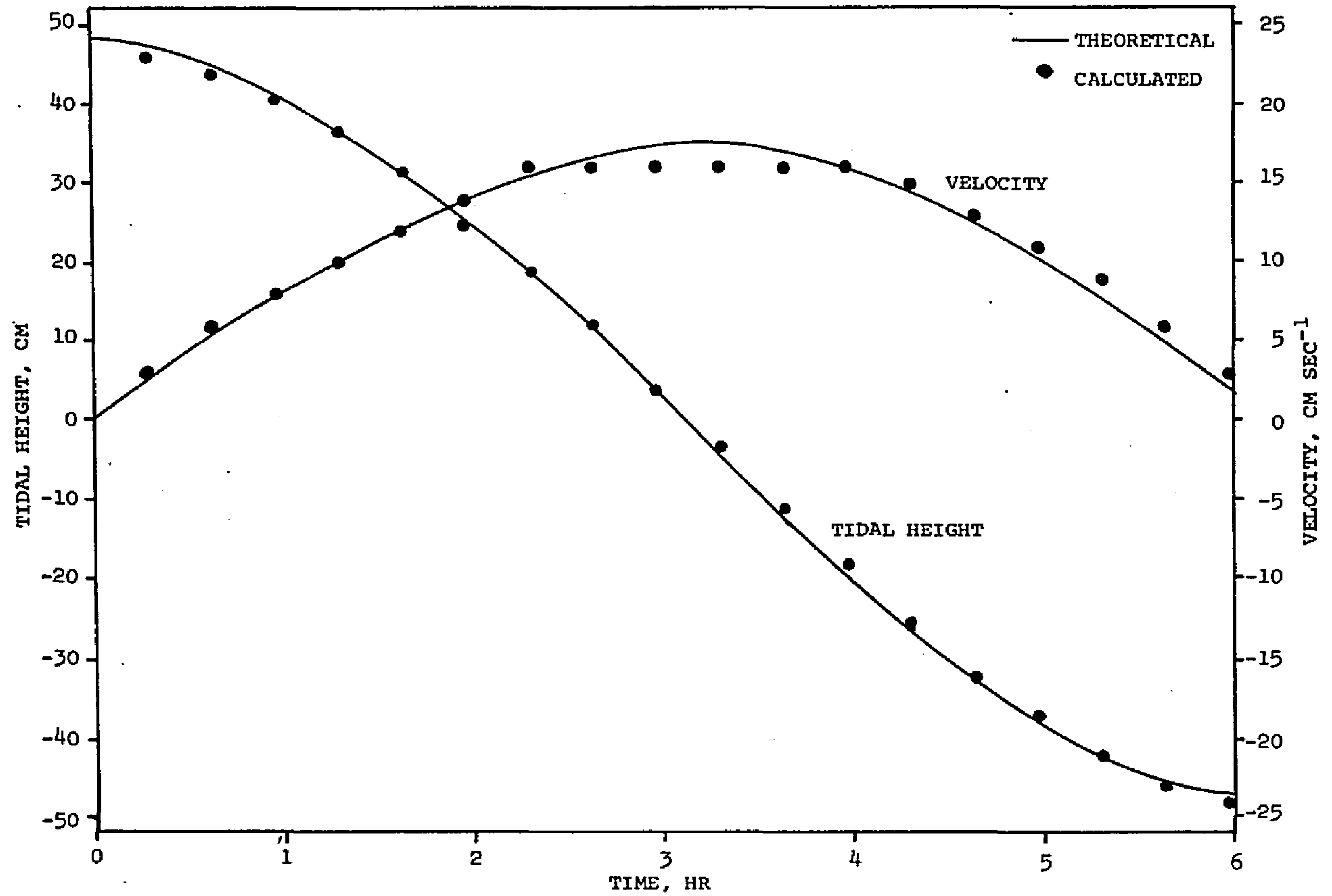

Figure 7
Tidal height as a function of time for grid point
(m = 15, n = 25)

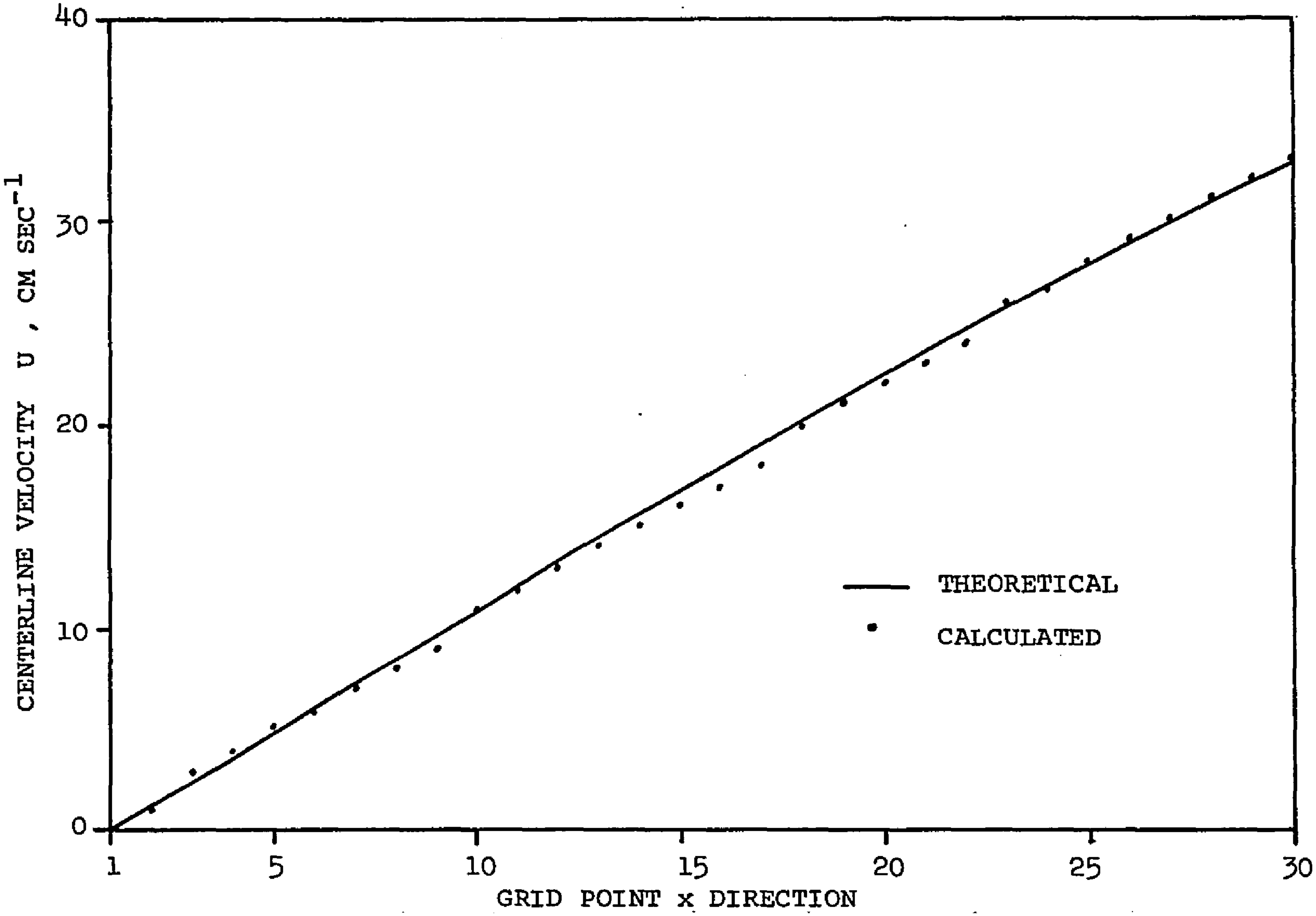

Figure 8 - Maximum theoretical and computed velocity as a function of distance in x direction, wave reflection

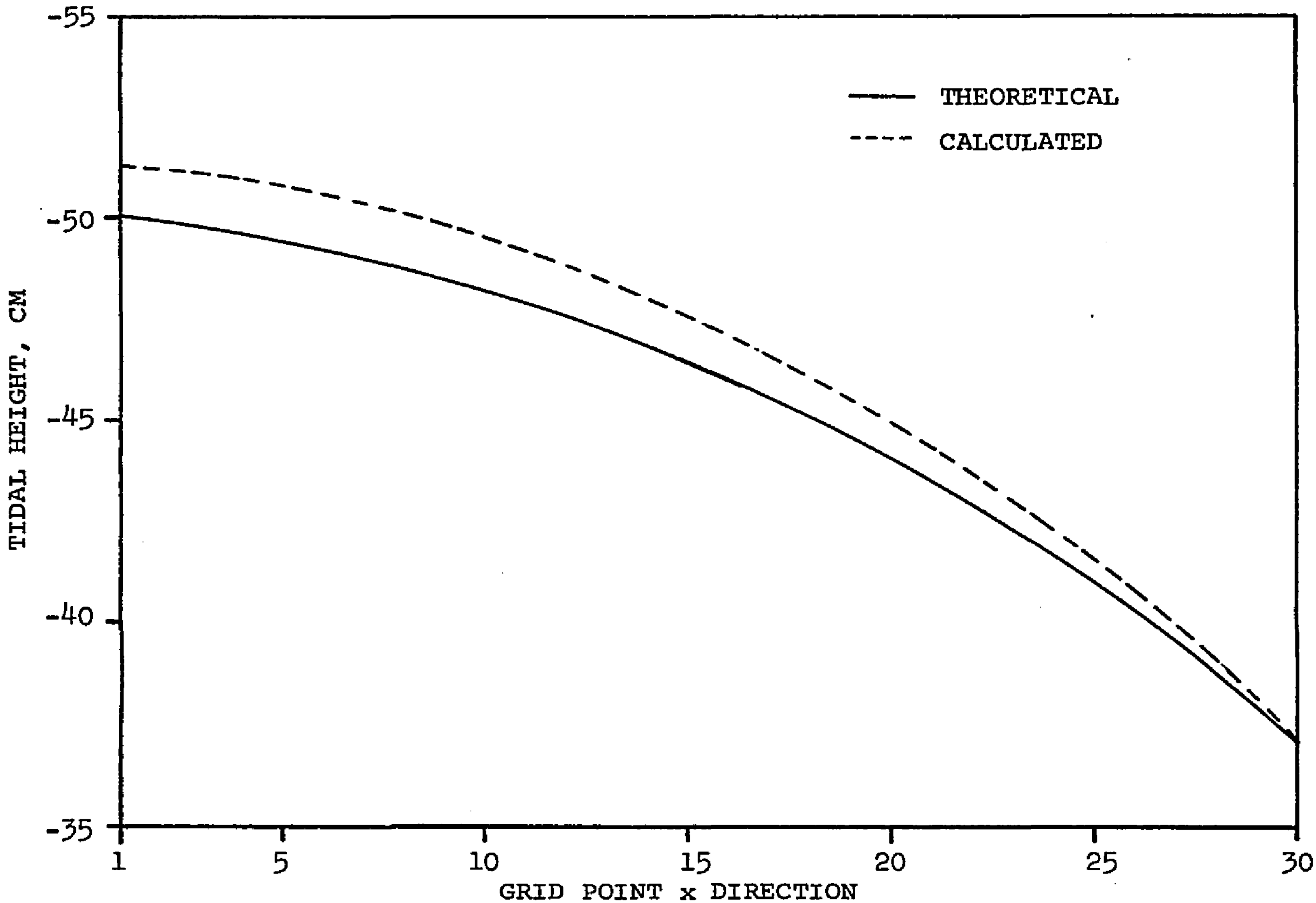

Figure 9 - Maximum theoretical and computed tidal height as a function of distance in x direction, wave reflection

height (below MSL) along the same centerline used in Figure 8. In Figure 9 there is a maximum difference of slightly more than 1 cm at the wall which decreases to 0 at the open eastern boundary.

Results from the salinity calculations were not plotted since the values remained constant at all times and at all points within the flow field.

For stability, the Courant-Friedricks-Lewy criteria for a two-dimensional explicit scheme $\Delta t = \Delta L/\sqrt{2gh}$ gives a value of 128.3 sec for a gird spacing of ΔL = 179,640 cm. The solutions were found to be stable with a half time step of Δt = 150 sec used here.

Steady-State Jet

General - For this physical situation a 30 x 50 point grid was used as before, but the grid spacing was increased to ΔL = 359,280 cm (approximately 2 nm). The Courant-Friedricks-Lewy criteria for this grid spacing gave Δt = 256 sec. A value of 300 sec for each half time step was chosen so that a total time step of Δt = 600 sec, or 10 min, covered a complete iteration. No stability problems arose with this particular time step and grid spacing. Salinity was not calculated since it was held constant over the grid for all cases. Holding the salinity constant generated a situation in which the density was homogeneous both vertically and horizontally. Water depth was 1000 cm, and no wind stress was assumed. Bottom friction was used in all cases with a Chézy coefficient of 400 $cm^{1/2}$ sec^{-1}. This Chézy coefficient corresponded to a Manning coefficient of 0.036 and is similar to those used by Leendertse (1971) and Dronkers (1964).

Initial conditions were $U = V = \delta = 0$. A coastline was established at the left side of the grid, with an opening representing a Bay mouth 17.9 km (~10 nm) wide centered in the middle of the coast at $n = 25$, Figure 6. Boundary conditions for the x direction were velocity at the coast, $U = 0$, except at the Bay opening or jet where $U = f(y)$ and

$\delta = 0$ on the eastern boundary. The jet started at $U = 0$ and built to a maximum in 16 iterations (160 min) and then remained steady for 10 iterations (100 min). The jet was given a parabolic profile with a maximum centerline velocity (velocity integrated with respect to depth) of 25 cm sec^{-1}. Boundary conditions for the y direction were velocity for the northern edge of the grid, $V = 0$, or a linear variation from 0 at the wall to a maximum of -4 cm sec^{-1} and tidal height $\delta = 0$ for the southern edge. Using velocity as an open boundary condition on the top of the grid created no problems because the boundary was far enough from the Bay mouth so no complications arose. If the northern (velocity) boundary was moved close to the Bay entrance, the boundary acted as a wall and there was a deflection of the outflow.

Four cases for the steady-state jet with bottom friction were run: Case I, steady-state jet as described above; Case II, steady-state jet with side friction; Case III, steady-state jet with Coriolis force; and Case IV, steady-state jet with an ambient velocity. Vector plots (velocity vectors) and tidal height contours are for a time of 260 min after starting when the jet has reached a steady state.

<u>Case I</u> - Figures 10 and 11 show the vector plots and tidal height contours for the steady-state jet. Four distinguishing features can be seen in the vector plot:

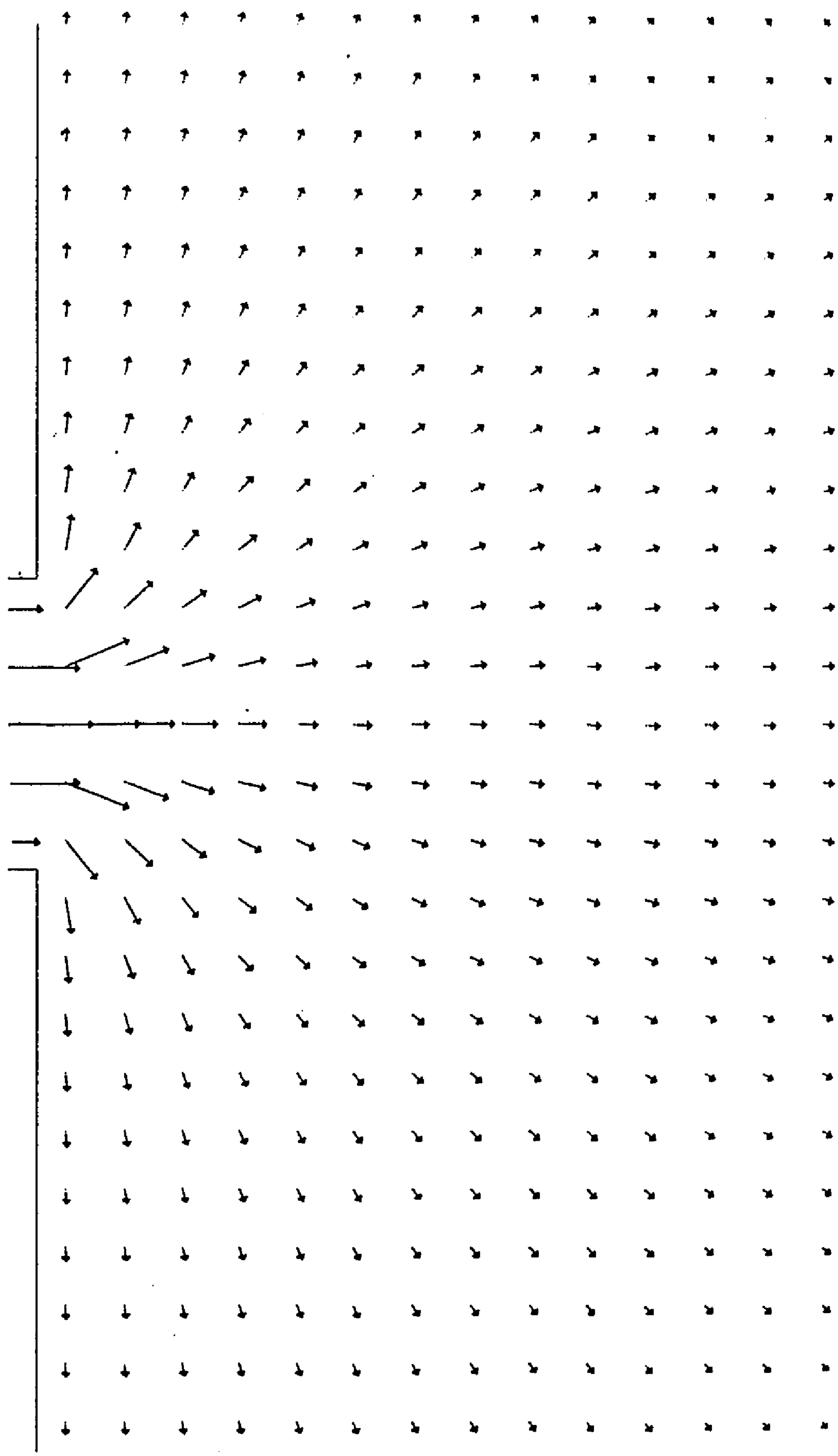

Figure 10 - Velocity vector plot, steady-state jet

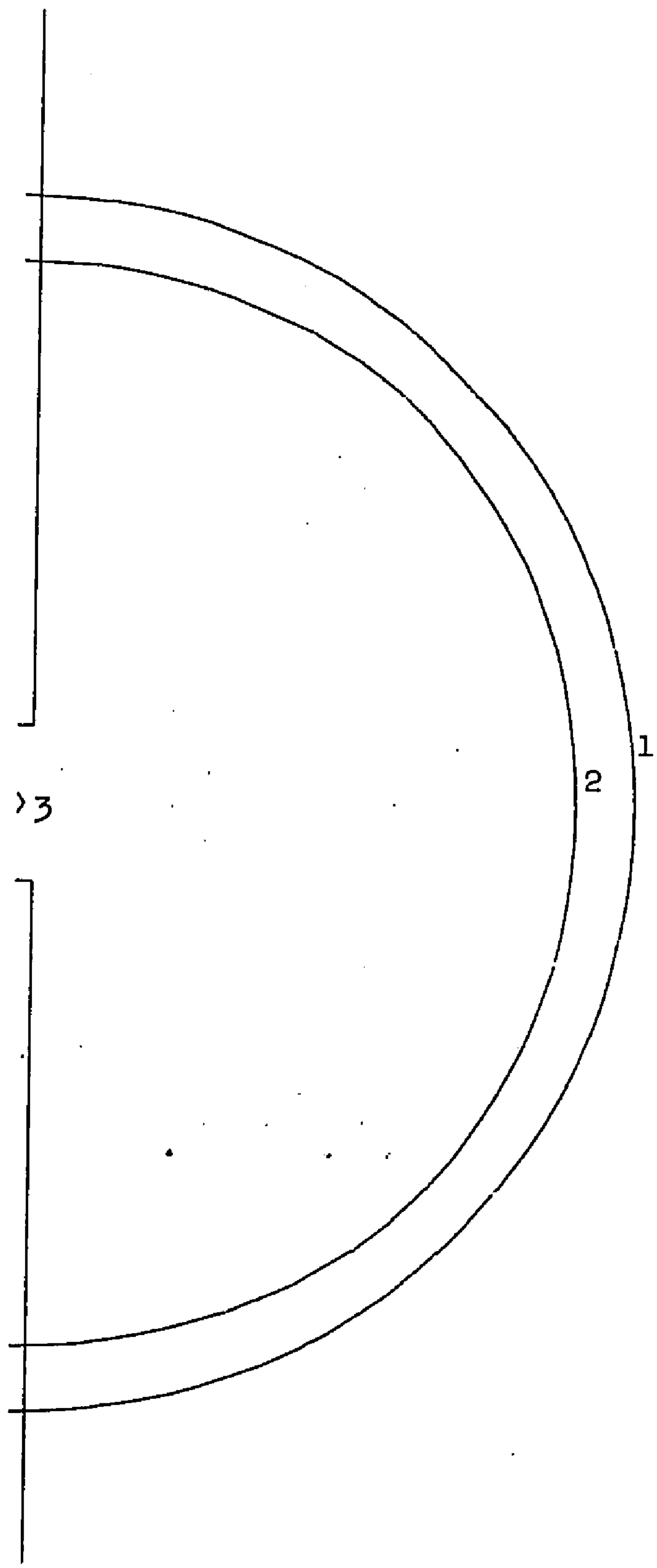

Figure 11 - Water level plot, steady-state jet, cm

first, the jet is dispersive (i.e., the velocity vectors diverge from the jet centerline) and not entraining (vectors converge toward the jet centerline); second, the centerline velocity U decreases sharply as a function of distance along the axis of the jet; third, there is a northern current along the coast above the jet and a southern current below it; and fourth, there are no eddies formed above or below the jet.

The dispersion of the jet is believed to be caused by a buildup of water (and therefore pressure gradient) around the Bay entrance and is shown by the plot of tidal height, Figure 11.[1] As the height of water above MSL is increased, a pressure gradient or head is generated in the x and y directions. This head causes the dispersion, since the water level at the boundaries, by virtue of the boundary conditions, does not go above datum (i.e., $\delta = 0$). Because of the above restriction, the water level inside the boundaries is an unknown and is allowed to fluctuate.

---

[1]In the derivations of Chapters II through IV, tidal height has been the term used to refer to the time-dependent level of the water above or below datum (MSL). In the steady-state case since there are no tides, the tidal height is really a water level (relative to mean sea level) that generates a pressure gradient and will be referred to as a water level in the following discussion.

The cause of the diverging flow in this case is similar to that reported by Bondar (1970) and Engelund and Pedersen (1973). Bondar (1970) reasoned that the river flow which was fresh and less dense was atop a more dense, saline wedge. This lens of less dense water created a hydraulic head, causing divergence or spreading of the flow of the surface layer. Bondar quotes angles of divergence of 40° or more for rivers emptying into the Black Sea and develops equations to predict the spread. Engelund and Pedersen (1973) take the same approach in studying the divergence of warm water jets emptying into a cooler body of water.

If the bottom friction is increased, the velocity in both the x and y directions decreases, causing the jet to shrink in size and the water level to increase, with the maximum increase at the Bay mouth. Figure 12 shows a plot of the centerline velocity U as a function of distance for three values of bottom friction. A decrease in C from 400 to 100 (increase in bottom friction) generated a small change in velocity at the same value of x/y, while a decrease in C from 100 to 5 caused a sharp change. Figure 12 indicates that bottom friction, while having some effect on the velocity, would have to be unreasonably large to cause a drastic change at a given point. Also, it shows

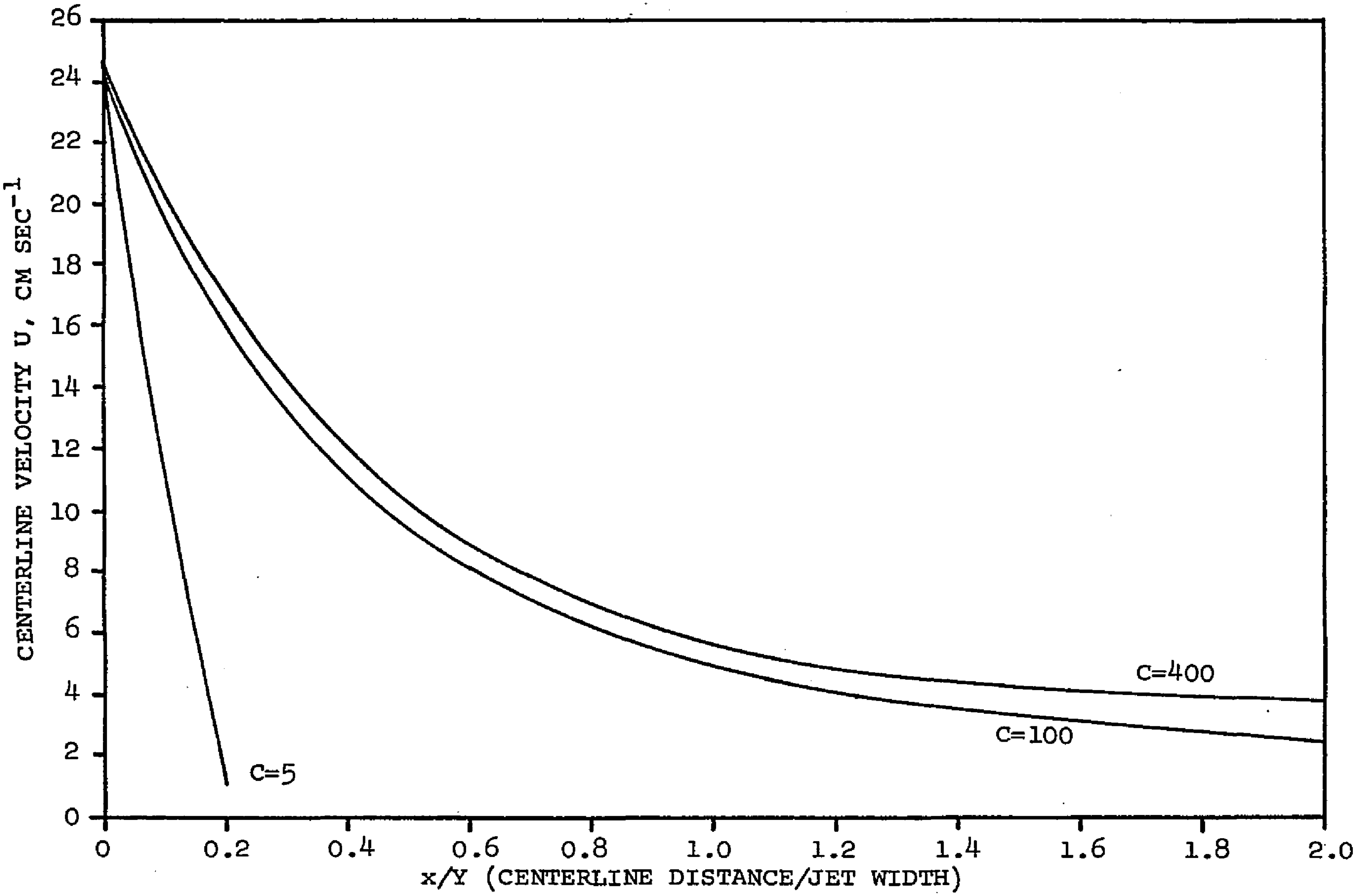

Figure 12 - Centerline velocity distribution resulting from different values of bottom friction, steady-state jet

that changes in C from 400 to 100 can cause the location (x/y) of velocities of 5 cm sec^{-1} or less to change rapidly. To try to understand how important friction is in this case, the jet was allowed to reach maximum velocity (25 cm sec^{-1}) after 160 min of buildup and was then cut off and the computations continued for 100 min. Upon termination of the jet, the remaining fluid that was in motion moved through the computational area, decreasing in velocity with time. The maximum positive velocity in the flow field as a function of time (after termination of the jet) is shown in Figure 13. The velocity decreases from a maximum of 25 cm sec^{-1} to 1/10 this amount in 100 min. By extrapolation (dashed line) velocities of 1 cm sec^{-1} should be reached in about 4 hr. This decrease in velocity suggests that bottom friction is dominant over rotation since the velocity decreases to near 0 in a time less than the inertial period for this latitude (19.9 hr).

Before comparing further the results of Case I with the classical plane jet, the results from Case II will be examined.

Case II - This case consisted of the steady-state jet used above, but with side as well as bottom friction. Here, α (equations 2.37 and 2.38) was given a value of 10,000, resulting in an eddy viscosity value of about

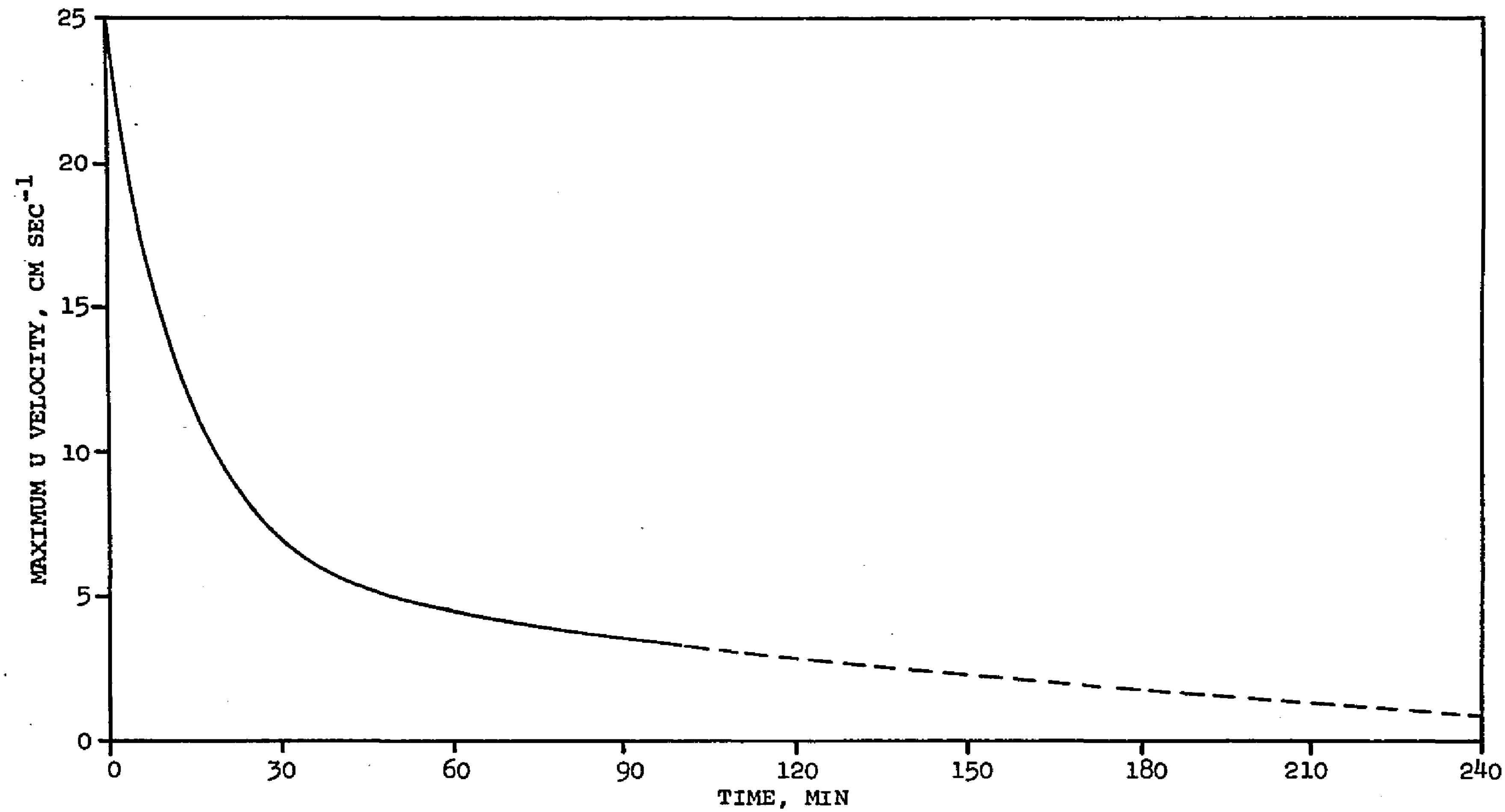

Figure 13
Decay time, steady-state jet

10^8 cm^2 sec^{-1}. Values in the literature vary from 10^5 to 10^8 (Sverdrup, et al (1941)). The results for the vector plot are shown in Figure 14. Four features are apparent: the jet is not as dispersive or does not spread laterally as much as in Case I; there is a decrease in the centerline velocity as a function of distance along the jet; the magnitude of velocity vectors adjacent to the coast above and below the jet, when compared to Case I, has decreased; and there are no eddies formed.

Figure 15 shows an x,y plot of the location of $U_o/2$ (half the centerline velocity) for Cases I and II. This figure verifies the decrease in lateral spread caused by the addition of side friction.

A comparison of the velocity as a function of distance in the x direction for Cases I and II is shown in Figure 16 by curves a and b (other parts of this figure will be discussed later). The velocity drops from a maximum of 25 cm sec^{-1} to less than 5 cm sec^{-1} in 30 km for both the bottom and side friction cases.

Bickley (1937) in his expansion of Schlichting's (1933) work derived the exact solution for the two-dimensional motion of an incompressible viscous fluid due to a side friction jet issuing from a long, narrow orifice. Albertson, et al (1950), summarized experimental data to determine

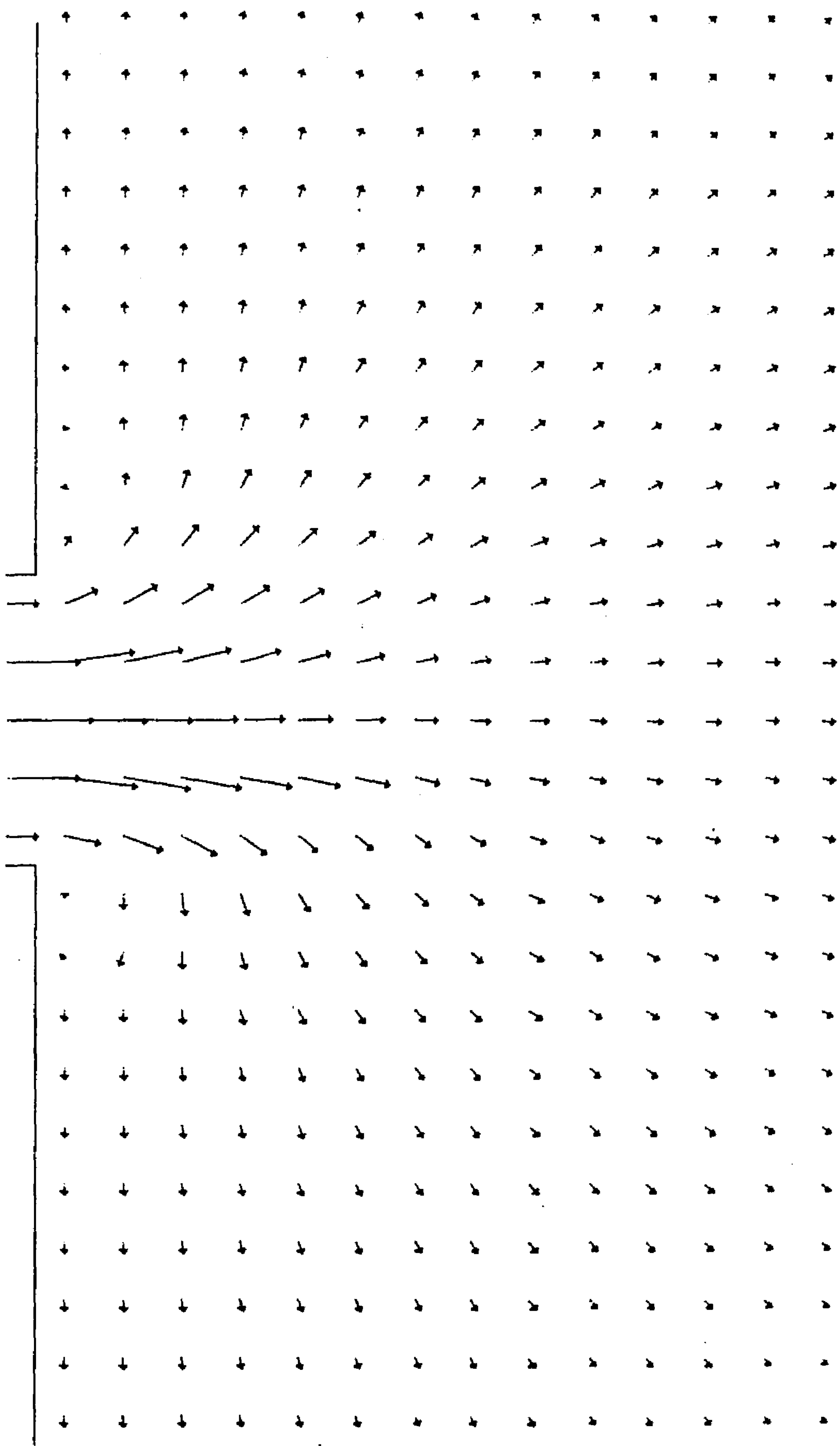

Figure 14 - Velocity vector plot
steady-state jet with side friction

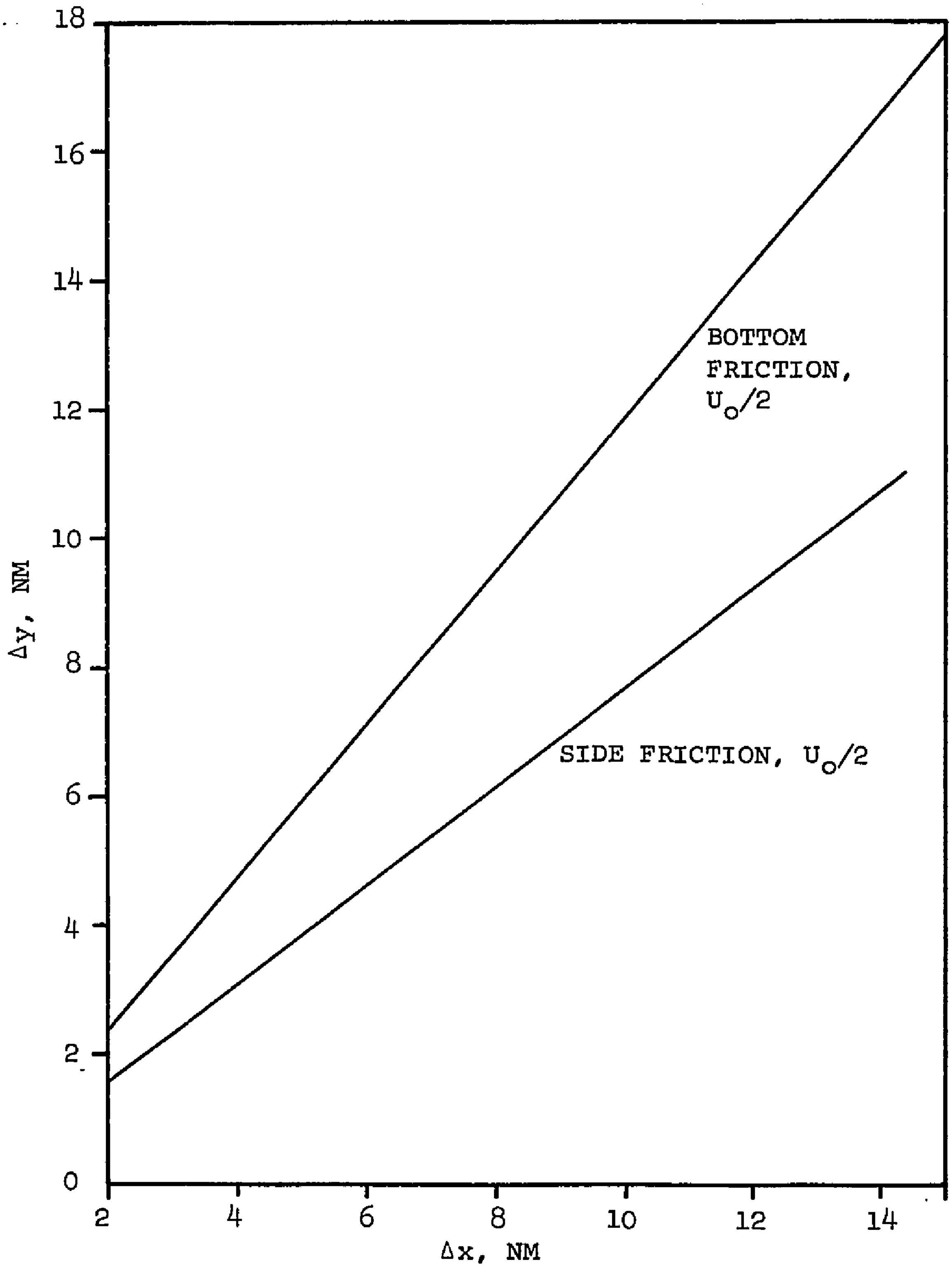

Figure 15 - $U_o/2$ as a function of x and y for side and bottom friction case steady-state jet

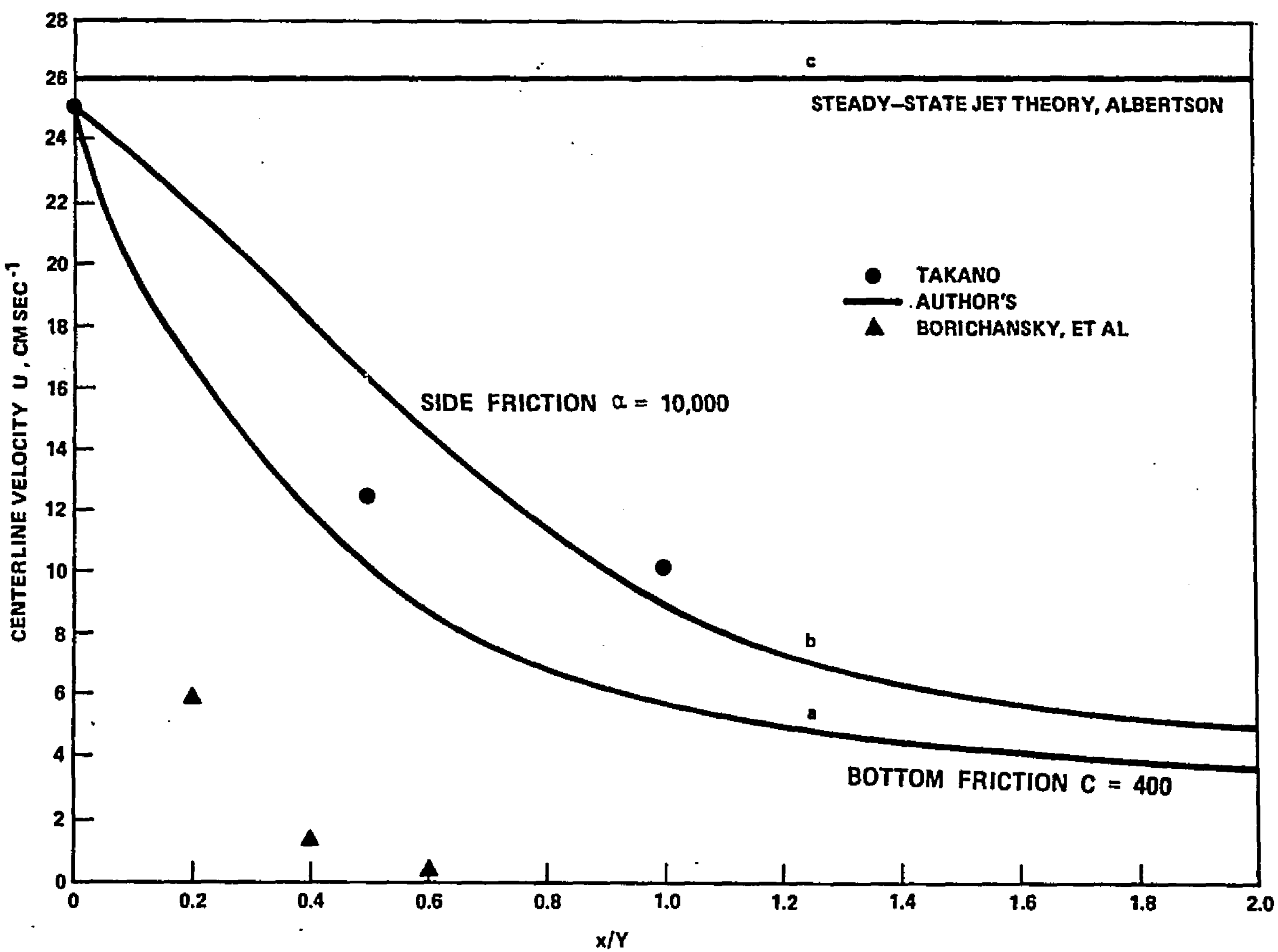

Figure 16 - Centerline velocity distribution for side and bottom friction case, steady-state jet

the velocity distribution and character of a side friction jet and to formulate empirical equations to predict the velocity distribution of a jet issuing from an orifice or slot. Albertson's (1950) summary of the side friction plane jet shows an entraining flow and a centerline velocity which begin to decrease only after a distance of six jet diameters. This would mean that, if a side friction plane jet theory were directly applicable to an estuary like Chesapeake Bay and the Bay flow were not tidal or deflected by the earth's rotation or other causes, the maximum centerline velocity would be detected unchanged up to a distance of 108 km from shore and the flow would be entraining.

Recent works by Takano (1954a) and Borichansky and Midhailov (1966) have attempted to evaluate the velocity distribution off the mouth of an estuary or river. Takano (1954a) derives the velocity distribution by not considering the inertia terms and by using only the side friction and pressure gradient terms. He assumes a thin layer of river water which is homogeneous and 1 or 2 meters thick resting on a more saline ocean wedge. In contrast, Borichansky and Mikhailov consider the inertia and side and bottom friction terms only. The results of both these investigations show a centerline velocity decreasing rapidly as a function of distance. Their velocity predictions for selected centerline points for an estuary of the type used in Case I are plotted as individual points in Figure 16 along with the prediction for a side friction jet (curve c) given by Albertson (1950). It can be seen that the centerline velocity results of Cases I and II agree in trend with the results of Takano (1954a) and Borichansky and Midhailov (1966) and not with the predictions of Albertson, et al (1950).

Gadgil (1971) was the first to make an attempt to look at both bottom (Case II) and side (Case III) frictions together. She used a laminar steady-state jet in a rotating container which had a rigid top and bottom. The rotation was used to generate an Ekman layer and, thus, bottom friction. While this is different from the steady-state jet considered here, bottom friction can exist without rotation (Case I), the results of her investigation are interesting to examine for similarities. Her results showed that if the rotation was strong, bottom friction dominated, the jet was dispersive, vorticity was decaying but not diffusing laterally, and momentum decreased with downstream distance. If there was little or no rotation and side friction dominated, the jet entrained fluid, vorticity was conserved but diffused laterally, and the momentum flux across the jet remained constant. Gadgil (1971) also was able to predict the distance it would take the velocity of a side or bottom friction jet to decrease to zero. In general, the distance required for her jet to decrease to zero was greater for a side friction case than for a bottom friction case.

Gadgil also points out that, in cases where bottom friction dominates, if side friction is considered it will control the flow pattern near the mouth of the jet and give way to a bottom friction velocity distribution as the distance from the jet entrance increases. This could be an explanation for the flow pattern observed in Figure 14.

In summary, for the velocity along the centerline it can be concluded that the distribution for an estuary or river discharging into a continental sea will decrease rapidly, in a form similar to that shown in Figure 15, if the jet is considered a bottom friction type. For this type of jet the flow will be dispersive (i.e., velocity vectors diverge away from the jet centerline). If the jet is dominated by side friction, it will follow a distribution along the centerline similar to that described by Albertson (1950) and the flow will be entraining (velocity vectors converging toward jet centerline). For a case in which side and bottom frictions exist, the flow pattern will be a combination of the two as described by Gadgil (1971).

Another interesting comparison of the U component of velocity is in the transverse direction. Bickley (1937) in his solution found the transverse distribution of the U component of velocity was a function of the hyperbolic secant squared ($U = f(\text{sech}^2 y)$). Albertson, et al (1950), in their work assumed that the transverse distribution of the component of velocity was Gaussian. The normalized transverse velocity distribution U/U_o (U component of velocity located at distance y from centerline/centerline velocity) was plotted against y/b (distance from centerline of U/distance from centerline of 1/2 U_o) for Case I, Figure 17. It can be seen from this figure that the data indeed follow a $\text{sech}^2 y$ curve.

As mentioned, the velocity vectors along the shore above and below the jet have decreased in intensity. It should be noted that a shoreward movement of water near the coast both above and below the jet has been generated.

Case III - This case consisted of the addition of the Coriolis force for a jet of the type in Case I. The Coriolis parameter was for a latitude of 37° and was calculated to be 0.00008 $\sec^{-1}$. The computational results

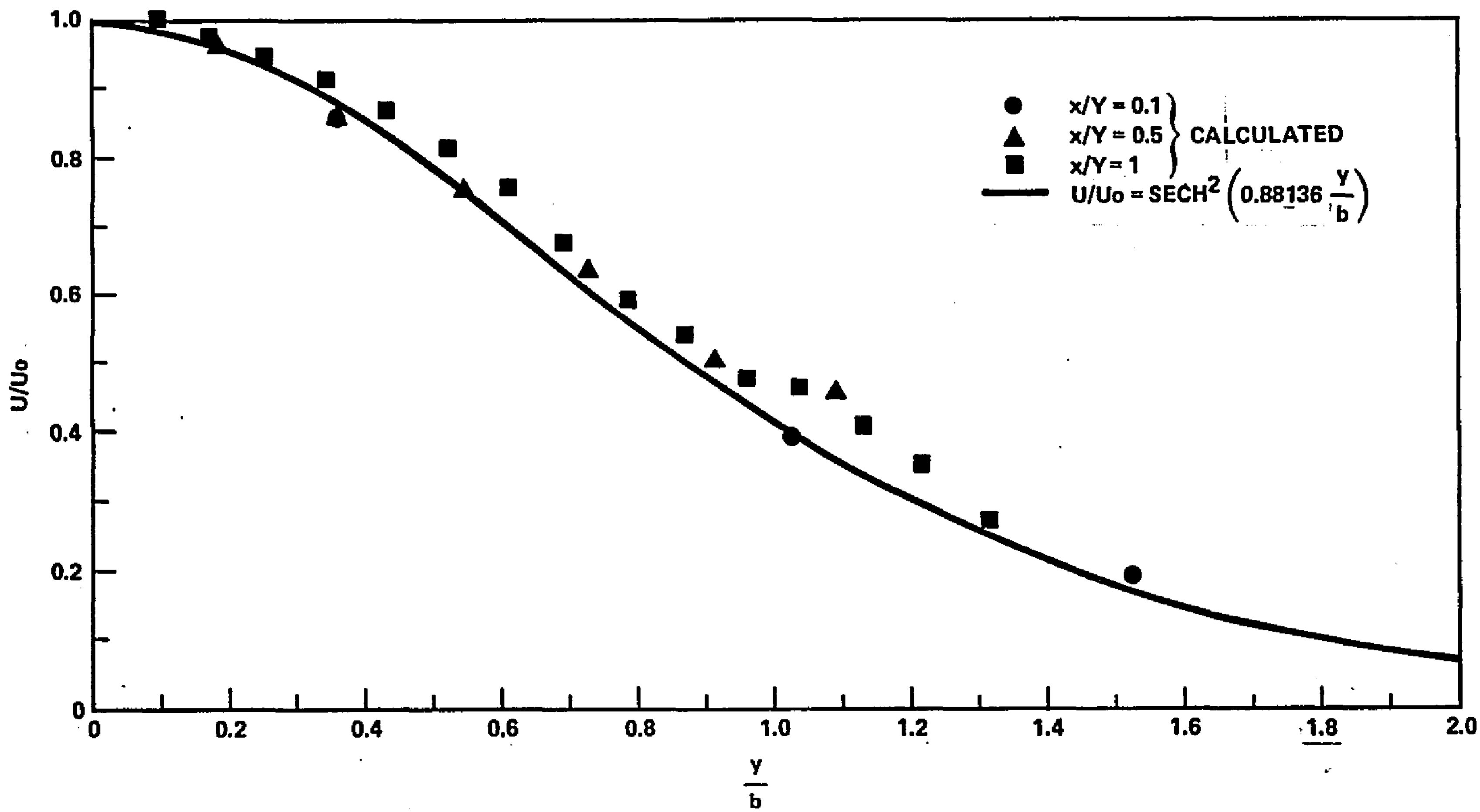

Figure 17
Cross-stream velocity distribution
steady-state jet

for the vector plot are shown in Figure 18, and the water level contours are shown in Figure 19. The same four features recognized and described for the vector plot of Case I are apparent here. Comparing Figure 18 with the vector plot of Case I, Figure 10, shows no major differences. There is a slight rotation of the vectors to the southern half of the plot, but nothing that is very noticeable. Plots of the centerline velocity for this case are the same as those of Case I and are not shown. The plot of water level, Figure 19, when compared with the water levels of Case I, Figure 11, also shows a slight difference, with some water being piled up to the south.

At this point it is helpful to consider two dimensionless quantities, the Ekman and Rossby numbers. The Ekman number is used to determine the relative importance of friction and rotation and is defined as $A_z/\Omega H^2$, where A_z is the vertical eddy viscosity. An A_z corresponding to a Chézy coefficient of 400 $cm^{-1/2}$ sec can vary from about 76.5 to 133.9 cm^2 sec^{-1}, depending on the type of vertical velocity profile assumed. (See Appendix D.) These values of vertical eddy viscosity are in the range of those quoted by Sverdrup, et al (1942), Neumann and Pierson (1966), and Dyer (1973). The corresponding Ekman number for the above range of turbulent eddy viscosity varies from 1.05 to 1.83.

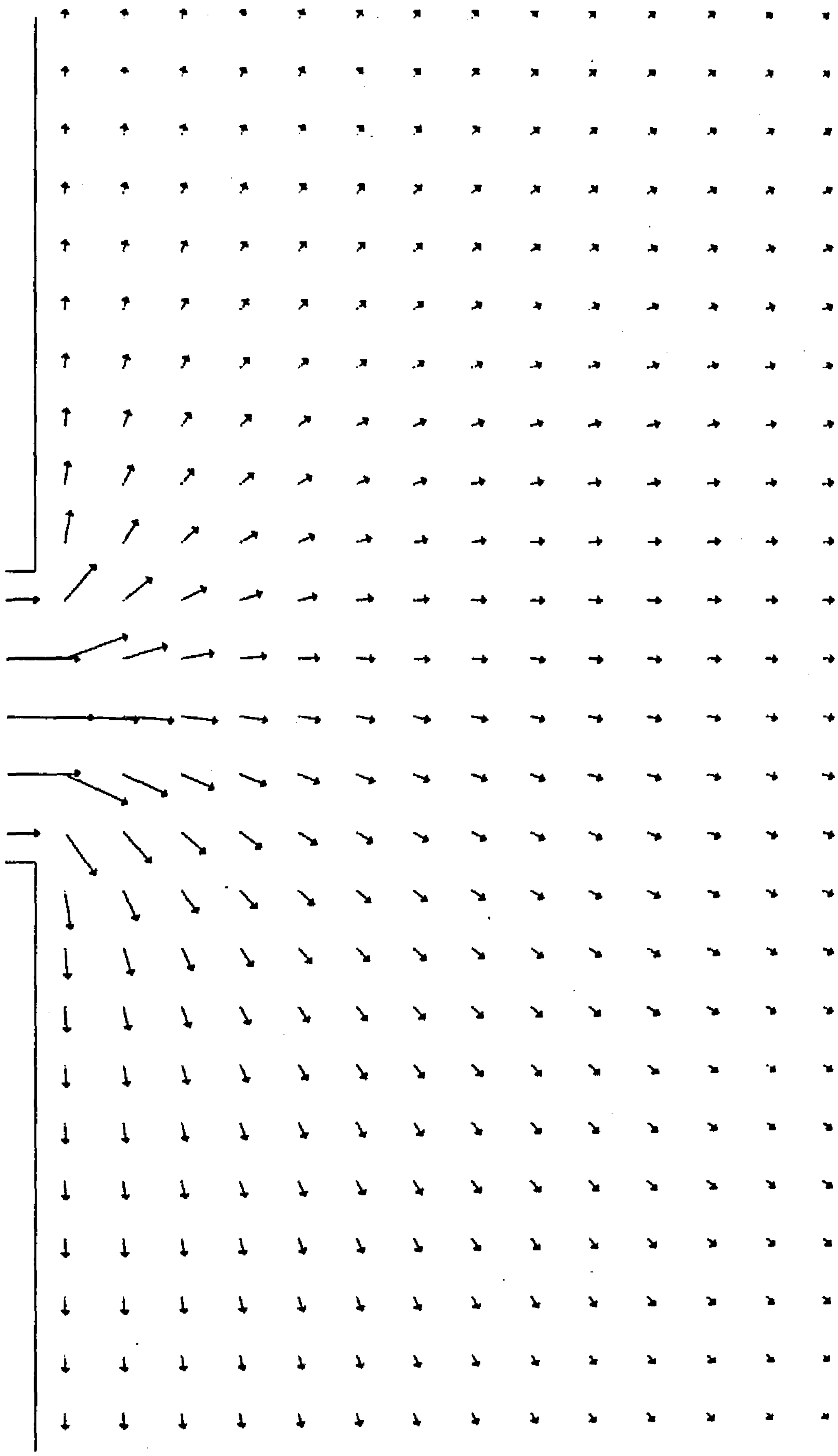

Figure 18 - Velocity vector plot
steady-state jet with Coriolis force

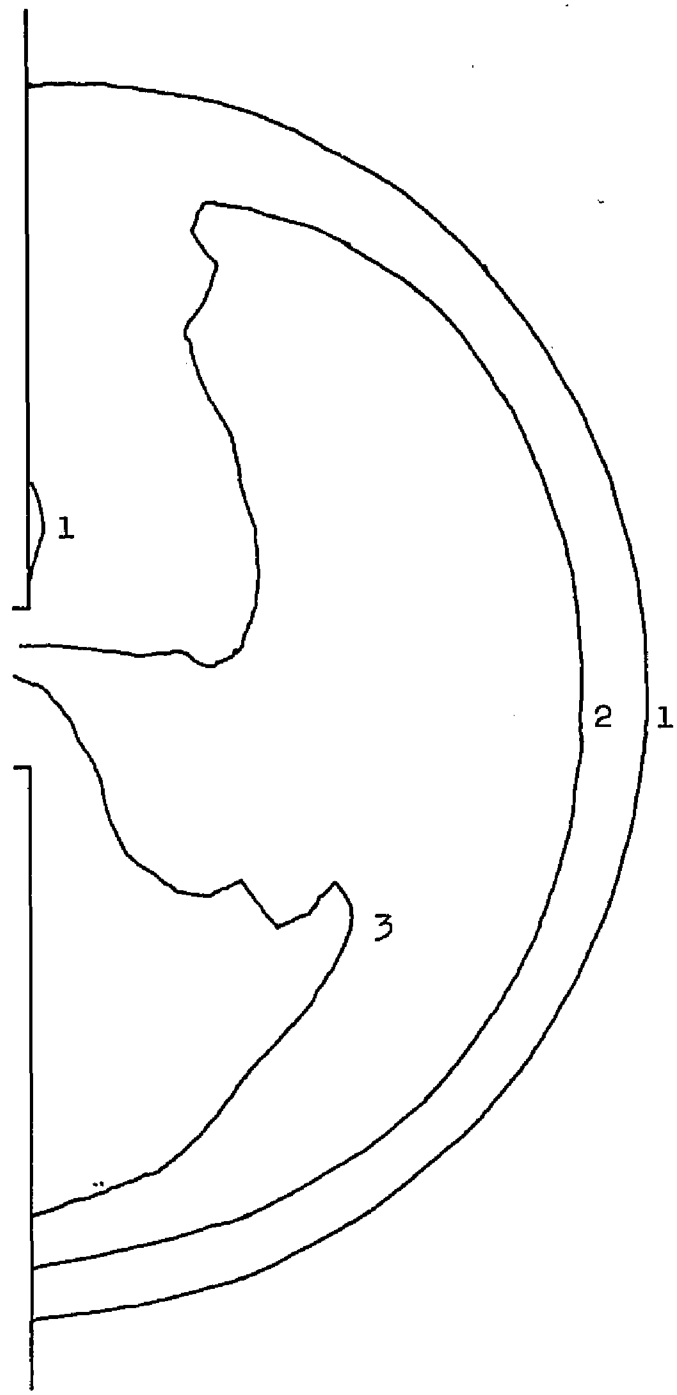

Figure 19
Water level plot
steady-state jet with Coriolis force, cm

It can be considered that in this case the flow is frictionally dominated for the higher values of the Ekman number, i.e., >1.

The Rossby number, $R_o = U/\Omega L$, is used to determine the relative importance of the inertial terms to those of rotation. For a characteristic length L = 359,280 cm (one-grid spacing) and velocity change of 25 cm sec^{-1} over this distance, the Rossby number is 0.9. This is a maximum value. While not one, it is much larger than the Rossby numbers usually found in laboratory experiments where rotation is considered dominant and shows that the inertial terms have increased in importance but are still not controlling. Takano (1955), when investigating the effect of the seaward flow off a river mouth, concluded that for his analytical equations, the Coriolis term could be insignificant if the inertial terms were large (i.e., large Rossby number).

Thus, for this case the friction terms can dominate those of rotation, while the inertial terms might not. This should help to explain the lack of a significant deflection of the outflow due to rotation and verifies the results of the jet decay experiment in Case I.

Case IV - This case consists of the addition of a southward flowing velocity to the situation of Case I.

Surface velocities in the Chesapeake Bight region are highly variable and depend on distance from shore and on season. Values in the literature range from 1.2 cm sec^{-1} to 32.4 cm sec^{-1} (Harrison, et al (1967)). A value of 4 cm sec^{-1} to the south was chosen and varied linearly from 0 at the coast to a maximum of -4 cm sec^{-1} at the right side of the computational grid. The results of the computation are shown as a vector plot in Figure 20. Here the northern flow along the coast decreased, and the jet was deflected and turned south as a wide band of flow. Again, there are no visible eddies. This case suggests that, for a frictionally dominant flow, an ambient southern velocity is more important in the turning of the Bay effluent to the south than the Coriolis force.

The northern flow along the coast above the Bay mouth still persists, as seen in Figure 19. Bumpus (1969) has described reversals or northern flow in the surface waters in the Mid-Atlantic Bight. His results are derived from surface drifters, and the reversals described exist at several locations on the coast and mainly during the summer. These reversals occur during a season of light winds so that the flow patterns established by a layer of lighter water on a more dense saline wedge, along with an imposed ambient current, could cause the time averaged surface flow described by Bumpus and shown by Figure 20.

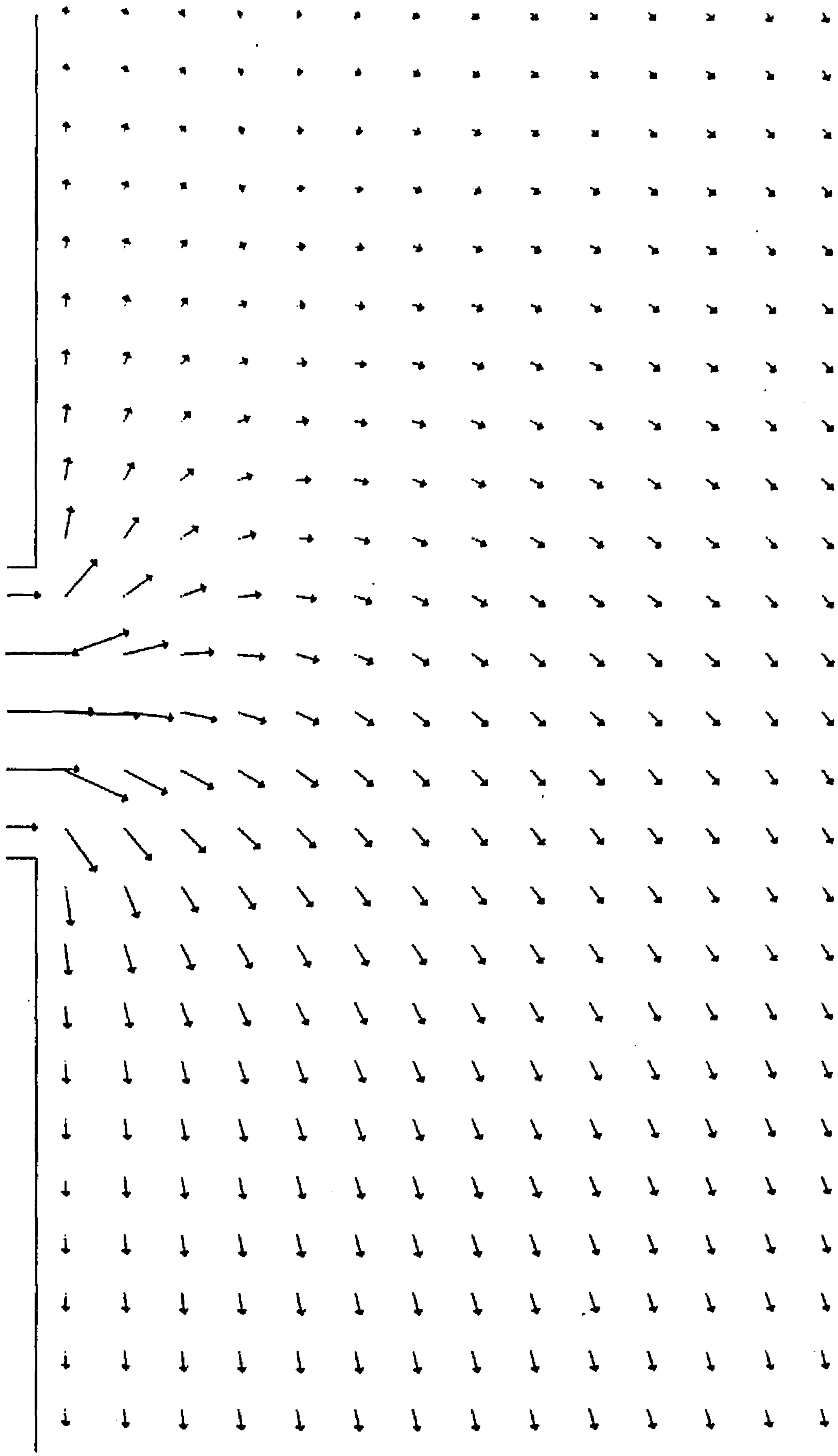

Figure 20 - Velocity vector plot, steady-state jet with southerly ambient velocity.

Oscillating Jet

General - For this physical situation, grid size, time step, grid spacing, Bay entrance, coastline, and bottom friction were the same as those for the steady-state jet. The Courant-Friedricks-Lewy stability criterion was also the same, and no problems were encountered in using an oscillating jet as a boundary condition. Salinity was not calculated, as for the steady-state jet, since it was held constant over the grid for all cases.

The initial conditions for the grid were the same as for a steady jet, but the boundary conditions were changed. In the east-west direction, velocity and tidal height were the boundary conditions as before, with the only change being at the Bay mouth. Here, the jet was made to oscillate sinusoidally with a period of 12.42 hr (semi-diurnal tide) and a maximum centerline velocity (integrated with respect to depth) of 25 cm sec^{-1}. The velocity profile across the Bay mouth remained parabolic. Boundary conditions in the north-south direction were changed, due to the problem of reflection from the northern boundary, so that tidal height was used on both boundaries. For all cases, except that of an ambient southward flowing velocity, the tidal height on the northern and southern boundaries remained zero.

Six different cases for an oscillating jet with bottom friction were run: Case I, oscillating jet; Case II, oscillating jet with Coriolis force; Case III, oscillating jet with sloping bottom; Case IV, oscillating jet with wind from east; Case V, oscillating jet with wind from north; and Case VI, oscillating jet with ambient velocity from the north.

In computing data for all the above cases, the program was run through two complete tidal cycles, with data for the vector plots and water level contours taken from the last tidal cycle. The term water level is used here as in the steady-state case because, although the velocity varies with a period equal to that of a semi-diurnal tide, the tidal height on the open boundaries is not fluctuating with time.

Case I - Figure 21 shows a plot of the water level and velocity as a function of time through both tidal cycles for two points on the grid ($m = 1$, $n = 25$ and $m = 6$, $n = 25$). In one tidal cycle the velocity and water level adjust so that they are out of phase by about 90° and remain this way throughout the second tidal cycle. The velocity and water level can be seen to decrease as a function of distance from the Bay mouth, when like curves in Figure 21 are compared. This figure suggests that the data taken during

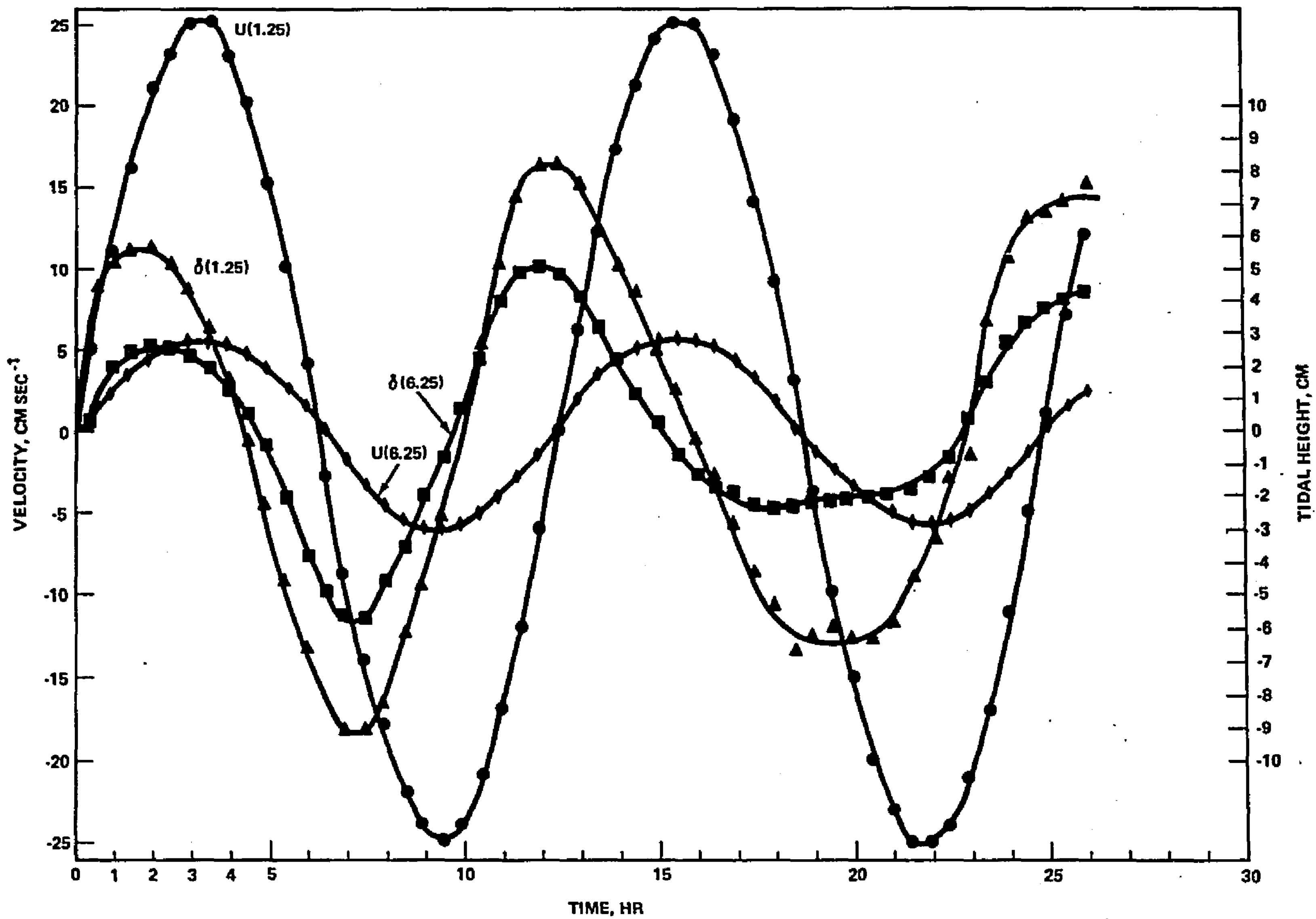

Figure 21 - Velocity and water level as a function of time at two grid points, oscillating jet

the second tidal cycle are for a jet which has reached equilibrium.

Figures 22 through 26 show the vector and water level plots for an oscillating jet during the second tidal cycle. Figures 22 and 25 are the plots of the water level at slack before ebb and at slack before flood, respectively. The contours show symmetry around the Bay entrance, as did Figure 11 for the steady-state jet. The height of the water is referenced to datum, and the effect of a head or pressure gradient caused by the height of the water above and below datum can be seen. The vector plots are given in Figures 23, 24, and 26. Figure 23 is a vector plot of the flow at maximum ebb, and Figure 24 is a vector plot for the time when the centerline jet velocity at the Bay mouth is 12 cm sec^{-1}. Figure 26 shows the vector plot at maximum flood. The main features of the flow in these figures are: the flow is dispersive for an ebb tide and convergent toward the Bay entrance for a flood tide, the velocity decreases as a function of distance along the centerline, there is a strong flow along the coast above and below the jet for both flood and ebb tides, and there are no eddies in these figures (which are instantaneous pictures). To further check for eddies, the flow was averaged over a tidal cycle to remove the tidal component for

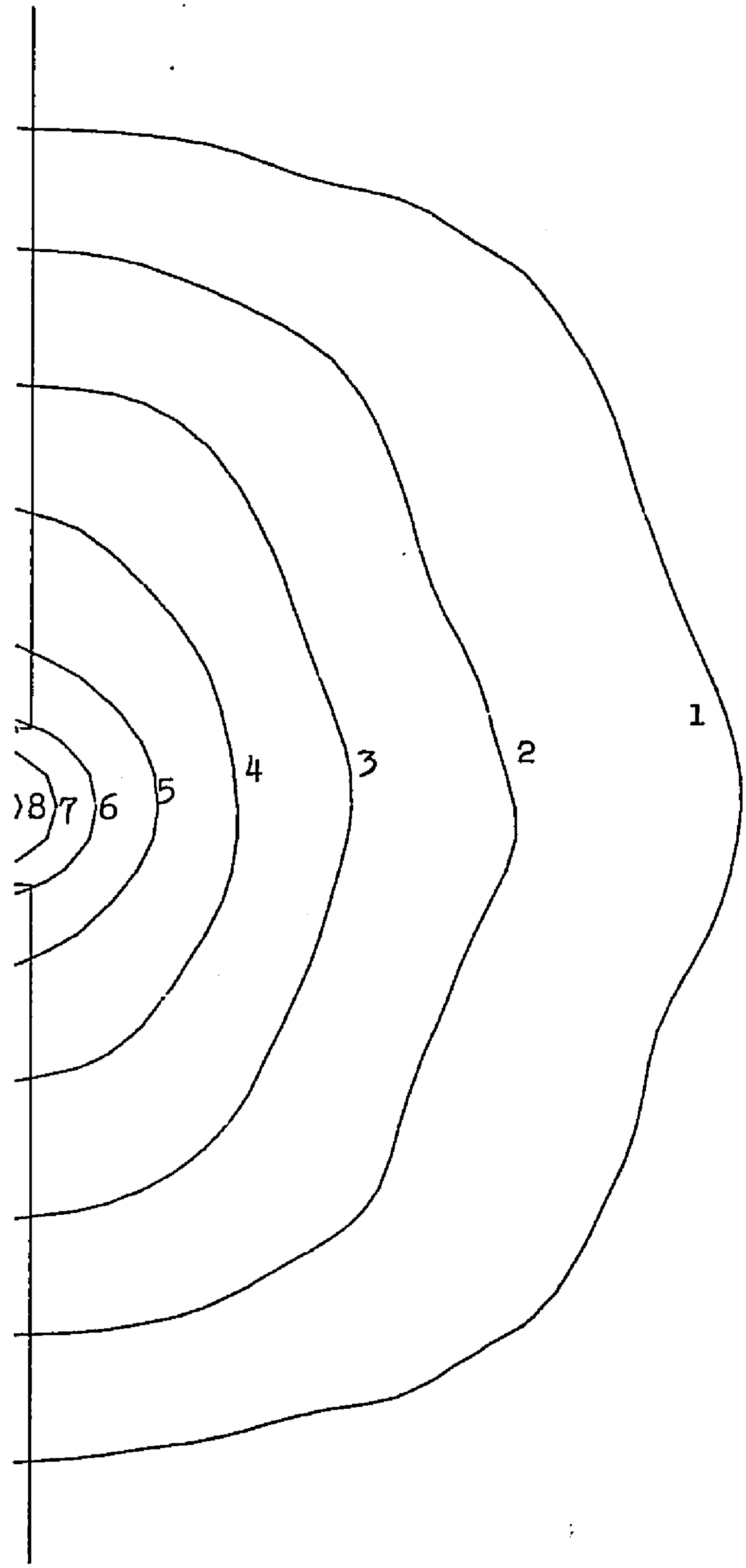

Figure 22
Water level plot
oscillating jet at slack before ebb, cm

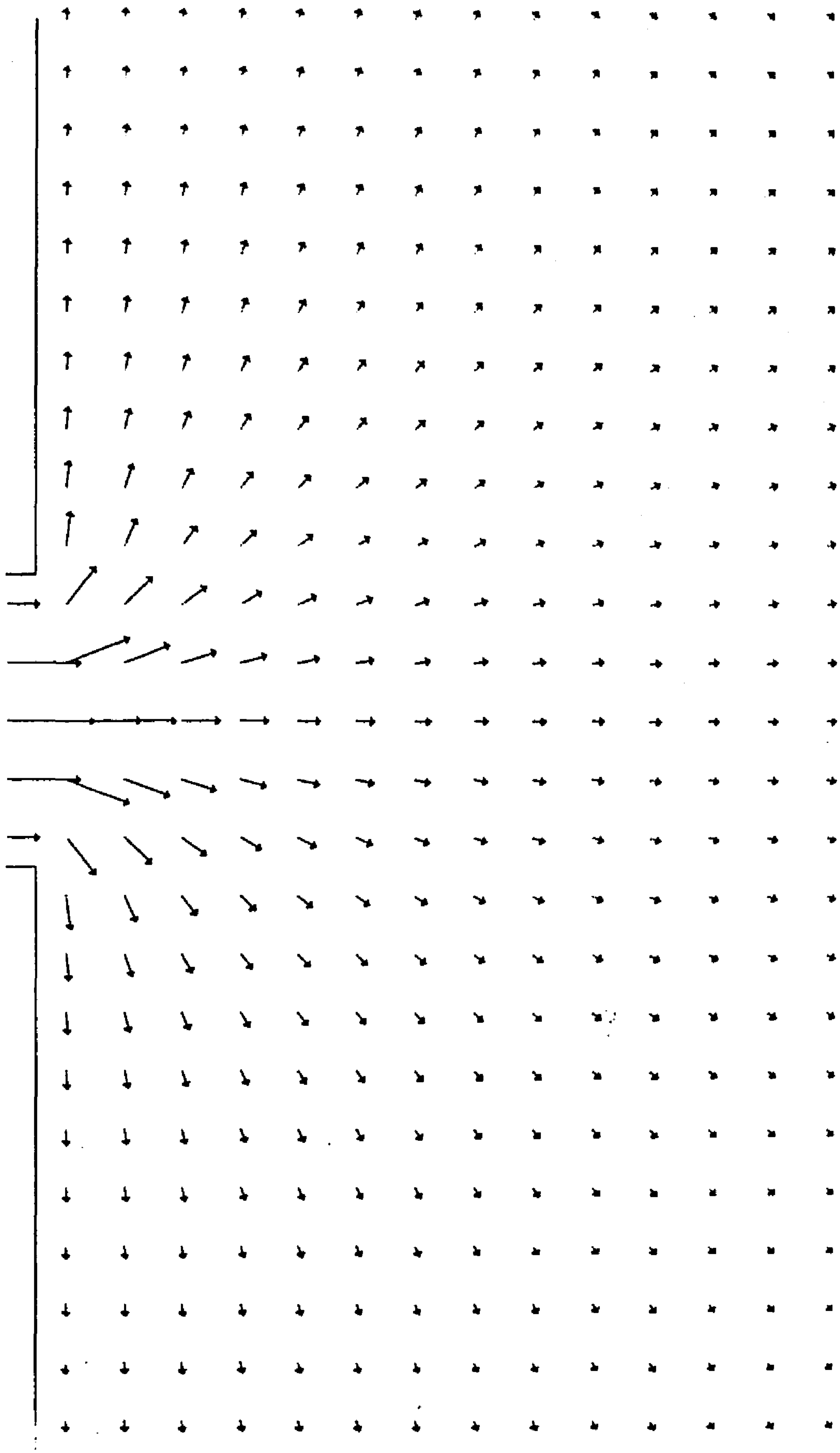

Figure 23 - Velocity vector plot
oscillating jet at maximum ebb

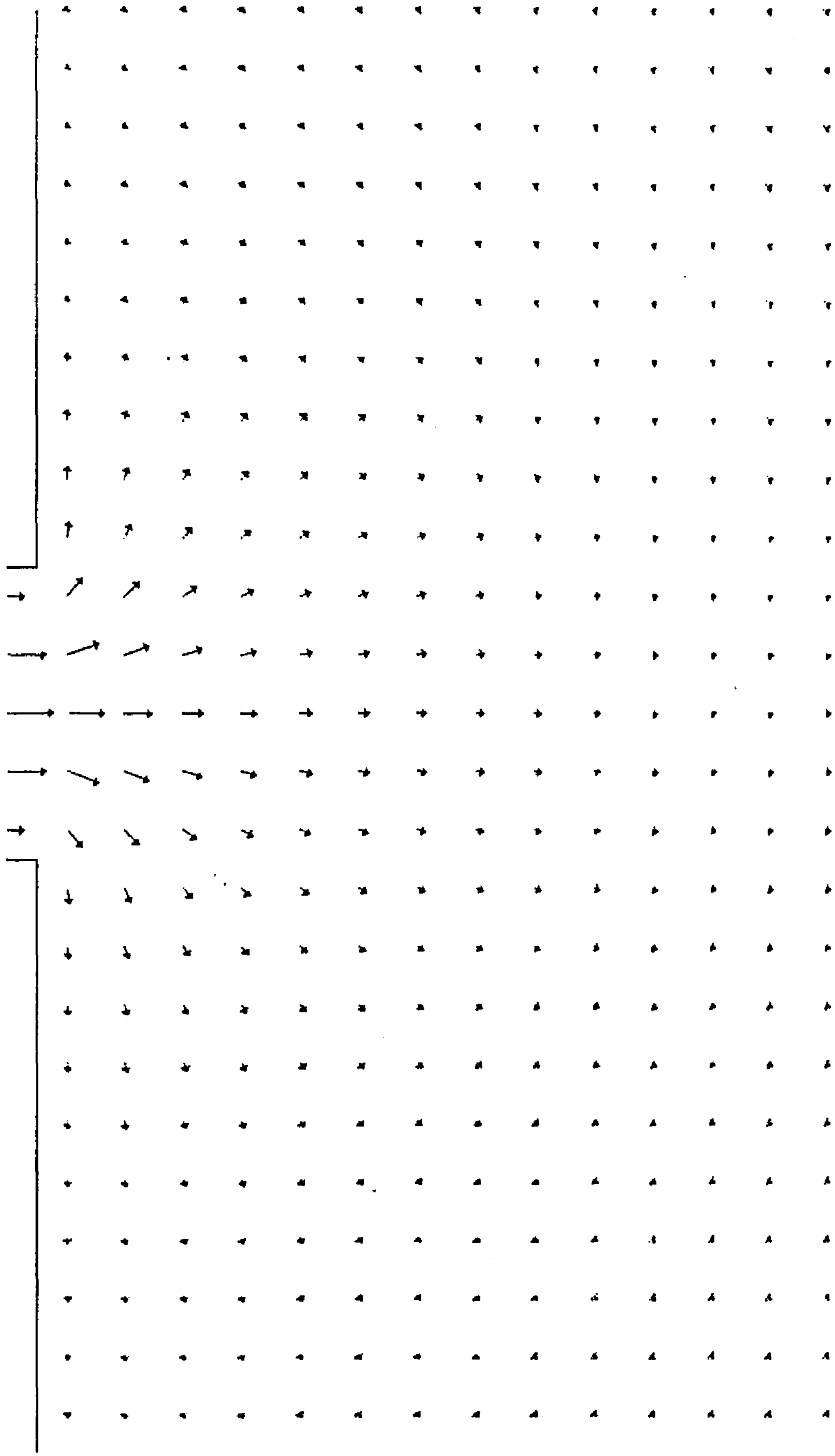

Figure 24 - Velocity vector plot, oscillating jet at a maximum centerline velocity of 12 cm sec^{-1}

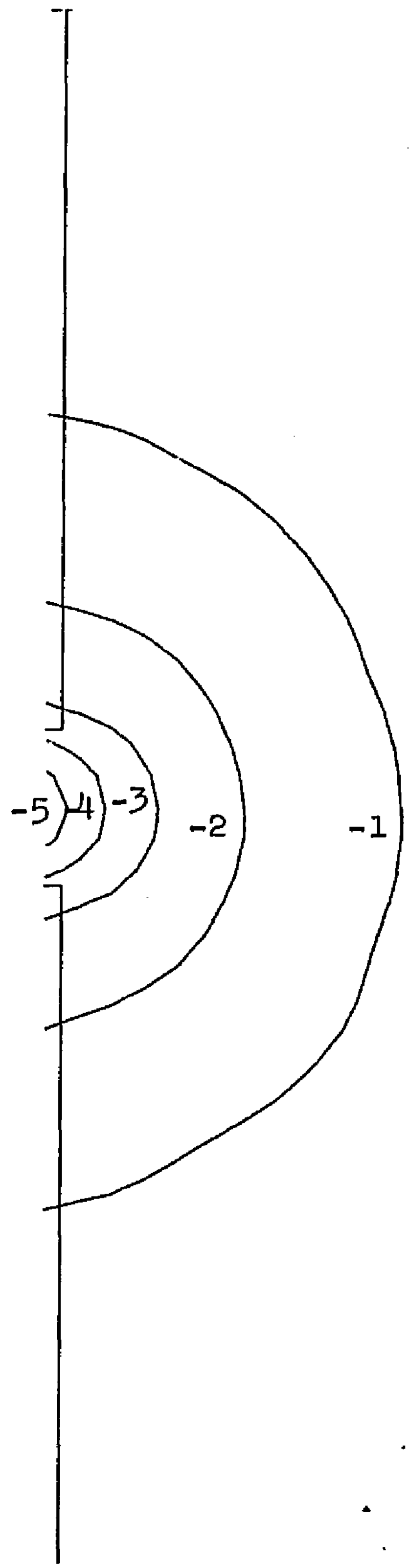

Figure 25
Water level plot
oscillating jet at slack before flood, cm

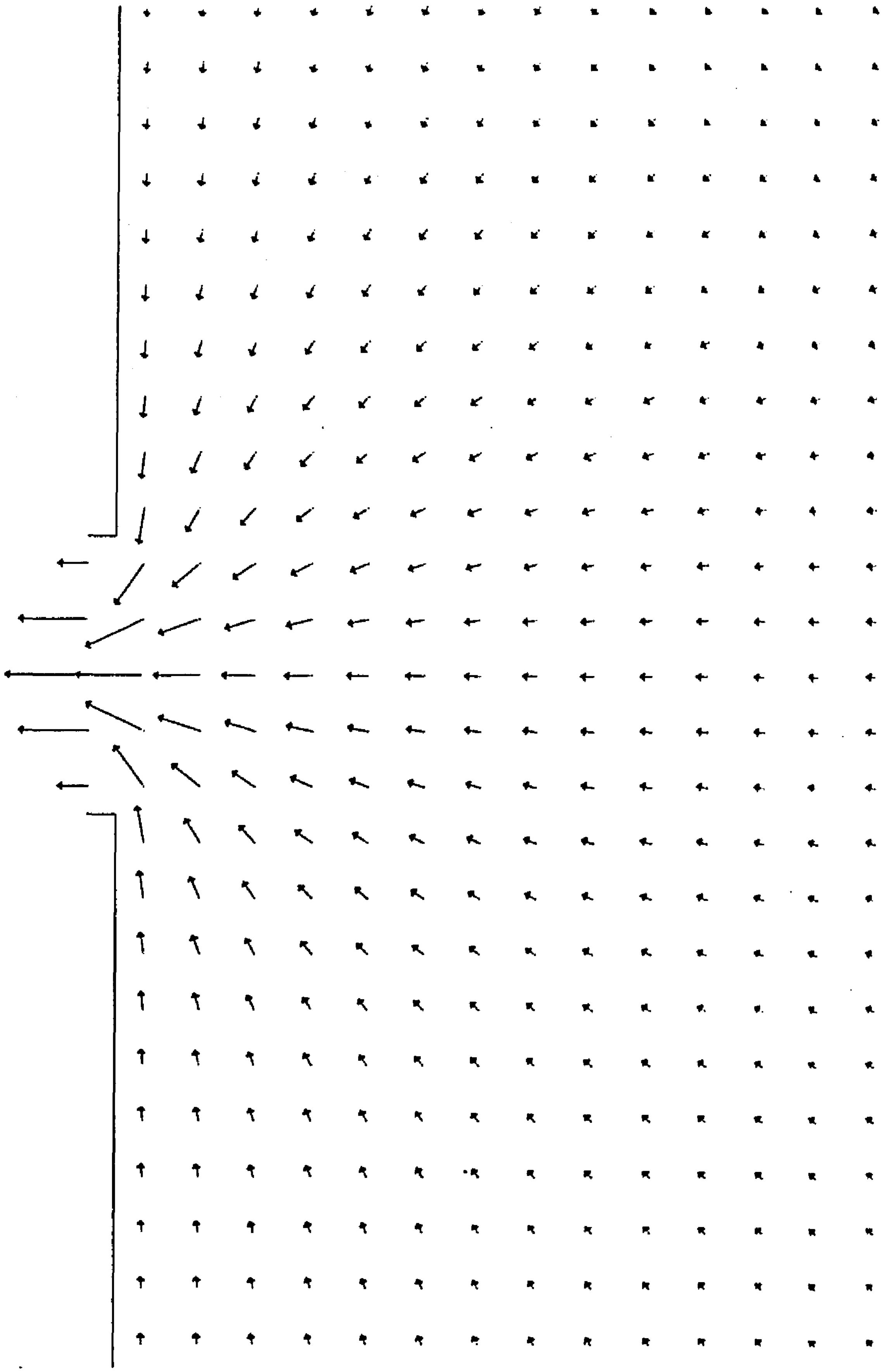

Figure 26 - Velocity vector plot
oscillating jet at maximum flood

the grid points in the vicinity of the Bay mouth. Only the southern portion of the Bay entrance was examined since the flow is symmetrical. The results of this summation are shown in Figure 27. Here it can be seen that, from an Euleran point of view, there is a weak residual clockwise circulation. This corresponds to the results of Harrison, et al (1962), in their measurement and inference of an eddy south of the Bay entrance near Virginia Beach, Virginia. It is believed this net circulation is the result of the non-linear terms, in the equations of motion, on the tidal velocity fluctuation.

The dispersion and convergence characteristics of the oscillating jet are believed to be caused by a pressure gradient. This gradient is generated by the water level varying above and below datum, as shown in Figures 22 and 26, and is the same mechanism that causes the dispersion of the steady-state jet.

The centerline velocity behaves in the same manner as described for the steady-state jet, in that it decreases as a function of distance from the Bay mouth. This condition holds for both flood and ebb and can be seen in Figures 23, 24, and 26; it is shown as velocity versus distance in Figure 28 for the ebb condition only.

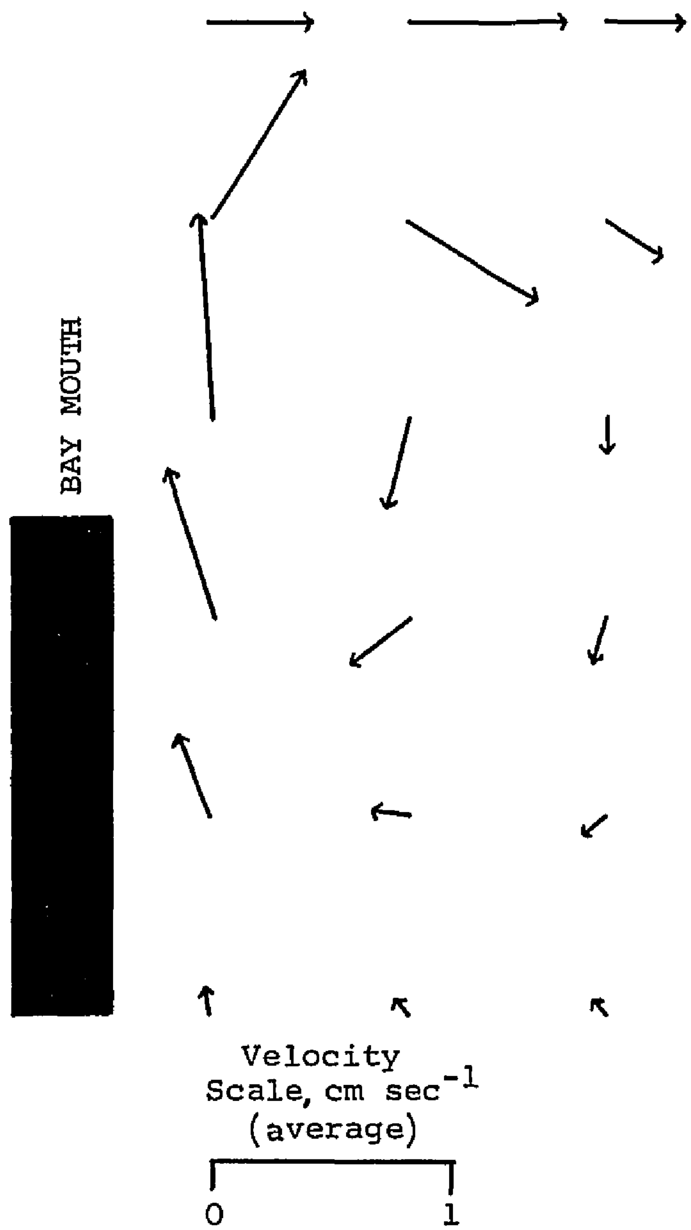

Figure 27
Tidal averaged flow, oscillating jet

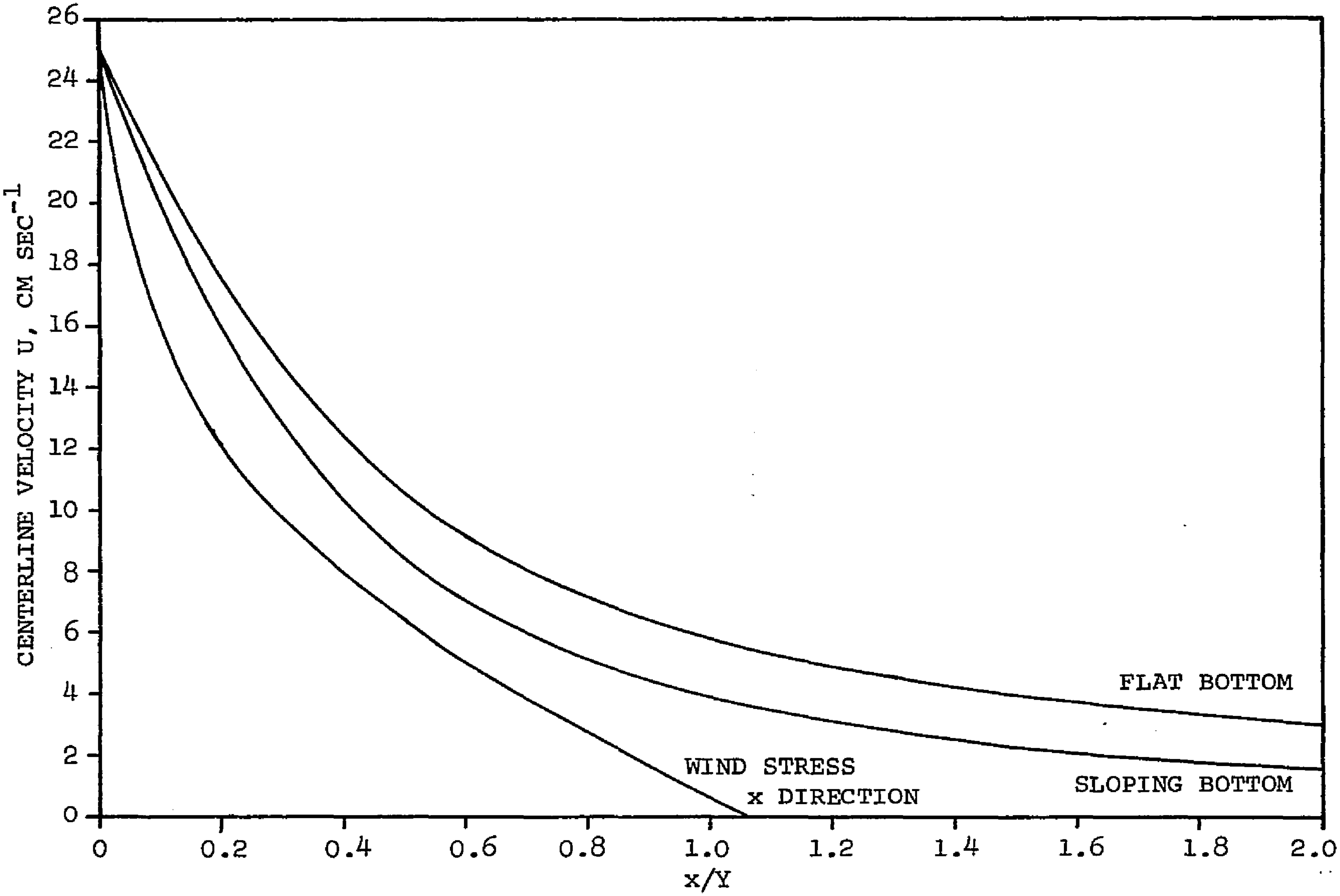

Figure 28 - Centerline velocity distribution for flat and sloping bottom, oscillating jet

The strong coastal flow away from the jet above and below the Bay entrance for the ebb flow reverses itself during the flood stage. In both cases a strong coastal current is apparent.

One final interesting aspect can be discussed in this case. The Amazon River has flow features that are very similar to this case. These features are: (1) There is no Coriolis effect since the Amazon is located on the equator; (2) the Amazon is unique in that it has no salt wedge; and (3) it is tidal and the width of the mouth reported by Gibbs (1970) is between 10 and 20 km, similar to the 17.9 km for the Chesapeake Bay. However, there are some differences worth noting: (1) The depth at the mouth of the Amazon is 2 to 4.5 times that used here; (2) the tidal range is 5 times that of the Chesapeake Bay; and (2) the volume of discharge is 100 times that of the Chesapeake Bay.

If Figures 2 and 3 of Gibbs (1970) are examined, with attention paid to the 20 % isohaline, and compared with Figures 10 and 11 for the steady-state jet and Figures 22 and 25 for the oscillating jet, the similarities in the fan-like spread of the Amazon effluent can be seen.

<u>Case II</u> - This case consisted of the addition of the Coriolis force to an oscillating jet of the type in Case I. The same value of the Coriolis parameter, f, applied in

Case III of the steady-state jet was used. The results of the calculations are given in the vector plots, Figure 29 for maximum ebb and Figure 30 for maximum flood. The four main features seen and described for the vector plots of the previous case apply here with little difference seen between Figures 23 and 29 and between Figures 26 and 30.

As for Case I, the tidal component was averaged out to observe the eddy effect. This is shown in Figure 31. Here it can be seen that the Coriolis effect strengthens the northern and weakens the southern flow of the eddies.

<u>Case III</u> - This case is different from any described thus far. In this run the shape of the bottom was changed from flat to gently sloping for the Case I oscillating jet. The bottom varied from 1000 cm in depth (~32 ft) at the coast to 13,000 cm in depth (~425 ft) 104 km from the coast, giving a slope of 1/1354. Bottom friction was held constant and not allowed to vary with depth, and the Coriolis force was not considered.

Figures 32 and 33 show the vector plots at maximum ebb and flood for the second tidal cycle. The same four general features recognized for the vector plot of Case I of the oscillating jet are again seen here. However, there are some differences: First, the gradual sloping of the bottom

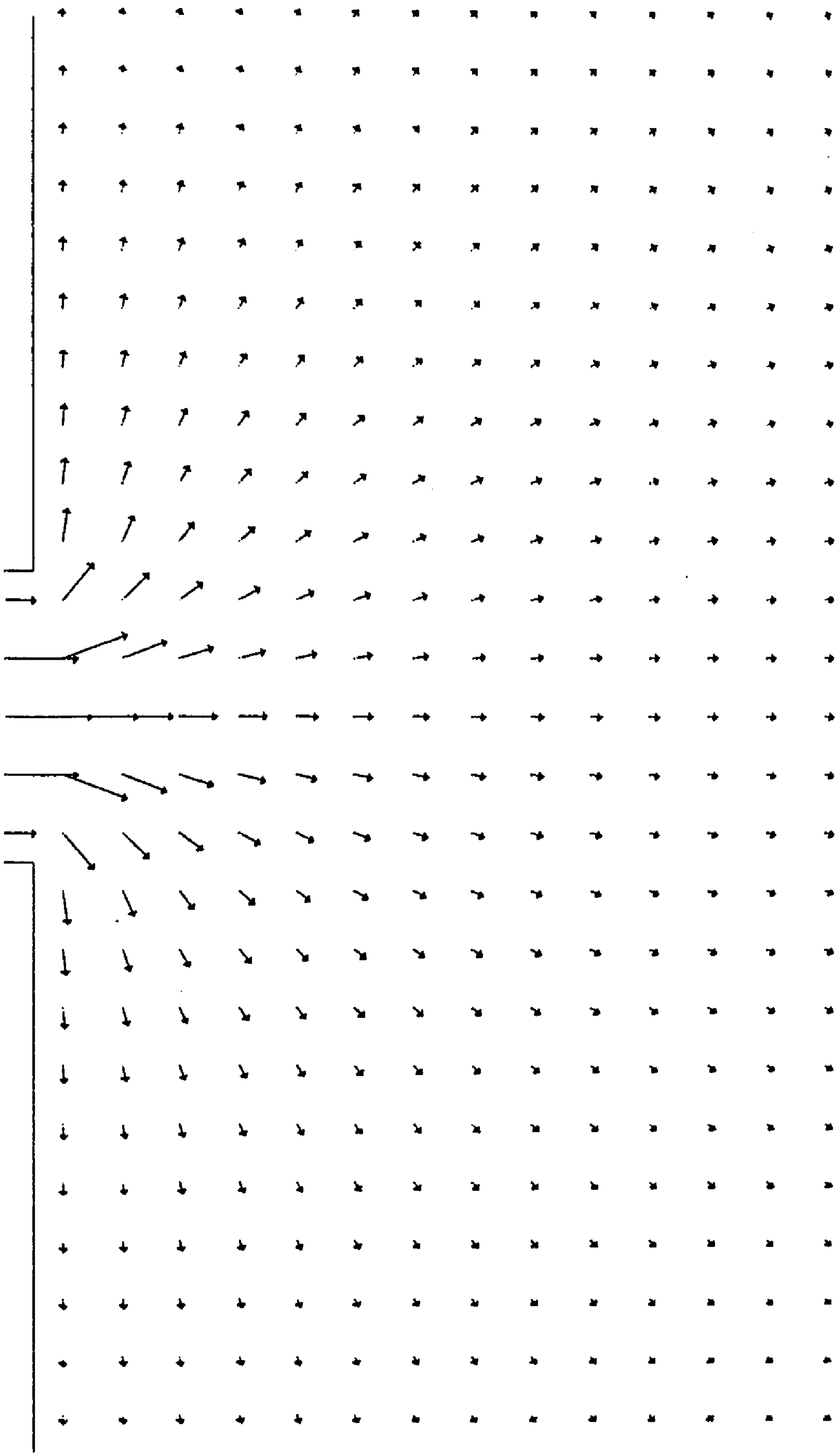

Figure 29 - Velocity vector plot, oscillating jet at maximum ebb and with Coriolis force

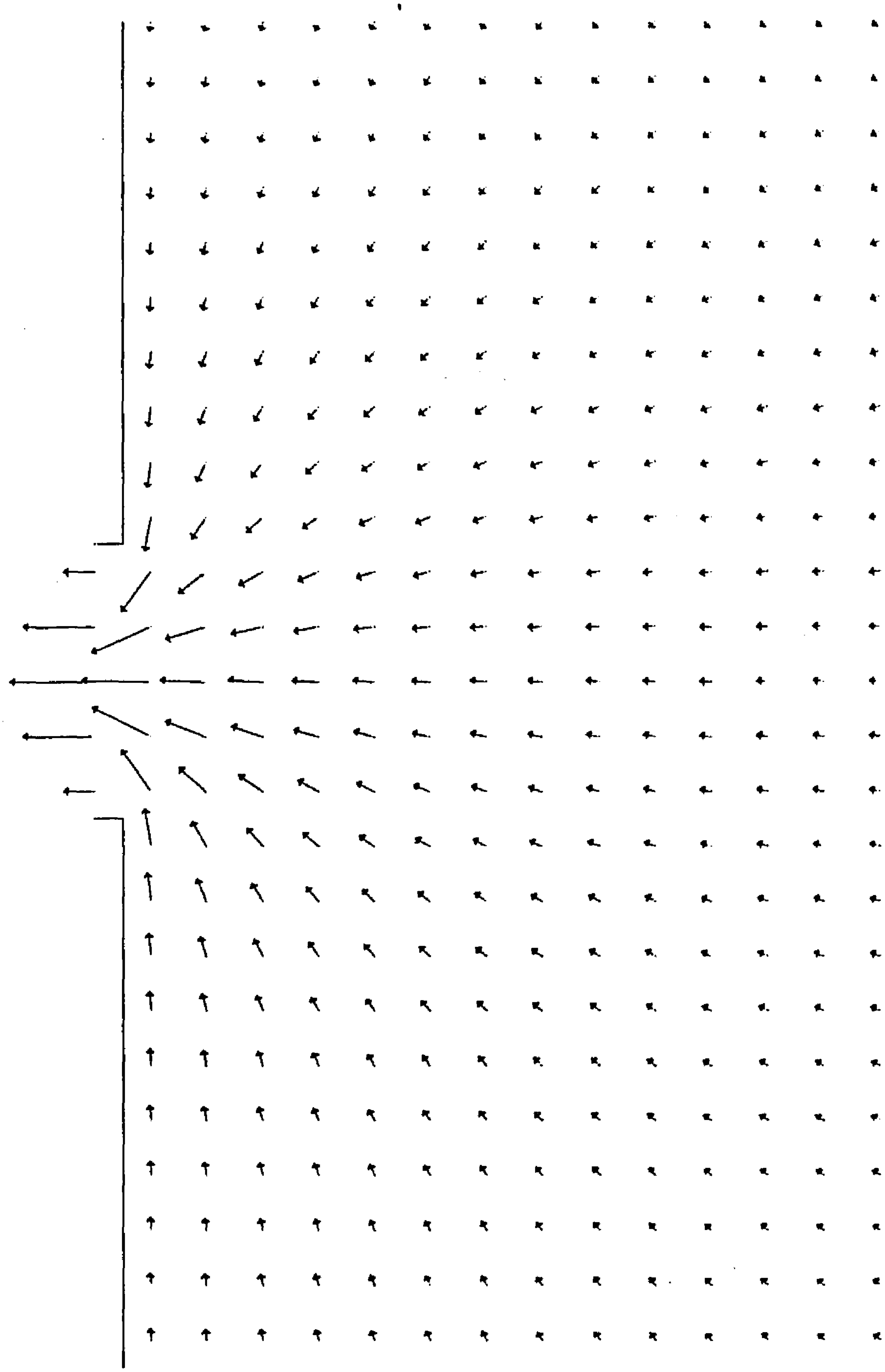

Figure 30 - Velocity vector plot, oscillating jet at maximum flood and with Coriolis force

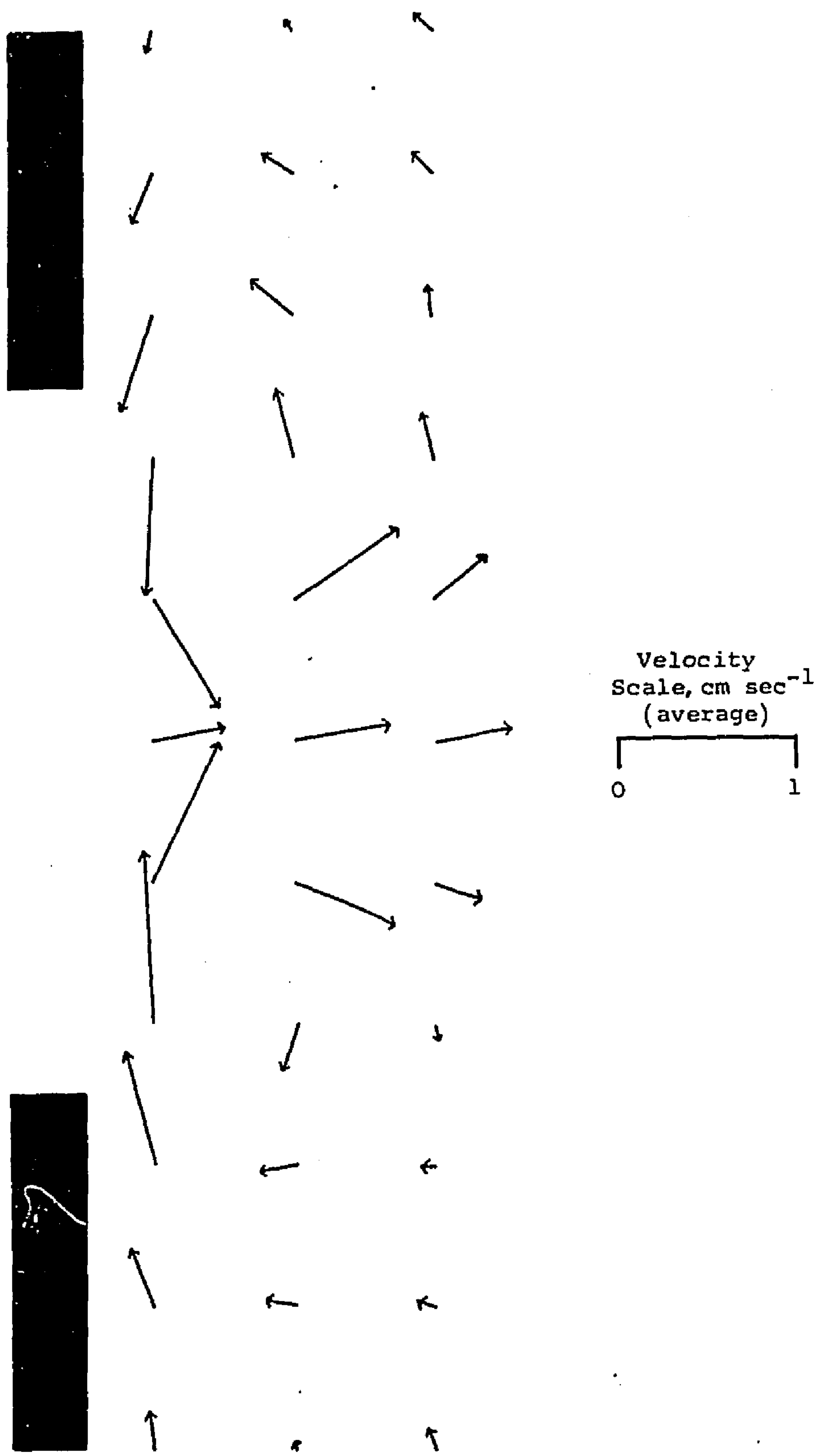

Figure 31
Tidal average flow, oscillating jet with Coriolis force

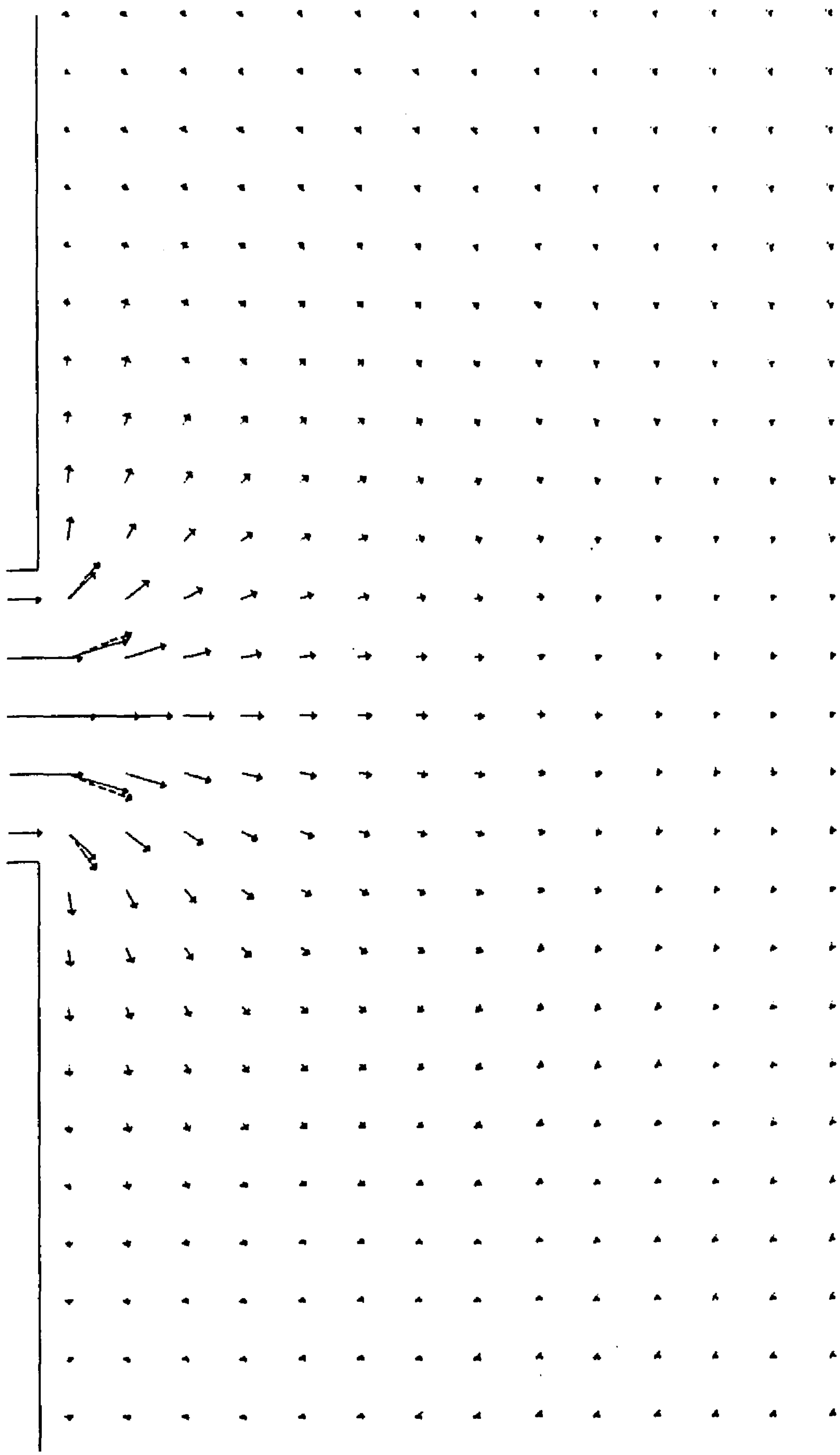

Figure 32 - Velocity vector plot, oscillating jet at maximum ebb and with sloping bottom

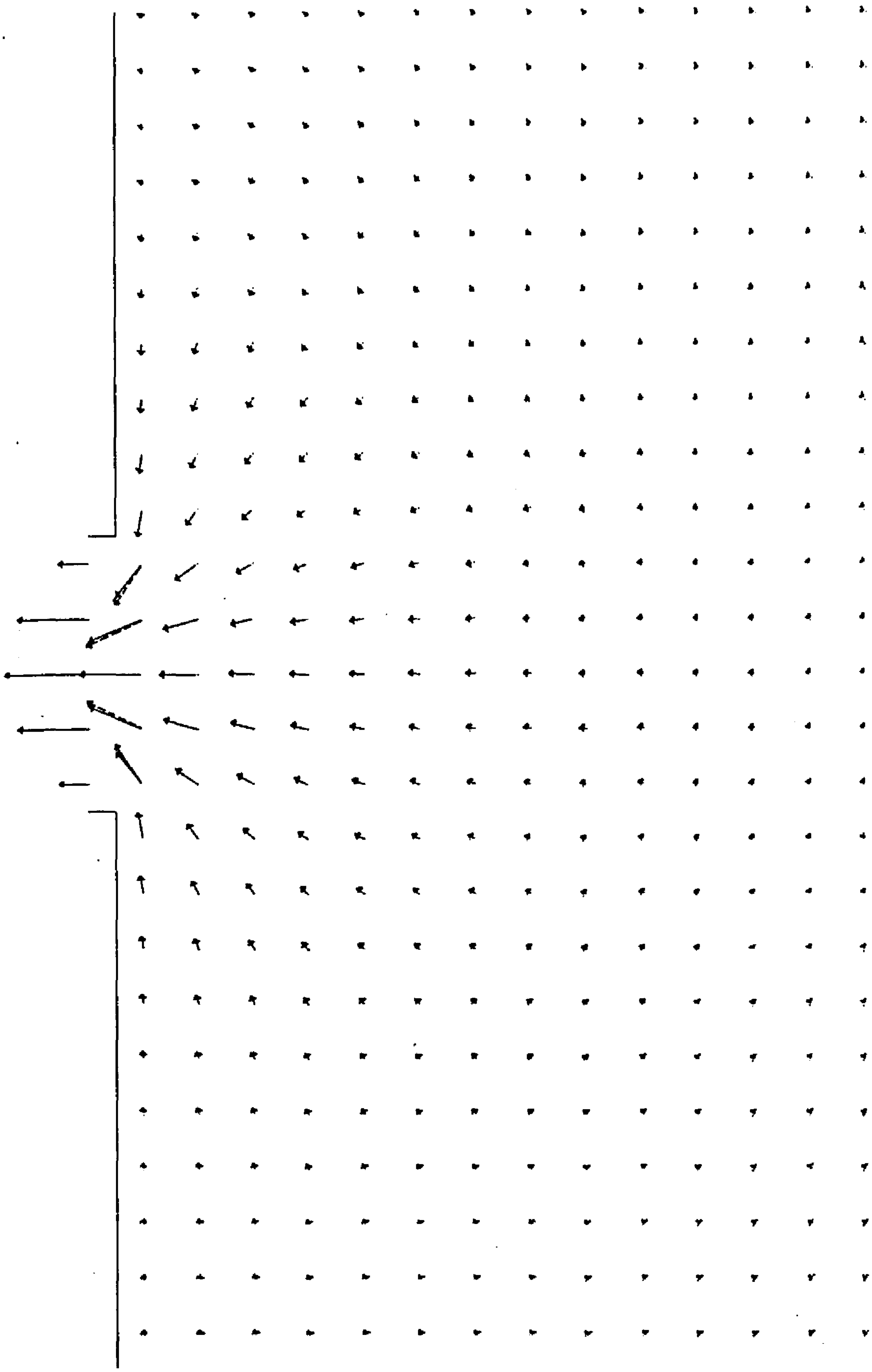

Figure 33 - Velocity vector plot, oscillating jet at maximum flood and with sloping bottom

causes the jet to change slightly in shape. This is illustrated by the dashed vector lines in Figures 32 and 33. The dashed lines located near the mouth of the Bay are the vectors for the Case I oscillating jet at the same grid point and time. From the comparison of the dashed and solid vector lines in Figures 32 and 33, it can be concluded that the sloping bottom causes the jet to be less dispersive during the ebb and less convergent during the flood in the vicinity of the Bay entrance. This result for the ebb case agrees with the laboratory modeling results of Borichansky and Mikhailov (1966), in their work on the interaction of river and seawater in the absence of tides. Further, if the lengths of the vectors are compared for the two cases, it will be seen that generally the magnitudes of the vectors for the flat bottom case are larger than those for the sloping bottom. This is illustrated by the centerline velocity during ebb, Figure 28.

Finally, it is believed that the causes of the dispersive and convergent characteristics of the jet are the same as those described for Case I of the oscillating and Case I of the steady-state jets.

Cases IV and V - These cases are for the effect of wind stress and are discussed below. The value of the wind stress τ^s used was for a wind of 15 knots. The wind stress is defined as $\tau^s = 2.6 \times 10^{-3} \rho_a'(W')^2$, where ρ_a is the density of air in gm cm^{-3} and W' is the wind speed in cm sec^{-1} at a height of 15 meters above the sea surface. This gave a value of τ^s of 1.9 dyne cm^{-2} for a wind speed of 15 knots (750 cm sec^{-1}). Two cases were run: Case IV, where the wind was on-shore, and Case V, for a northerly wind. The results are shown in Figures 34 through 37.

Case IV - Figures 34 and 35 show the vector plots at maximum ebb and flood, respectively. During maximum ebb, the outflow along the center of the jet is retarded and the jet is split and deflected, symmetrically, north and south. A plot of the centerline velocity as a function of distance for maximum ebb is shown in Figure 28. This type of situation creates an area of minimum velocity where the centerline velocity goes to zero. Also, the jet when split is driven parallel and close to the shore.

For the maximum flood case the wind stress drives water toward the Bay and shore, causing two areas of zero velocity above and below the jet.

These two plots are somewhat representative of the flow features for an on-shore wind but must be interpreted with caution. The major difference between the representation in these figures and that which exists in nature is that here the jet mass transport does not change with an on-shore

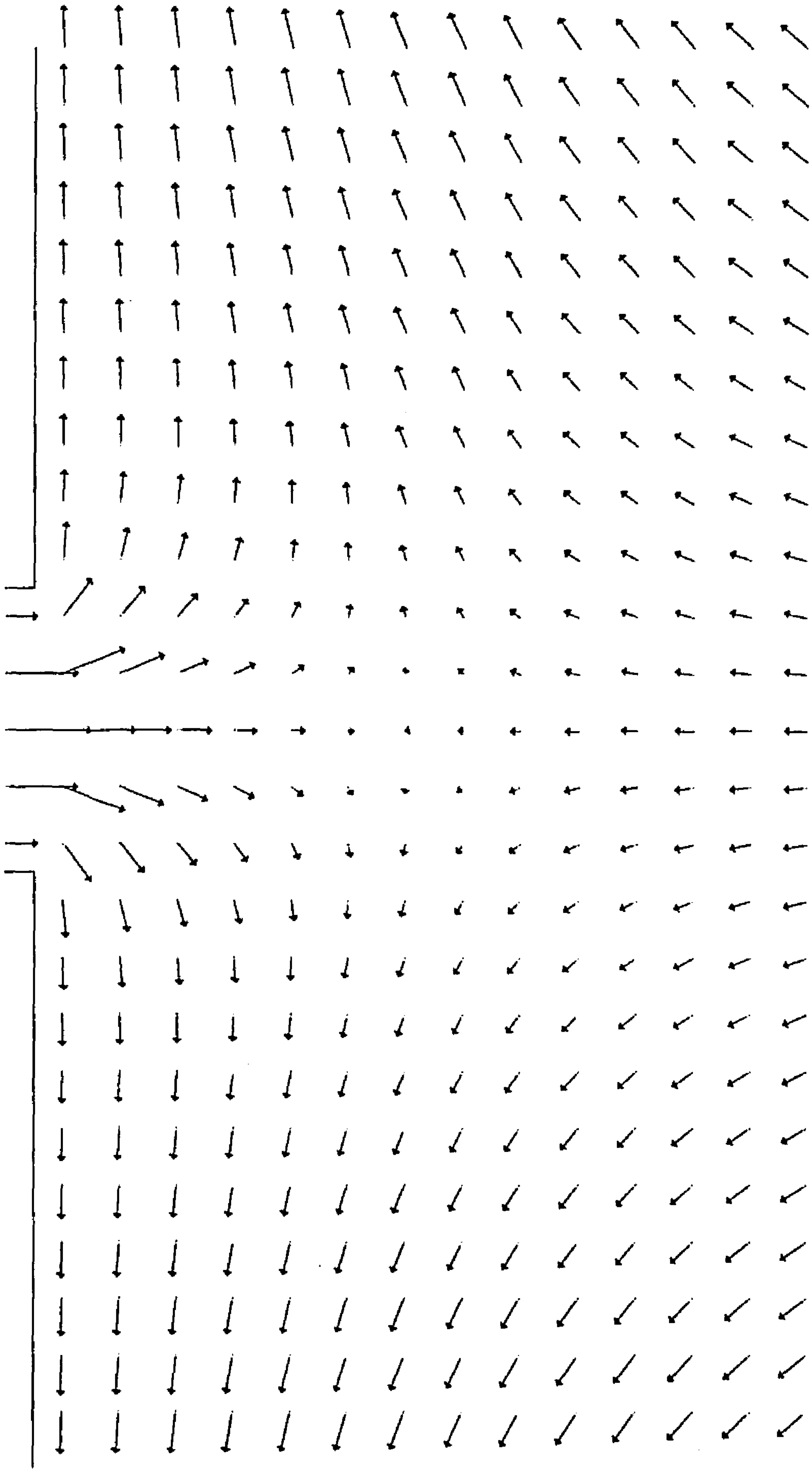

Figure 34 - Velocity vector plot, oscillating jet at maximum ebb and with onshore wind

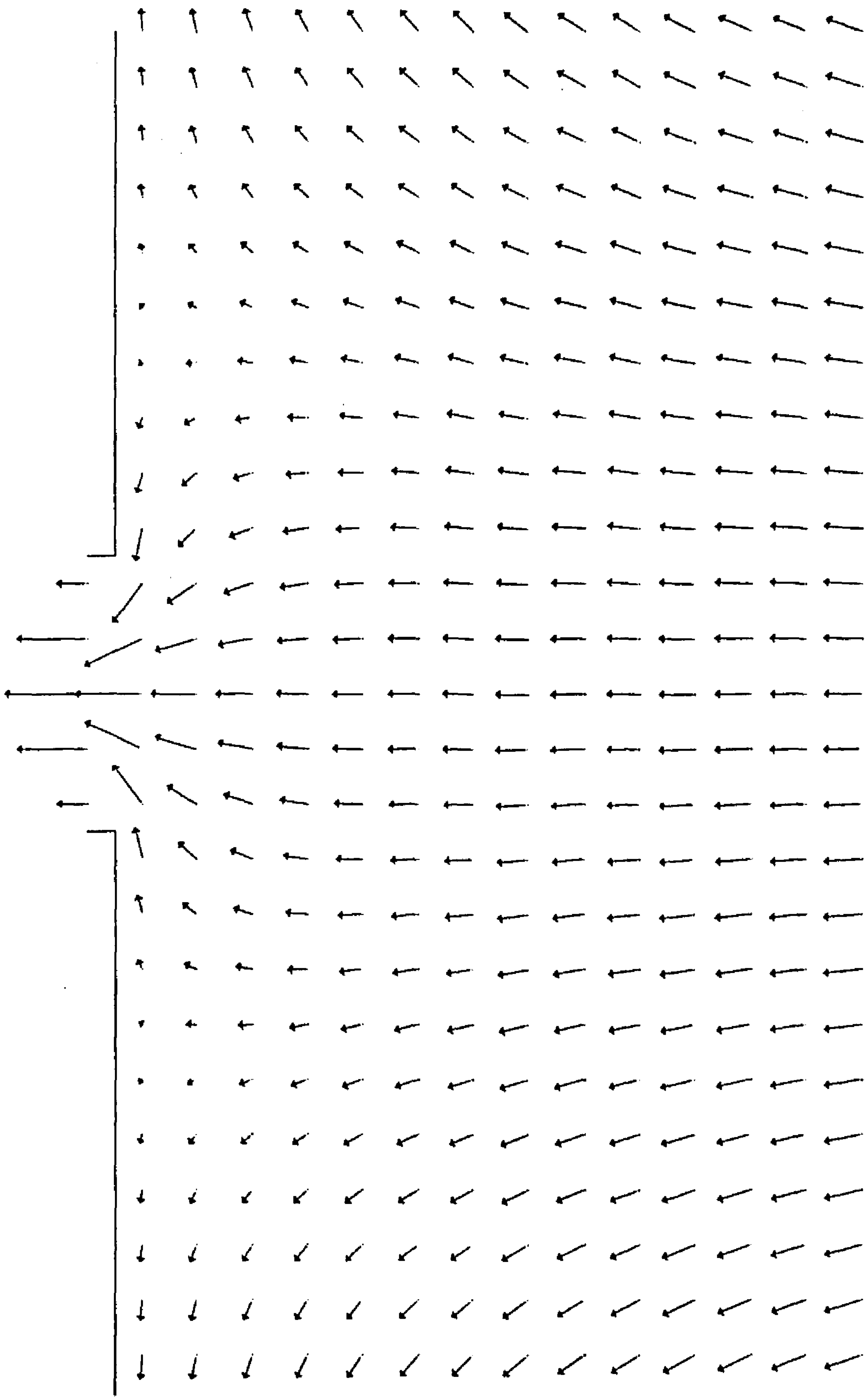

Figure 35 - Velocity vector plot, oscillating jet at maximum flood and with onshore wind

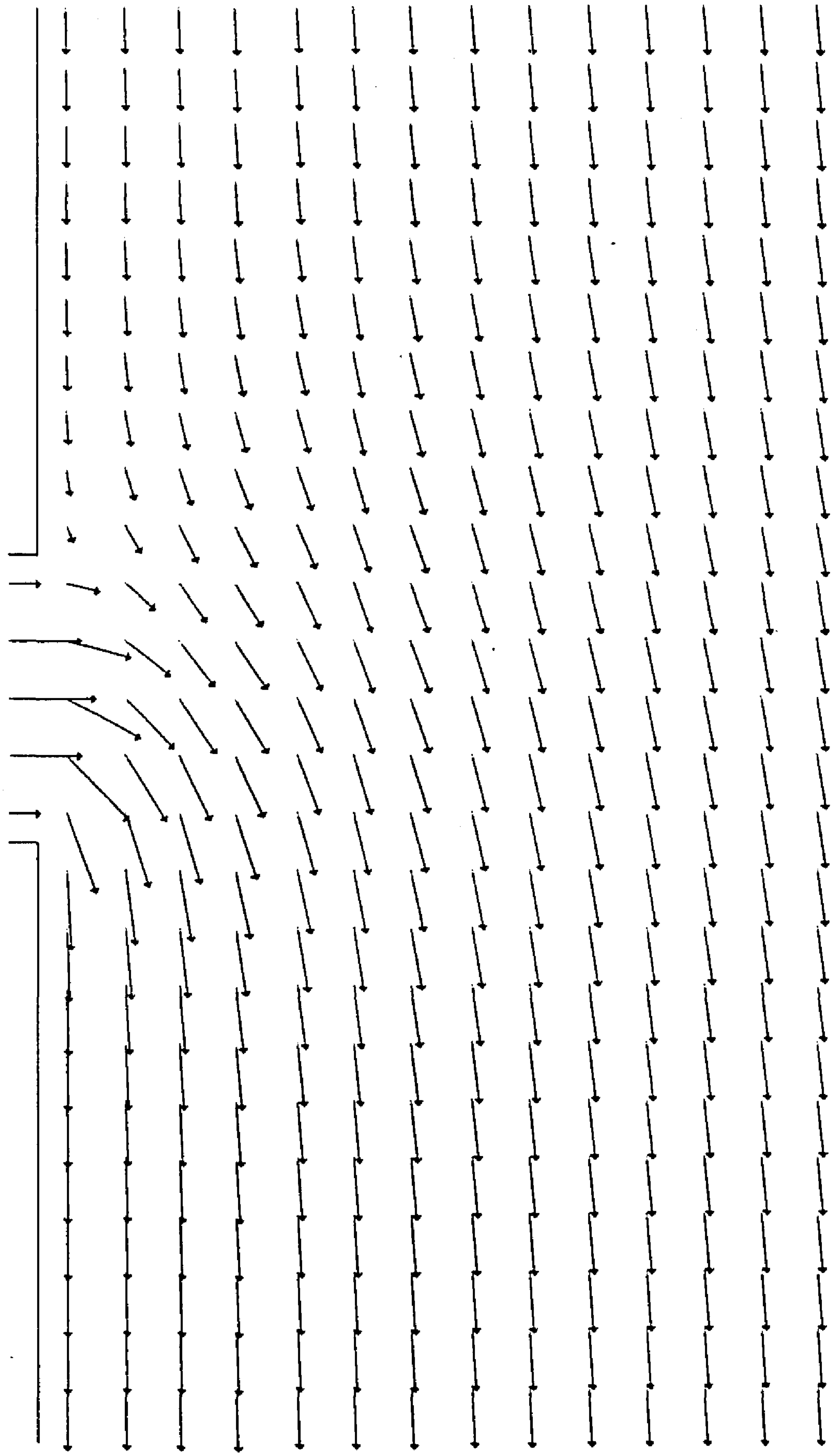

Figure 36 - Velocity vector plot, oscillating jet
at maximum ebb and with northerly wind

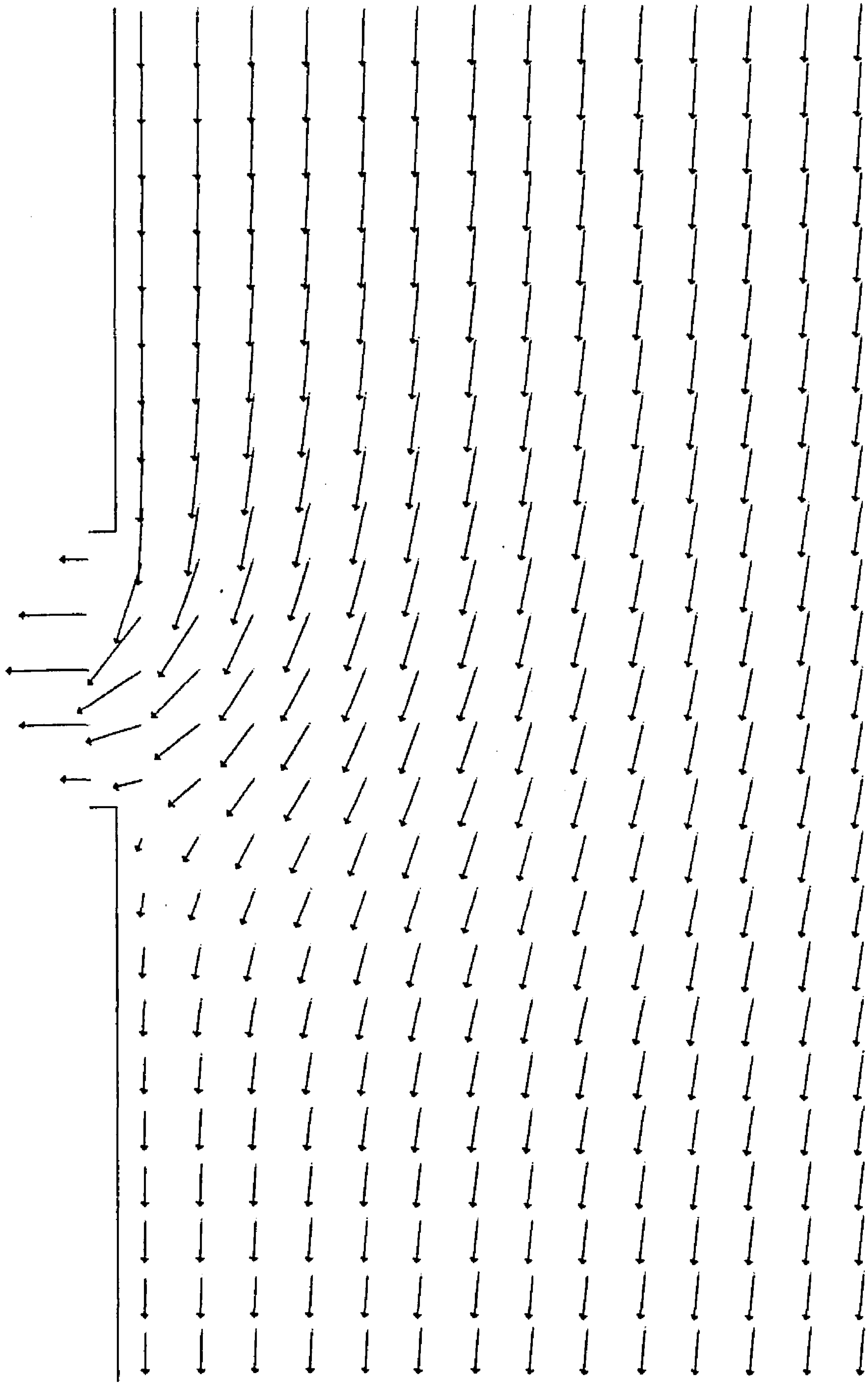

Figure 37 - Velocity vector plot, oscillating jet at maximum flood and with northerly wind

wind. Stated another way, there is no provision made for mass movement into the Bay, caused by the wind, using the velocity as a boundary condition. Therefore, the plots as shown in Figures 34 and 35 probably have features which would not be seen in a true coastal situation. The important conclusion from studying these two figures is that an on-shore wind can be very effective in changing the flow pattern, and the features given by Figures 34 and 35 are a very general representation of what probably takes place with an on-shore wind.

Case V - Figures 36 and 37 show the results of a north wind blowing over the shallow continental sea. Here the flow is deflected south on the ebb and deflected into the Bay on the flood. There seems to be a point of low velocity during the flood stage south of the jet and also a deflection of the vectors toward shore.

Boicourt (1973) and Stommel and Leetmaa (1972), in their studies of the circulation of the water on the continental shelf, pointed out the importance of wind in driving the shelf circulation. Boicourt (1973) and others have noted that a strong west wind will drive water out of the Bay, while a strong on-shore wind will cause an increase in water level in the Bay. While the results of Case IV do not show the mass flux into the Bay by an on-shore wind due to the oscillating jet boundary condition, the flow patterns generated do indicate that, if a mass flow across the boundary were allowed, there would be a net flow into the Bay.

The effect of the wind parallel to shore has also been noted in the literature. Budringer, et al (1964), and Duxbury, et al (1966), as quoted by Boicourt (1973), in their description of the Columbia River outflow, assign the cause of outflow deflection to the north in the summer and to the south during the winter to the prevailing winds present during these seasons.

The results from Case V indeed suggest that the stress caused by the wind is a much more dominant force than the Coriolis force and is just as effective as an ambient velocity in deflecting the outflow.

Finally, it will be noted that eddies were not generated in either Case IV or Case V.

Case VI - The final case is one with an ambient velocity imposed upon the situation of Case I. Because the north-south boundary conditions for an oscillating jet are tidal heights, the initial and boundary conditions had to be changed from those of Cases I through IV. The ambient velocity was generated by raising the northern boundary either 5 or 11 cm above datum to give a velocity flowing south of approximately 5 and 10 cm sec^{-1}, respectively, across the shelf.

This slope is not a unique condition. Stommel and Leetmaa (1972) in their model of the shelf circulation pointed out the importance of the sea surface slope in their coastal model. Sturges (1974) has discussed the slope of the sea surface in this region and described the seasonal variation of sea level at Norfolk, Virginia. Sturges (1974) estimates the slope of the sea surface in the region being modeled as 2.0 ± 0.4 cm/degree or 0.023 to 0.04 cm/nm. For the grid used here the slope was 0.052 and 0.104 cm/nm. It is recognized that most reported shelf velocities for this region are estimated to be 5 cm sec^{-1} or less; thus, a slope of 0.052 cm/nm approaches a more realistic situation. The importance of small changes in water level here and in the previous cases for both the steady-state and oscillating jets illustrates the need for a good understanding of the permanent, seasonal, and daily variations of the sea surface in order to accurately predict the flow.

Initial conditions for the run were $U = V = 0, \delta = f(y)$. Boundary conditions for the western boundary remained the same, while for the eastern boundary $\delta = f(y)$. For the northern boundary $\delta = 5$ or 11, and for the southern boundary

$\delta = 0$. The results of the computations are shown in Figures 38 through 41 for the maximum ebb and flood of the second tidal cycle with a northern boundary of $\delta = 5$ and 11, respectively.

For Figures 38 and 40 several features can be noted: a quicker turning of the jet by the ambient current than for Case IV of the steady-state jet, a northern velocity which goes to zero along the coast and above the jet, and a confinement of the jet closer to shore.

The rapid turning of the flow by the ambient velocity once it leaves the Bay (Figures 38 and 40) is caused by three factors. First, the ambient velocity is almost constant across the shelf and, therefore, its value near shore is not zero as in the case for the steady-state jet. Second, the magnitudes of the ambient currents used are greater than the 4 cm sec^{-1} used for the steady-state case. Third, the jet velocity is not maintained constant at maximum ebb speed.

Thus, the ambient velocity in these two cases is a more effective factor for the deflection of the jet than the Coriolis force.

The northern velocity along the coast above the Bay entrance has been verified by several observers, Harrison, et al (1967), Bumpus (1969), and discussed in Case IV of

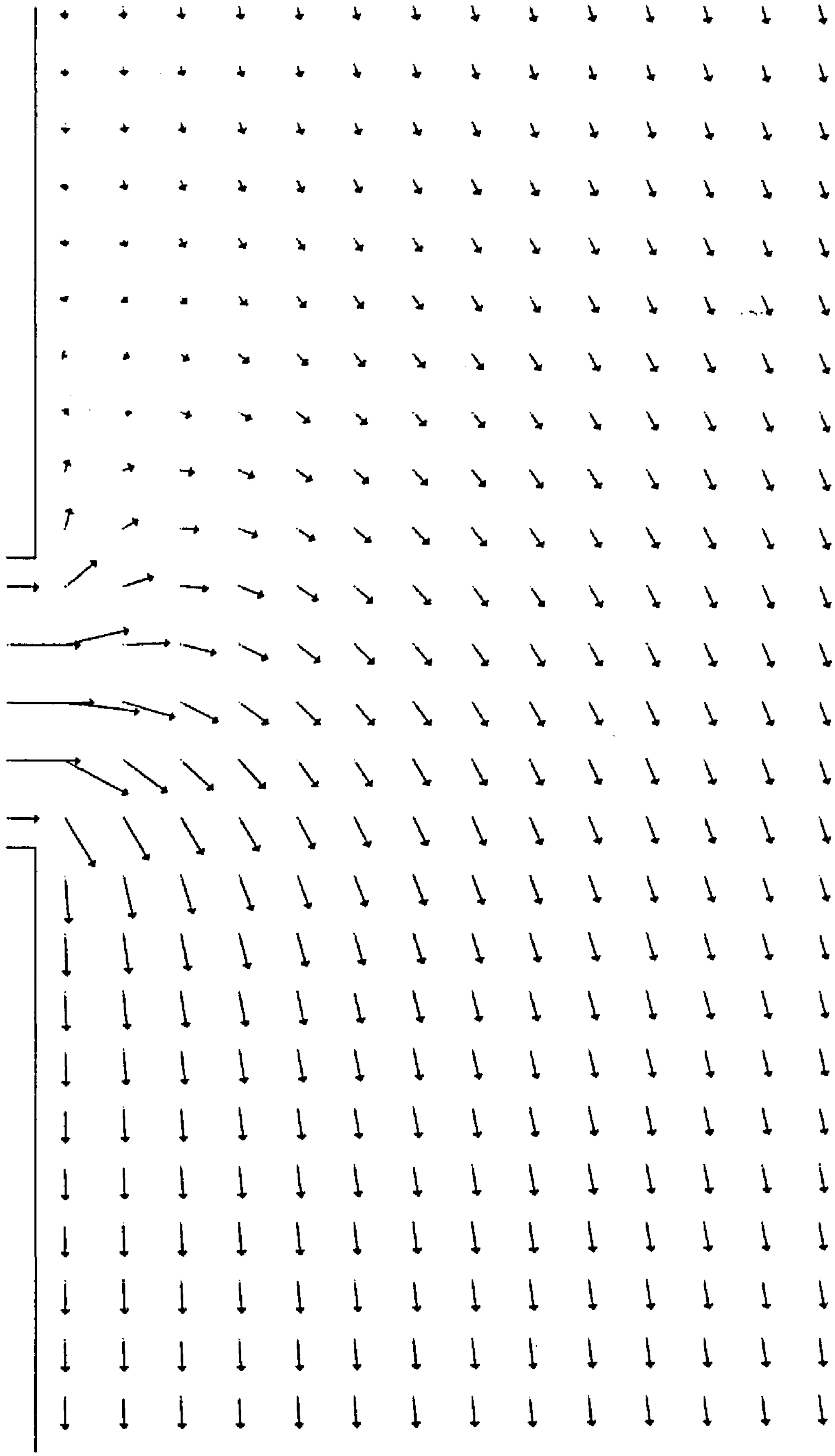

Figure 38 - Velocity vector plot, oscillating jet at maximum ebb and with a southerly ambient velocity of 5 cm sec^{-1}

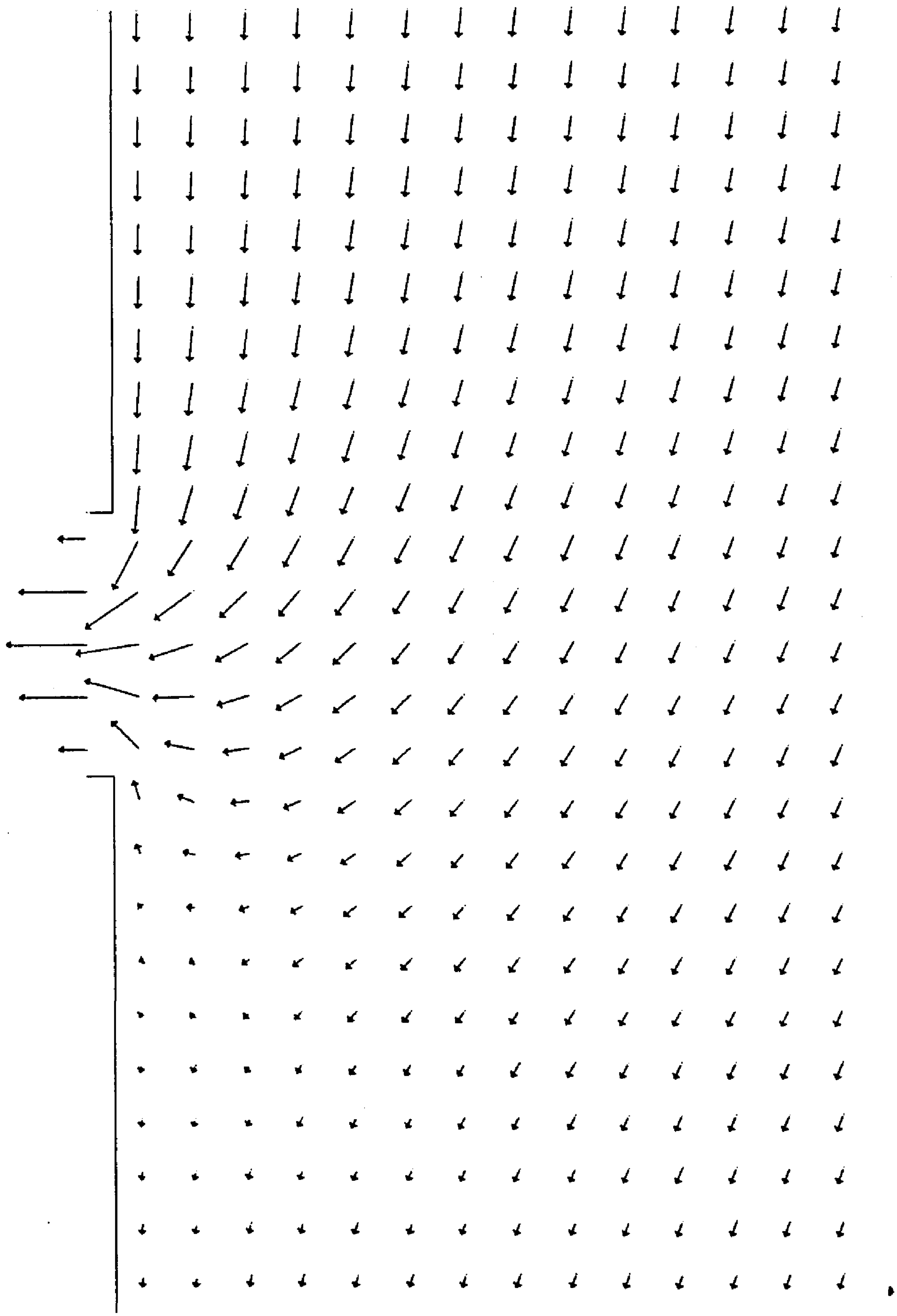

Figure 39 - Velocity vector plot, oscillating jet at maximum flood and with a southerly ambient velocity of 5 cm sec^{-1}

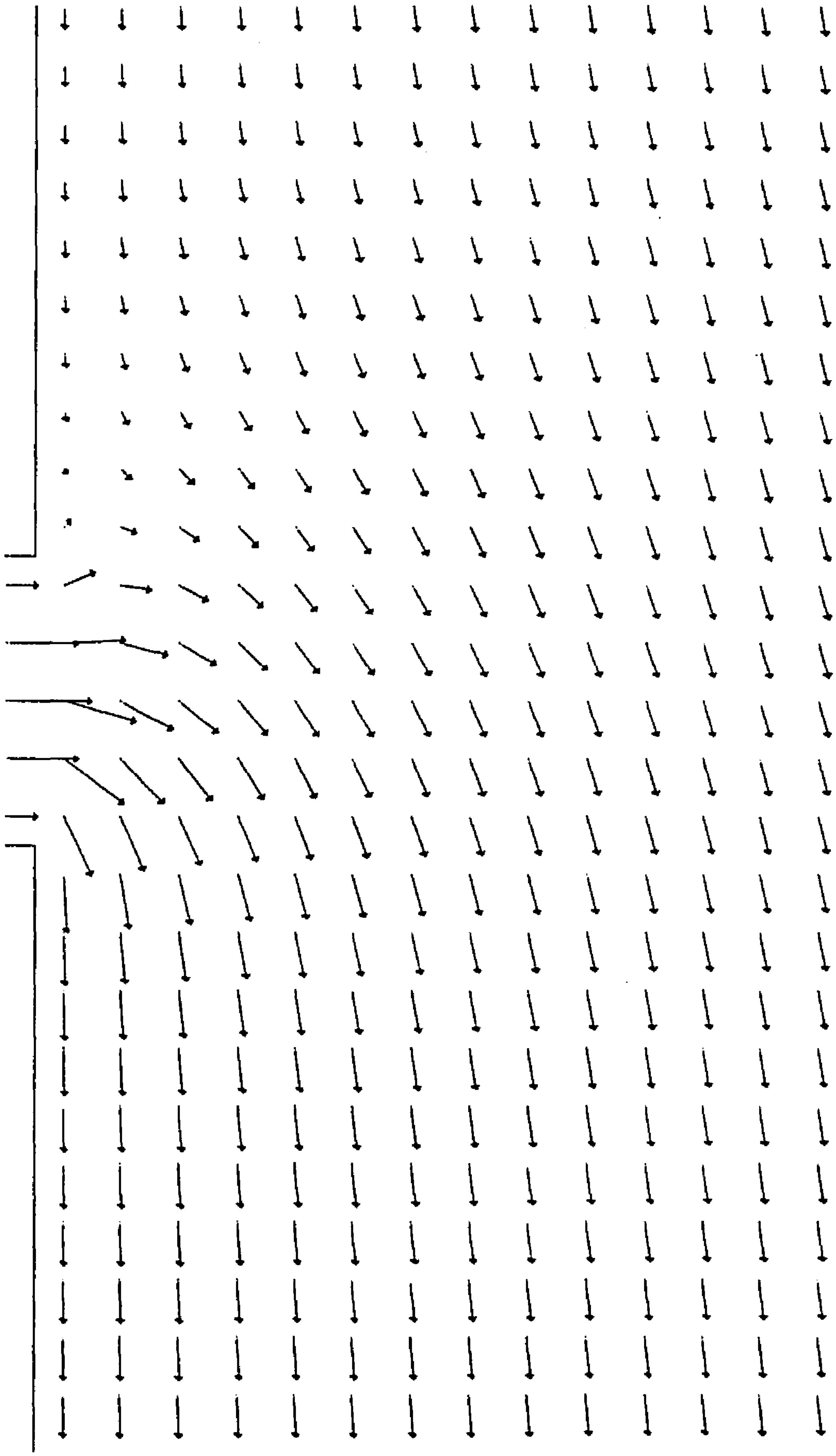

Figure 40 - Velocity vector plot, oscillating jet at maximum ebb and with a southerly ambient velocity of 10 cm sec^{-1}

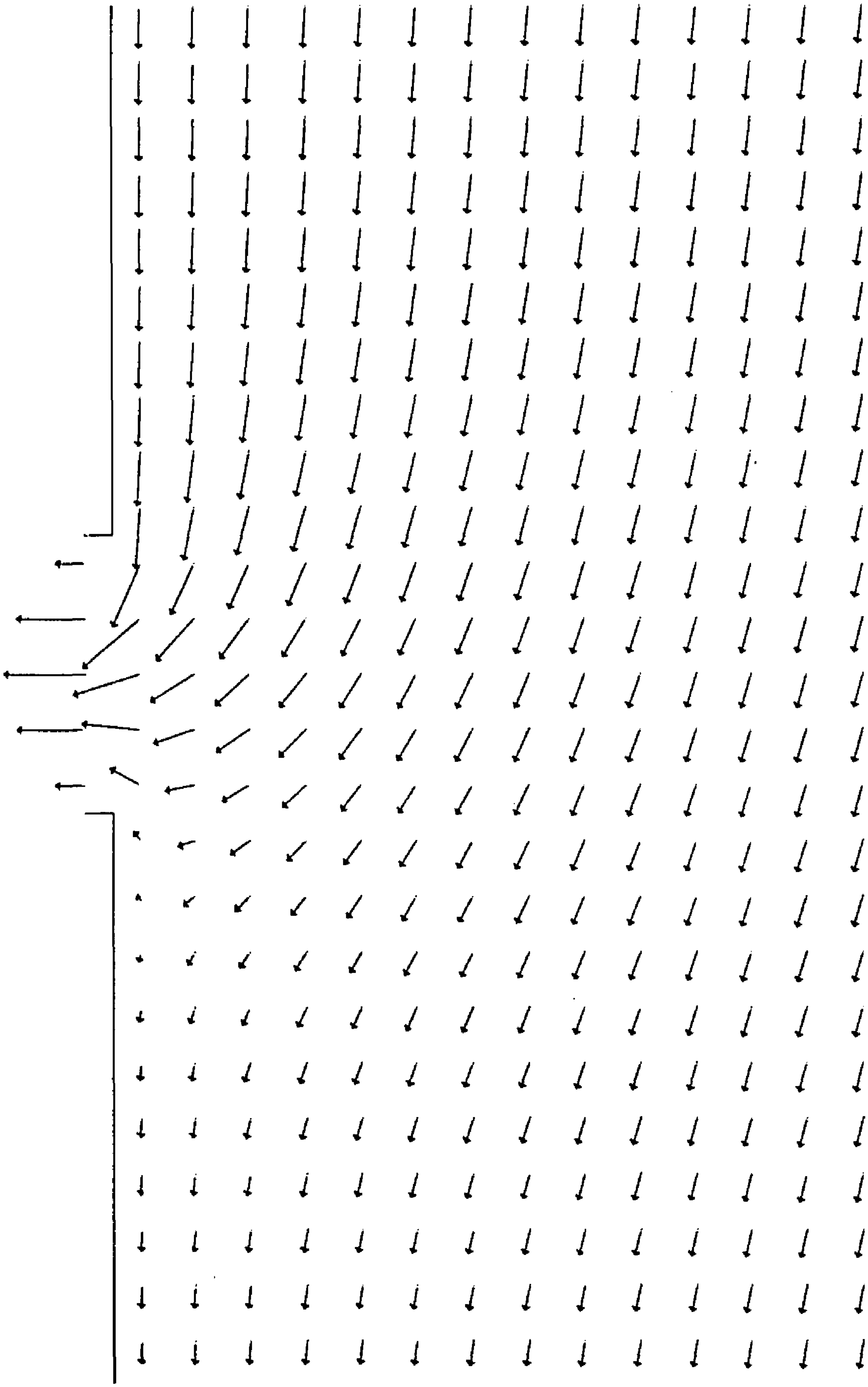

Figure 41 - Velocity vector plot, oscillating jet at maximum flood and with a southerly ambient velocity of 10 cm sec^{-1}

the steady-state jet. Figures 38 and 40 show the way this feature could be limited to an area of coastline just above the Bay entrance and how it can vary with strength of the wind and outflow from the Bay.

Figure 42 is a plot of the salinity distribution on the continental shelf for the month of July 1972. This figure outlines the direction of flow from the Chesapeake Bay when it leaves the entrance. The similarity of the flow pattern of Figure 42 when compared with Figures 38 and 40 is apparent. However, there are some differences which should be noted.

Boicourt (1973) points out that the isohalines leave the Bay entrance at an angle. Current meter observations of Boicourt (1973) and Kuo (Virginia Institute of Marine Sciences, private communication) indeed show that the currents at places in the Bay entrance exit in a direction more southeasterly than due east. This is probably caused by the main channel which also exits in a southeast direction. This fact, along with the ambient southern velocity, probably causes the current to be confined along the coast in a more narrow band than is shown in Figures 38 and 40. Boicourt (1973) has also pointed out that the salinity pattern off the Bay entrance will be a function of the wind and volume of flow out of the Bay. Thus, while the salinity

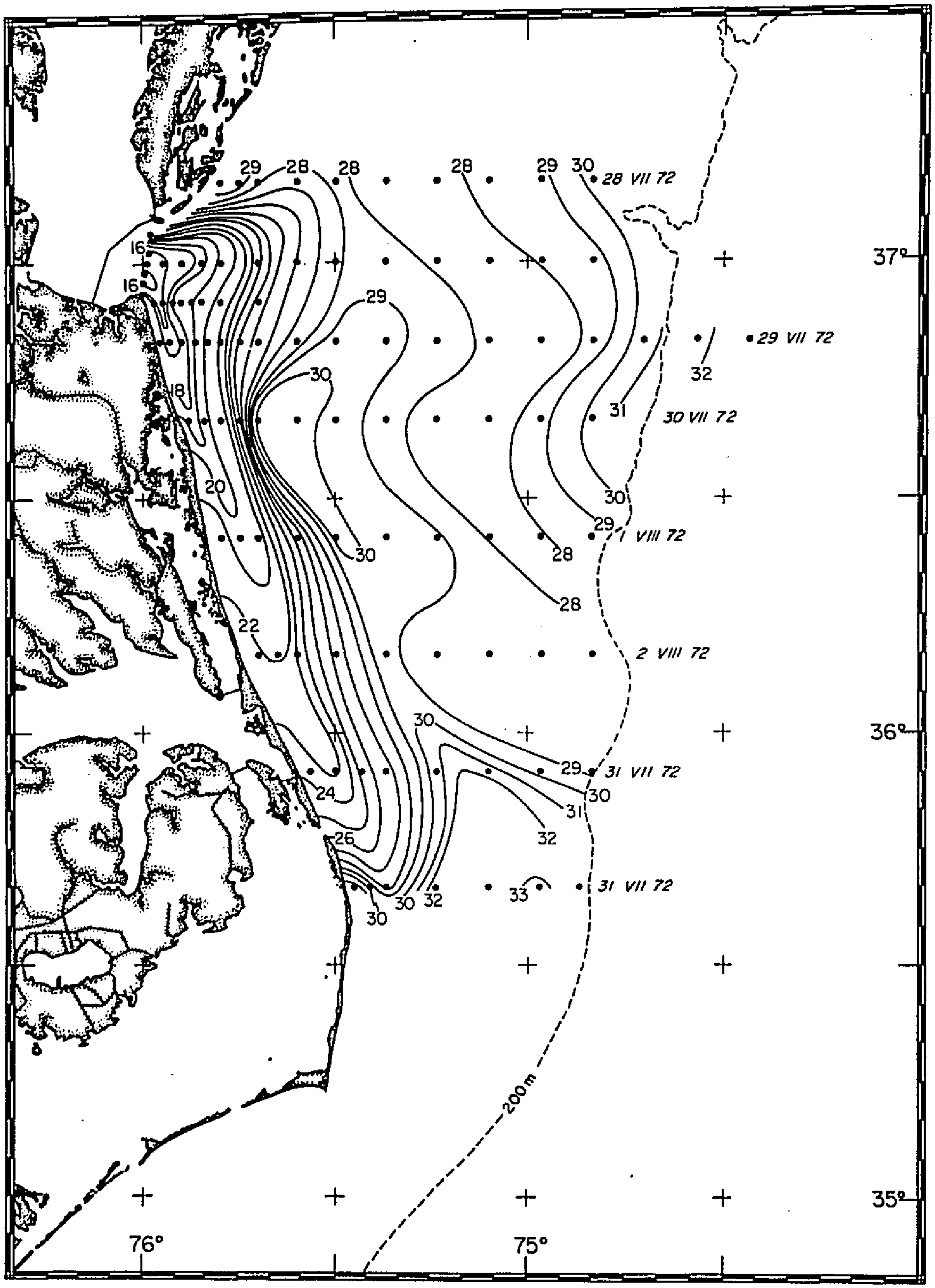

Figure 42
Chesapeake Bight surface salinity distribution
July-August 1972

pattern of Figure 42 verifies in a general way the flow pattern of Figures 38 and 40, the final results will be functions of many variables, some not considered in the discussion of this case.

The flow patterns for the flood tide, Figures 39 and 41, also show three prominant characteristics: a turning of the southerly flow into the Bay, a point of minimal velocity south of the Bay entrance where the flow seems to split, and a weakness of the southerly flow below the Bay entrance. Figures 39 and 41 compare well with the flow patterns into the Bay composed by Boicourt (1973) and described by Harrison, et al (1967).

The flow was averaged over a tidal cycle (for the same points used in Cases I and II) to see if there was an eddy present. The southward, 5 cm sec^{-1}, flowing ambient velocity wiped out the eddy so that no traces of it were found. From an Eulerian standpoint, the eddy has been destroyed.

Finally, Figure 43 shows a series of vector plots for selected points and conditions over a complete tidal cycle. Figure 43a shows for comparison the vectors for Case I at the point $m = 3$ and $n = 22$ (above the Bay mouth). This figure shows a slight rotary characteristic for the tide. Figure 43b is for the same point but with an ambient velocity of 5 cm sec^{-1} south. Figure 43c is for the point

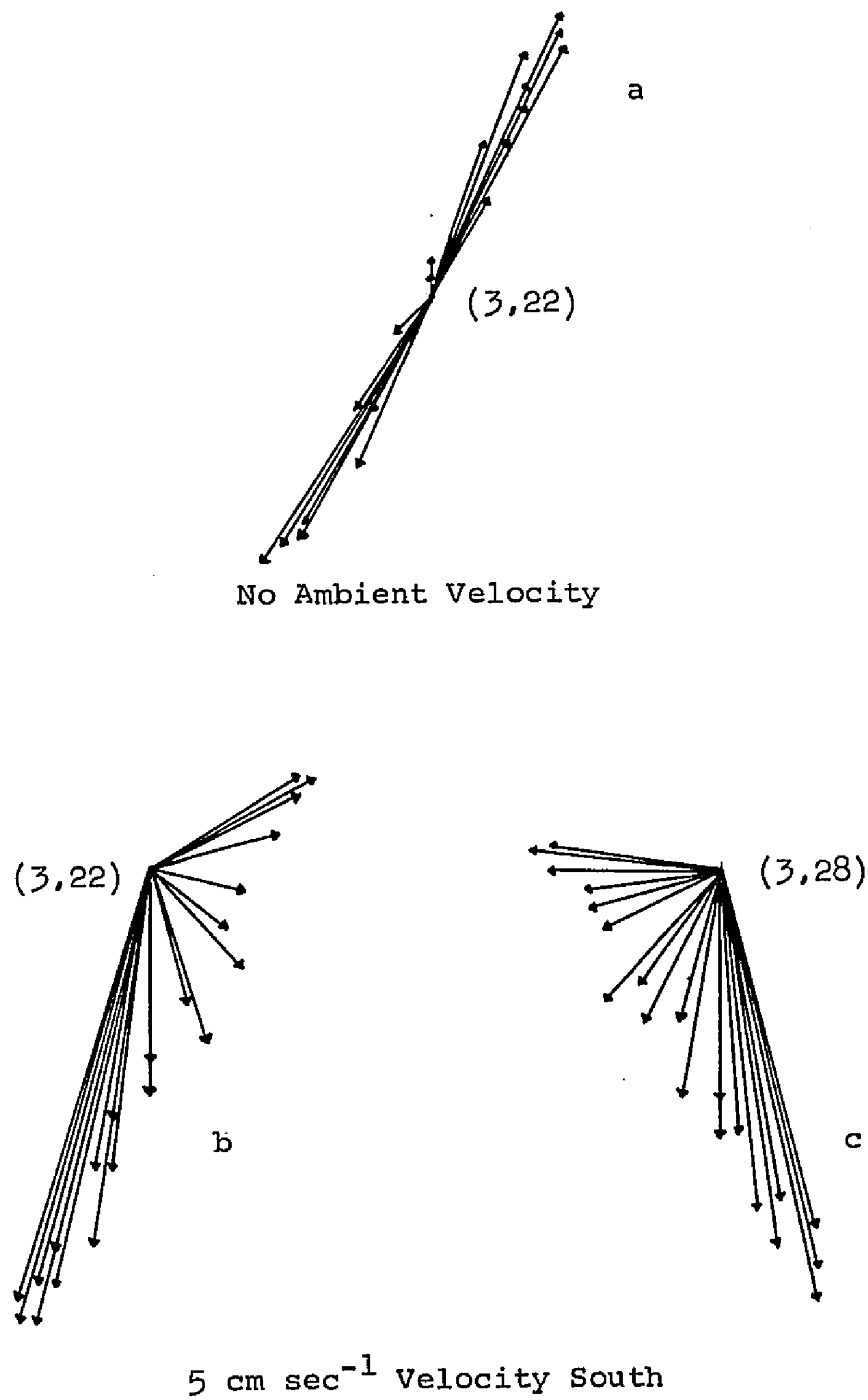

Figure 43
Velocity vector roses at two grid points

$m = 3$, $n = 28$ (below the Bay mouth) and with an ambient current of 5 cm sec^{-1}. Both of these figures show a more diversive spread of the vectors due to the ambient current.

CHAPTER VII

CONCLUSIONS AND RECOMMENDATIONS

The intent of this investigation was to discern the resultant flow fields arising from the discharge of a tidal estuary or river onto the continental shelf using the continuity, momentum, and mass balance equations. The approach was to numerically model the area, simplify the geometry and physical situation where possible, and determine the relative effect of different physical factors on the flow. The model developed in Chapters II through V and the results of its application given in Chapter VI have accomplished this. The results, while for much simpler cases than arise in nature, nevertheless are useful and applicable toward understanding natural situations.

Conclusions

From the results and discussion of Chapter VI it can be concluded that the outflow from a tidal or non-tidal estuary or river onto a continental shelf can be broken into three types: dispersive, in which the velocity vectors diverge from the centerline; entraining, in which the velocity vectors converge toward the centerline; or a combination of the two. The final type will be governed by the degree of bottom and side frictions, the bottom slope, and the level of the water above datum at the Bay entrance.

The centerline velocity of the bottom friction steady-state jet studied was found to decrease much more rapidly than the side friction cases reported in the literature. Cross-stream U velocities for the same bottom friction case were a function of $\operatorname{sech}^2 y$. For a steady-state jet which considers both side and bottom friction, the centerline velocity profile was found to be a combination of the pure side and bottom friction cases.

For the model case of the Chesapeake Bay, it was determined that the outflow is dispersive, with a centerline velocity decreasing to less than half its maximum velocity in one jet width. Field observations of estuaries other than the Chesapeake Bay verify the rapid velocity decrease along the centerline, but no information was found on the characteristics of the cross-stream velocity distribution. The velocity distribution both along the centerline and laterally will be affected by the wind and ambient currents in the vicinity of the discharge so that field verification of these profiles will be difficult.

From the results of all the cases studied, the slope of the sea surface relative to mean sea level is very important in controlling the movement of the shelf waters, as previously mentioned. For the area studied (Chesapeake Bight) the sea surface slope needed to generate an ambient current, corresponding to currents found by field measurements, agreed with leveling observations by a factor less than two. Small value of the sea surface slope needed and the sensitivity of the model to it suggest that in a natural environment both the permanent sea level height and the seasonal and tidal variations should be accurately known in order to model and predict the shelf circulation, particularly if tidal heights are used as a boundary condition. For modeling purposes it is estimated that this water level should be known to within at least 1-2 cm.

The Coriolis force has often been considered to be the most important factor for generating the turning of an estuary or river (in nature) as it empties onto a shelf. In contrast, for the cases studied, the Coriolis force was not found to be a controlling factor in the turning of the outflow. This turning is believed to be masked by the effect of bottom friction and is illustrated by the large values of the Ekman number (≥ 1) for the cases used.

Thus, the cases studied suggest that, if in nature the bottom friction and the inertial terms are dominant, the wind and ambient current are more important factors in the deflection of the outflow than the Coriolis force.

For the steady-state jet no eddies were found in all four cases investigated. For the oscillating jet eddies were found for Cases I and II after the tidal component was averaged out. The effect of the Coriolis force in Case II was to decrease the strength of the southern flow of the eddies and increase the strength of the northern flow. This also confirms the results reported by other investigators.

This study substantiates the reversal of flow in the circulation pattern above the Bay entrance that has been reported by other investigators both for the Chesapeake Bay and other areas in the Mid-Atlantic Bight. From the model studies, the strength of this reversal will be a function of the strength of the ambient current, dispersion of the outflow from the Bay or river entrance, and wind. The flow can also be tidal dependent.

Results from the modeling efforts show that tidal height or velocity can be used for an open boundary condition. However, if velocity is used, care must be taken to assure that reflection from the boundary does not occur.

This problem can be eliminated by the use of tidal heights for the open boundary conditions, which most investigators use in a model of this type.

The multi-operational techniques used here have proven to be stable and fast. The technique is a more economical way to calculate data than a purely explicit scheme.

Recommendations

Recommendations for future work in the use of this or other models in studying the coastal flow in the vicinity of the Chesapeake Bay entrance can be divided into two general categories: intermediate and advanced.

For the intermediate step, several features and/or factors which were not included in this study should be examined. These are: (1) a more detailed evaluation of the mass conservation of the numerical scheme to verify Leendertse's work; (2) incorporation and use of the mass transport equation to study the effect of simple salinity and density variations on the flow patterns; (3) altering the Bay's discharge to the southeast to observe the difference in flow characteristics above and below the Bay entrance; (4) sloping the bottom to approach a depth of zero near the coast and varying the bottom friction terms to more accurately represent the near shore circulation; (5) development and use of the side friction terms; and (6) use of a jet (to simulate the Bay discharge) interacting with a tidal wave propagating normal to the coast to more nearly approximate the true environmental situation in the Chesapeake Bight.

For the advanced category expansion of the models to three dimensions to investigate the layered flow in the Chesapeake Bight is desirable. However, the cost of developing and using a model of this type may be prohibitive. Further, sufficient field data on the tidal and non-tidal circulation in the coastal zone during a typical summer and winter condition are needed to calibrate both the two- and three-dimensional models. The size and cost of a field program of this nature would depend on the area of interest and extent of modeling undertaken.

APPENDIX A

ORDER OF MAGNITUDE ESTIMATE

Compare the magnitudes of

$$-\frac{g H^2}{\bar{\rho} L}\frac{\partial \bar{\rho}}{\partial x} \qquad \text{A.1}$$

and

$$-\frac{g}{\bar{\rho}}\frac{\partial}{\partial x}\int_{-h}^{\delta}\left(\int_{z}^{\delta}\rho' dz\right)dz. \qquad \text{A.2}$$

By using the first two terms of Taylor series, let

$$\rho(z) \approx \bar{\rho} + \left.\frac{\partial \rho}{\partial z}\right|_{z=z_o}(z-z_o) \qquad \text{A.3}$$

where z_o is the position in the vertical at which the density equals $\bar{\rho}$. Now using 2.21 and A.3 and evaluating $\partial\rho/\partial z$ at $z = z_o$ gives

$$\rho' = \rho - \bar{\rho} \approx \left.\frac{\partial \rho}{\partial z}\right|_{z_o}(z-z_o) \qquad \text{A.4}$$

Integrating A.4 from z to δ yields

$$\int_{z}^{\delta}\rho' dz \approx \frac{1}{2}\left.\frac{\partial \rho}{\partial z}\right|_{z_o}\left[(\delta-z_o)^2-(z-z_o)^2\right]. \qquad \text{A.5}$$

Integrating A.5 from -h to δ and combining terms gives

$$\int_{-h}^{\delta}\left(\int_{z}^{\delta}\rho' dz\right)dz \approx \frac{H}{2}\left.\frac{\partial \rho}{\partial z}\right|_{z_o}\left[\frac{2}{3}(\delta-z_o)^2+\frac{1}{3}(\delta-z_o)(h+z_o)-\frac{1}{3}(h+z_o)^2\right] \qquad \text{A.6}$$

Assuming $z_o = (-h + \delta)/2$ and substituting into A.6 gives

$$\int_{-h}^{\delta}\left(\int_{z}^{\delta}\rho' dz\right)dz \approx \frac{H^3}{12}\left.\frac{\partial \rho}{\partial z}\right|_{z_o}. \qquad \text{A.7}$$

Now substituting A.7 into A.2 yields A.8, a form of A.2 whose magnitude can be evaluated

$$-\frac{g}{\bar{\rho}}\frac{\partial}{\partial x}\left(\frac{H^3}{12}\frac{\partial \rho}{\partial z}\right) \approx \frac{g}{\bar{\rho}}\frac{H^2}{12}\frac{\partial}{\partial x}\Delta\rho \qquad \text{A.8}$$

where $\Delta\rho$ is the density variation over the water column. The relative magnitude of A.8 and A.1 is then

$$\frac{-\frac{g}{\bar{\rho}}\frac{H^2}{12}\frac{\partial \Delta\rho}{\partial x}}{-\frac{g}{\bar{\rho}}\frac{H^2}{2}\frac{\partial \bar{\rho}}{\partial x}} = \frac{1}{6}\,\frac{\frac{\partial}{\partial x}\Delta\rho}{\frac{\partial \bar{\rho}}{\partial x}} = R\,. \qquad \text{A.9}$$

Equation A.9 is a ratio of A.2 to A.1. If this ratio is ≤ 0.1 (A.1 > A.8 by a factor of 10 or more), then equations 2.39 and 2.40 are valid. Simple examples of density distributions where term A.2 can be ignored are shown below:

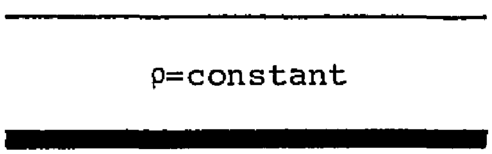

$$R = \frac{1}{6}\,\frac{0}{0} = \frac{0}{0}$$

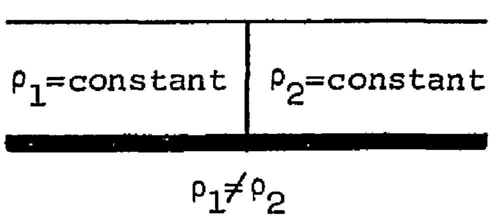

$$R = \frac{1}{6}\,\frac{0}{\frac{\partial \bar{\rho}}{\partial x}} = 0$$

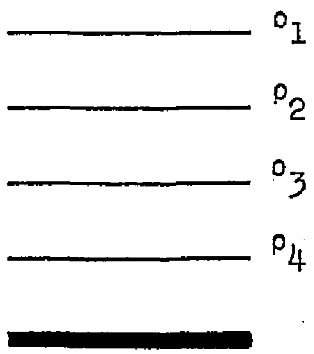

$\rho_1<\rho_2<\rho_3<\rho_4$

$$R = \frac{1}{6}\,\frac{0}{0} = \frac{0}{0}$$

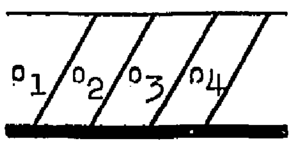

$\rho_1<\rho_2<\rho_3<\rho_4$

$$R = \frac{1}{6}\,\frac{0}{\frac{\partial \rho}{\partial x}} = 0$$

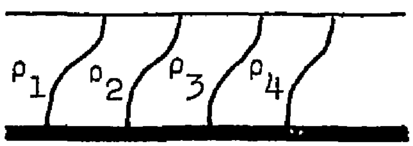

$\rho_1<\rho_2<\rho_3<\rho_4$

The general cases where the surfaces of constant density are approximately parallel.

If the density distribution in the water column gives a ratio $R > 0.1$, then term A.2 cannot be ignored and equations 2.39 and 2.40 are not valid. The case $R > 0.1$ would imply the existence of relatively strong vertical stratification and the simulation by a vertically integrated two-dimensional model will not be applicable. Therefore, in the framework of two-dimensional approximation, it may be assumed that equations 2.39 and 2.40 are valid.

APPENDIX B

TABLE OF EQUIVALENTS

Text Notation	Computer Notation
f	FC
g	G
h	H
$\bar{h}$	HAVG
m	J
n	K
x	X
y	Y
c	C*
D_i	DX,DY*
H^{it}_{jF}, H^{it}_{jB}	HXF,HYF,HXB,HYB*
s	S*
$\bar{U}$	U1A
U	U*
$\bar{V}$	V1A
V	V*
α	A1
δ	HL*
ρ	R*
τ^s_x, τ^s_y	WSX,WSY
ΔL	L
Δt	DT

Text Notation	Computer Notation
A_j	1/2DT
B_j	BX,BY
C_j	CX,CY
D_j	DX,DY
E_j	EX,EY
F_j	G/2L
H_j	HCX,HCY
P_j	PX,PY
Q_j	QX,QY
R_j	RX,RY
T_j	TX,TY
A'_j	AAX,AAY
B'_j	BBX,BBY
C'_j	CCX,CCY
D'_j	DDX,DDY
E'_j	EEX,EEY
F'_j	FFX,FFY

NOTE: Notations with an asterisk may have a 1 or 2 with them; i.e., S1, U2, HXF1. The variables without a 1 or 2 are the variables at the future time. With a 1 attached they are the variables at the present time, and with a 2 at the past time.

APPENDIX C

COMPUTER PROGRAM

```
      PROGRAM MODEL(INPUT=128,OUTPUT=128,TAPE4=1024,TAPE5=INPUT,
     1TAPE6=OUTPUT)
      REAL L,L1,L2,L3,L4
      DIMENSION U(30,50),U1(30,50),U2(30,50)
      DIMENSION V(30,50),V1(30,50),V2(30,50)
      DIMENSION HL(30,50),HL1(30,50),HL2(30,50)
      DIMENSION HAVG(30,50),PX(50),QX(50),RX(50),TX(50)
      DIMENSION EEX(50),FFX(50)
      DIMENSION PY(50),QY(50),RY(50),TY(50)
      DIMENSION EEY(50),FFY(50)
      DIMENSION S(30,50),S1(30,50),H(30,50),S2(30,50)
      DIMENSION UAN(50)
      DIMENSION TITLE(8)
      COMMON          HJMKM,HL1JK,HJKM1,JM1,KM1,JP1,KP1,HJK,HJM1K,
     1BX,CX,DCX,E1,E2,E3,EX,HC1A,HC1B,HC1D,HC1,HC2,HC3,HC4A,HC4B,HC4C,
     1HC4D,HC4,HC5,HC6,HC7,HCX,G,FC,        H,HL1,HL2,U,    U2,V,    V2,S,
     1S1,DX,DY,DX1,DY1,R1,C1,HXB1,HXF1,HYB1,HYF1,C,HXF,HXB,HAVG,V1A,A,
     1F,L1,L2,L3,L4,WSX,AA1,AA2,AA3,AA4,AAX,BB1,BB2,BBX,CC1,CC2,CC3,CC4,
     1CCX,DD1,DD2,DD3,DDX,C2,HL,S2,TX,EEX,FFX,RX,L,J,K
      COMMON BY,CY,DCY,EY,HCY,AAY,BBY,CCY,DDY,HYF,HYB,WSY,U1A,
     1C1JP,R1JP,DXJM,DY1KM,CJM,C1KM,C1KP,R1KP,DYKM,DX1JM,CKM,C1JM
      EQUIVALENCE (PX,EEX,PY,EEY)
      EQUIVALENCE (QX,FFX,QY,FFY)
      EQUIVALENCE (RX,RY),(TX,TY)
      EQUIVALENCE (U,U1),(V,V1)
      G=980.
      HAVG(1,1)=30.
      PX(1)=1.
      QX(1)=1.
      RX(1)=0
      TX(1)=1.
      HL(1,1)=.3
      S(2,1)=30.00
      UAN(1)=0
      FC=0
C INPUT OF INITIAL CONDITIONS
      READ(5,4)TITLE
    4 FORMAT(8A10)
      READ(5,5)JMAX,KMAX
    5 FORMAT(I4,I4)
      WRITE(6,50)JMAX,KMAX
   50 FORMAT(≠1INPUT DATA≠/≠ JMAX =≠I4/≠ KMAX =≠I4)
      READ(5,6)DT,L
    6 FORMAT(2F7.0)
      WRITE(6,60)DT,L
   60 FORMAT(≠ DT    =≠F7.0/≠ L     =≠F7.0)
      READ(5,7)ITMAX
    7 FORMAT(I4)
      WRITE(6,70)ITMAX
   70 FORMAT(≠ ITMAX=≠I4)
      READ(5,8)WSX,WSY
    8 FORMAT(2F8.2)
   80 FORMAT(≠ WSX  =≠F8.2/≠ WSY  =≠F8.2)
      WRITE(6,80)WSX,WSY
C TAPE WRITING STATEMENTS
      WRITE(4)TITLE
      WRITE(4)JMAX,KMAX,DT,L,ITMAX,WSX,WSY
```

```
      DO 3400 K=1,KMAX                                                  MODEL      59
      DO 3300 J=1,JMAX                                                  MODEL      60
      V1(J,K)=0                                                         MODEL      61
      V2(J,K)=0                                                         MODEL      62
      U1(J,K)=0                                                         MODEL      63
      U2(J,K)=U1(J,K)                                                   MODEL      64
      HL1(J,K)=0                                                        MODEL      65
      HL2(J,K)=HL1(J,K)                                                 MODEL      66
      H(J,K)=1000.0                                                     MODEL      67
      S1(J,K)=30.00                                                     MODEL      68
      S2(J,K)=30.00                                                     MODEL      69
 3300 CONTINUE                                                          MODEL      70
 3400 CONTINUE                                                          MODEL      71
      JMAXM=JMAX-1                                                      MODEL      72
      KMAXM=KMAX-1                                                      MODEL      73
      L3=1./(2.*(L**2))                                                 MODEL      74
      L4 = 1./(8.*L)                                                    MODEL      75
      L2 = L4 + L4                                                      MODEL      76
      L1 = L2 + L2                                                      MODEL      77
      A=1./DT                                                           ES75001     1
      F      = G/(2.*L)                                                 MODEL      79
      DO 200 K=2,KMAX                                                   MODEL      80
      DO 100 J=2,JMAX                                                   MODEL      81
      HAVG(J,K) = (H(J,K) + H(J,K-1) + H(J-1,K-1) + H(J-1,K))/4.        MODEL      82
  100 CONTINUE                                                          MODEL      83
  200 CONTINUE                                                          MODEL      84
      DO 300 IT=1,ITMAX                                                 MODEL      85
C INPUT OF BOUNORY CONDITIONS                                           MODEL      86
      LT=IT                                                             MODEL      87
      DO 3000 K=1,KMAX                                                  MODEL      88
      HL(JMAX,K)=0                                                      MODEL      89
      U(1,K)=0                                                          MODEL      90
      S(1,K)=30.00                                                      MODEL      91
      S(JMAX,K)=30.00                                                   MODEL      92
 3000 CONTINUE                                                          MODEL      93
C JET START UP                                                          MODEL      94
      DO 3001 K=23,25                                                   ES75001     2
      U(1,K)=25*(1-((((L*2.5)-((L/2)+(K-23)*L))**2)/((L*2.5)**2)))*     ES75001     3
     1SIN(.0001405*DT*((2*LT)-1))                                       ES75001     4
      U(1,50-K)=U(1,K)                                                  ES75001     5
 3001 CONTINUE                                                          MODEL     100
C CALCULATION OF CONSTANTS FOR U,HL                                     MODEL     108
      DO 600 K=2,KMAXM                                                  MODEL     109
      DO 700 J=2,JMAXM                                                  MODEL     110
      CALL INDEX                                                        MODEL     111
      CALL CONUH                                                        MODEL     112
      RX(1)=0                                                           MODEL     113
      TX(1)=U(1,K)                                                      MODEL     114
      PX(J)=BX/(A-CX*RX(JM1))                                           MODEL     115
      QX(J)=(DCX-CX*TX(JM1))/(A-CX*RX(JM1))                             MODEL     116
      RX(J)=F/(EX+PX(J)*F)                                              MODEL     117
      TX(J)=(F*QX(J)+HCX)/(EX+PX(J)*F)                                  MODEL     118
  700 CONTINUE                                                          MODEL     119
C CALCULATION OF U,HL                                                   MODEL     120
  140 J=JMAXM                                                           MODEL     121
  110 U(J,K)=TX(J)-RX(J)*HL(J+1,K)                                      MODEL     122
      HL(J,K)=QX(J)-PX(J)*U(J,K)                                        MODEL     123
```

```
            J=J-1                                                       MODEL    124
            IF(J-2) 120,110,110                                         MODEL    125
        120 CONTINUE                                                    MODEL    126
        600 CONTINUE                                                    MODEL    127
      C EXTRAPOLATION OF U,HL                                           MODEL    128
            DO 801 K=2,KMAX                                             MODEL    129
            U(JMAX,K)=U(JMAXM,K)                                        ES75001    6
        801 CONTINUE                                                    MODEL    131
            DO 800 K=23,27                                              ES75001    7
            HL(1,K)=(HL(2,K)-HL(3,K))+HL(2,K)                           MODEL    133
        800 CONTINUE                                                    MODEL    134
            DO 900 J=1,JMAXM                                            MODEL    135
            JP1=J+1                                                     MODEL    136
            HL(J,1)=0                                                   ES75001    8
            U(JP1,1)=0                                                  ES75001    9
            HL(JP1,KMAX)=0                                              MODEL    139
            U(JP1,KMAX)=0                                               ES75001   10
        900 CONTINUE                                                    MODEL    141
      C PRINT STATEMENTS                                                MODEL    142
      C     VELOCITY IN THE X DIRECTION                                 MODEL    143
            TMX=((2*IT-1)*DT)/60.                                       MODEL    144
            IF(MOD(IT,3).NE.0) GO TO 4100                               ES75001   11
            WRITE(6,91)TMX                                              MODEL    145
         91 FORMAT(≠1 TIME(MIN.) FOR HALF TIME STEP X-DIRECTION= ≠F6.1) MODEL    146
            WRITE(6,51)IT,DT                                            MODEL    147
         51 FORMAT(≠ COMPUTED FROM IT,DT=≠I5,F10.5)                     MODEL    148
            WRITE(6,95)                                                 MODEL    149
         95 FORMAT(/, ≠ VELOCITY IN X DIRECTION≠)                       MODEL    150
            DO 902 IK=1,KMAX                                            MODEL    151
            WRITE(6,92) (U(IJ,IK),IJ=1,JMAX )                           MODEL    152
        902 CONTINUE                                                    MODEL    153
         92 FORMAT( ≠ ≠,30F4.0)                                         MODEL    154
            LT=IT                                                       MODEL    155
      C     TIDAL HEIGHT FOR THE X DIRECTION.                           MODEL    156
            WRITE(6,96)                                                 MODEL    157
         96 FORMAT(/, ≠ TIDAL HEIGHT IN X DIRECTION≠)                   MODEL    158
            DO 903 IK=1,KMAX                                            MODEL    159
            WRITE(6,92) (HL(IJ,IK),IJ=1,JMAX )                          MODEL    160
        903 CONTINUE                                                    MODEL    161
       4100 CONTINUE                                                    MODEL    162
      C TAPE WRITING STATEMENTS                                         MODEL    163
            IDIR=1HX                                                    MODEL    164
            WRITE(4)IDIR,TMX                                            MODEL    165
            WRITE(4) ((U(J,K),J=1,JMAX),K=1,KMAX)                       MODEL    166
            WRITE(4) ((HL(J,K),J=1,JMAX),K=1,KMAX)                      MODEL    167
            GO TO 4200                                                  ES75001   12
      C CALCULATION OF CONSTANTS FOR S,X-DIRECTION                      MODEL    168
            DO 1000 K=2,KMAXM                                           MODEL    169
            DO 1100 J=2,JMAXM                                           MODEL    170
            CALL INDEX                                                  MODEL    171
            CALL CONSX                                                  MODEL    172
            EEX(1)=0                                                    MODEL    173
            FFX(1)=S(1,K)                                               MODEL    174
            EEX(J)=CCX/(BBX-AAX*EEX(JM1))                               MODEL    175
            FFX(J)=(DDX-AAX*FFX(JM1))/(BBX-AAX*EEX(JM1))                MODEL    176
       1100 CONTINUE                                                    MODEL    177
      C CALCULATION OF S,X-DIRECTION                                    MODEL    178
```

```
  180 J=JMAXM                                                           MODEL    179
  150 S(J,K)=FFX(J)-EEX(J)*S(J+1,K)                                     MODEL    180
      J=J-1                                                             MODEL    181
      IF(J-2) 160,150,150                                               MODEL    182
  160 CONTINUE                                                          MODEL    183
 1000 CONTINUE                                                          MODEL    184
C EXTRAPOLATION OF S                                                     MODEL    185
      DO 400 J=1,JMAX                                                   MODEL    186
      S(J,1)=30.00                                                      MODEL    187
      S(J,KMAX)=30.00                                                   MODEL    188
  400 CONTINUE                                                          MODEL    189
C PRINT STATEMENTS                                                      MODEL    190
C     SALINITY FOR THE X DIRECTION                                      MODEL    191
      IF(MOD(IT,3).NE.0) GO TO 4200                                     ES75001   13
      WRITE(6,98)                                                       MODEL    192
   98  FORMAT(≠1 SALINITY FOR X-DIRECTION≠)                             MODEL    193
      DO 904 IK=1,KMAX                                                  MODEL    194
      WRITE(6,92)  (S(IJ,IK),IJ=1,JMAX )                                MODEL    195
  904 CONTINUE                                                          MODEL    196
 4200 CONTINUE                                                          MODEL    197
C TAPE WRITING STATEMENTS                                               MODEL    198
      GO TO 4250                                                        ES75001   14
      WRITE(4)  ((S(J,K),J=1,JMAX),K=1,KMAX)                            MODEL    199
 4250 CONTINUE                                                          ES75001   15
      DO 1200 J=1,JMAX                                                  MODEL    200
      DO 1300 K=1,KMAX                                                  MODEL    201
      S(J,K)=30.0                                                       ES75001   16
      S2(J,K)=S1(J,K)                                                   MODEL    202
      S1(J,K)=S(J,K)                                                    MODEL    203
      HL2(J,K)=HL1(J,K)                                                 MODEL    204
      HL1(J,K)=HL(J,K)                                                  MODEL    205
      V2(J,K)=V1(J,K)                                                   MODEL    206
 1300 CONTINUE                                                          MODEL    207
 1200 CONTINUE                                                          MODEL    208
C INPUT OF BOUNDRY CONDITIONS                                           MODEL    209
      LT=IT                                                             MODEL    210
      DO 4000 J=1,JMAX                                                  MODEL    211
      S(J,1)=30.00                                                      MODEL    212
      S(J,KMAX)=30.00                                                   MODEL    213
      HL(J+1,1)=0                                                       ES75001   17
      HL(J+1,KMAX)=0                                                    ES75001   18
      HL(J,KMAX)=0                                                      MODEL    215
 4000 CONTINUE                                                          MODEL    216
 4050 CONTINUE                                                          MODEL    217
C CALCULATION OF CONSTANTS FOR V,HL                                     MODEL    218
      DO 1400 J=2,JMAXM                                                 MODEL    219
      K=1                                                               ES75001   19
      CALL INDEX                                                        ES75001   20
      CALL CONVH                                                        ES75001   21
      E1=A/2+(L1*2*(V2(J,K)-V2(J,KP1)))                                 ES75001   22
      E2=(((V2(J,K))**2)+(.0625)*((U1A)**2))**0.5                       ES75001   23
      E3=(HYB1*((C1KP+C1)/2)**2)                                        ES75001   24
      EY=((E2/E3)*G)+E1                                                 ES75001   25
      PY(1)=0                                                           ES75001   26
      RY(1)=-(F/(EY-PY(1)*F))                                           ES75001   27
      TY(1)=(HCY-F*HL(J,1))/(EY-PY(1)*F)                                ES75001   28
      DO 1500 K=2,KMAXM                                                 MODEL    220
```

```
      CALL INDEX                                                        MODEL   221
      CALL CONVH                                                        MODEL   222
      PY(K)=CY/(A-BY*RY(KH1))                                           MODEL   225
      QY(K)=(DCY-BY*TY(KH1))/(A-BY*RY(KH1))                             MODEL   226
      RY(K)=-(F/(EY-PY(K)*F))                                           MODEL   227
      TY(K)=(HCY-F*QY(K))/(EY-PY(K)*F)                                  MODEL   228
 1500 CONTINUE                                                          MODEL   229
C CALCULATION OF V,HL                                                   MODEL   230
  240 K=KHAXH                                                           MODEL   231
  210 CONTINUE                                                          MODEL   232
      KP1=K+1                                                           MODEL   233
      V(J,K)=TY(K)-RY(K)*HL(J,KP1)                                      MODEL   234
      HL(J,K)=QY(K)-PY(K)*V(J,K)                                        MODEL   235
      K=K-1                                                             MODEL   236
      IF(K-2) 220,210,210                                               MODEL   237
      V(J,1)=TY(1)-RY(1)*HL(J,2)                                        ES75001  29
  220 CONTINUE                                                          MODEL   238
 1400 CONTINUE                                                          MODEL   239
C EXTRAPOLATION OF V,HL                                                 MODEL   240
      DO 2100 J=2,JHAXH                                                 MODEL   241
      HL(J,1)=0                                                         ES75001  30
      V(J,1)=V(J,2)                                                     ES75001  31
      V(J,KHAX)=V(J,KHAXH)                                              ES75001  32
 2100 CONTINUE                                                          MODEL   244
      DO 2200 K=1,KHAXH                                                 MODEL   245
      KP1=K+1                                                           MODEL   246
      HL(1,K)=0                                                         MODEL   247
      V(1,K)=0                                                          MODEL   248
      HL(JHAX,K)=0                                                      MODEL   249
      V(J,KHAX)=V(JHAX,1)                                               ES75001  33
 2200 CONTINUE                                                          MODEL   251
      DO 2300 K=23,27                                                   ES75001  34
      HL(1,K)=(HL(2,K)-HL(3,K))+HL(2,K)                                 MODEL   253
      V(1,K)=0                                                          MODEL   254
 2300 CONTINUE                                                          MODEL   255
C PRINT STATEMENTS                                                      MODEL   256
      THY=(IT*DT*2)/60.                                                 MODEL   257
      IF(MOD(IT,3).NE.0) GO TO 4300                                     ES75001  35
      WRITE(6,93) THY                                                   MODEL   258
   93 FORMAT(≠1 TIME(MIN.) FOR HALF TIME STEP Y-DIRECTION= ≠,F6.1)      MODEL   259
      WRITE(6,51)IT,DT                                                  MODEL   260
C     VELOCITY V IN THE Y DIRECTION                                     MODEL   261
  101 FORMAT(/, ≠ VELOCITY  Y  DIRECTION≠)                              MODEL   262
      WRITE(6,101)                                                      MODEL   263
      DO 905 IK=1,KMAX                                                  MODEL   264
      WRITE(6,92) (V(IJ,IK),IJ=1,JMAX )                                 MODEL   265
  905 CONTINUE                                                          MODEL   266
C     TIDAL HEIGHT FOR THE Y DIRECTION                                  MODEL   267
  103 FORMAT(/,≠ TIDAL HEIGH IN Y DIRECTION≠)                           MODEL   268
      WRITE(6,103)                                                      MODEL   269
      DO 906 IK=1,KMAX                                                  MODEL   270
      WRITE(6,92) (HL(IJ,IK),IJ=1,JMAX )                                MODEL   271
  906 CONTINUE                                                          MODEL   272
 4300 CONTINUE                                                          MODEL   273
C TAPE WRITING STATEMENTS                                               MODEL   274
      IDIR=1HY                                                          MODEL   275
      WRITE(4)IDIR,THY                                                  MODEL   276
```

```
      WRITE(4) ((V(J,K),J=1,JMAX),K=1,KMAX)                             MODEL    277
      WRITE(4) ((HL(J,K),J=1,JMAX),K=1,KMAX)                            MODEL    278
      GO TO 4400                                                        ES75001   36
C CALCULATION OF CONSTANTS FOR S,Y-DIRECTION                            MODEL    279
      DO 1900 J=2,JHAXM                                                 MODEL    280
      DO 2000 K=2,KMAXM                                                 MODEL    281
      CALL INDEX                                                        MODEL    282
      CALL CONSY                                                        MODEL    283
      EEY(1)=0                                                          MODEL    284
      FFY(1)=S(J,1)                                                     MODEL    285
      EEY(K)=CCY/(BBY-AAY*EEY(KM1))                                     MODEL    286
      FFY(K)=(DDY-AAY*FFY(KM1))/(BBY-AAY*EEY(KM1))                      MODEL    287
 2000 CONTINUE                                                          MODEL    288
C CALCULATION OF S,Y-DIRECTION                                          MODEL    289
  280 K=KMAXM                                                           MODEL    290
  250 CONTINUE                                                          MODEL    291
      S(J,K)=FFY(K)-EEY(K)*S(J,K+1)                                     MODEL    292
      K=K-1                                                             MODEL    293
      IF(K-2) 260,250,250                                               MODEL    294
  260 CONTINUE                                                          MODEL    295
 1900 CONTINUE                                                          MODEL    296
C EXTRAPOLATION OF S                                                    MODEL    297
      DO 500 K=1,KMAX                                                   MODEL    298
      S(1,K)=30.00                                                      MODEL    299
      S(JMAX,K)=30.00                                                   MODEL    300
  500 CONTINUE                                                          MODEL    301
C PRINT STATEMENTS                                                      MODEL    302
C     SALINITY FOR THE Y DIRECTION                                      MODEL    303
      IF(MOD(IT,3).NE.0) GO TO 4400                                     ES75001   37
      WRITE(6,105)                                                      MODEL    304
  105 FORMAT(≠1 SALINITY FOR Y-DIRECTION≠)                              MODEL    305
      DO 907 IK=1,KMAX                                                  MODEL    306
      WRITE(6,92) (S(IJ,IK),IJ=1,JMAX )                                 MODEL    307
  907 CONTINUE                                                          MODEL    308
 4400 CONTINUE                                                          MODEL    309
C TAPE WRITING STATEMENTS                                               MODEL    310
      GO TO 4450                                                        ES75001   38
      WRITE(4) ((S(J,K),J=1,JMAX),K=1,KMAX)                             MODEL    311
 4450 CONTINUE                                                          ES75001   39
      DO 2500 K=1,KMAX                                                  MODEL    312
      DO 2600 J=1,JMAX                                                  MODEL    313
      S(J,K)=30.0                                                       ES75001   40
      HL2(J,K)=HL1(J,K)                                                 MODEL    314
      HL1(J,K)=HL(J,K)                                                  MODEL    315
      S2(J,K)=S1(J,K)                                                   MODEL    316
      S1(J,K)=S(J,K)                                                    MODEL    317
      U2(J,K)=U1(J,K)                                                   MODEL    318
 2600 CONTINUE                                                          MODEL    319
 2500 CONTINUE                                                          MODEL    320
      WRITE(6,90) IT                                                    MODEL    321
   90 FORMAT( ≠ CYCLES COMPLETED= ≠,I4)                                 MODEL    322
  300 CONTINUE                                                          MODEL    323
      WRITE(6,7852)                                                     MODEL    324
 7852 FORMAT(≠ THIS IS THE END≠)                                        MODEL    325
C TAPE WRITING STATEMENTS                                               MODEL    326
      I1=10HTHIS IS TH                                                  MODEL    327
      I2=10HE END                                                       MODEL    328
```

```
            WRITE(4)I1,I2                                     MODEL
            ENDFILE4                                          MODEL
  345       REWIND4                                           MODEL
            STOP                                              MODEL
            END                                               MODEL
```

```
      SUHROUTINE CONUH                                                  CONUH      2
      RFAL L,L1,L2,L3,L4                                                CONUH      3
      DIMENSION U(30,50),U1(30,50),U2(30,50)                            CONUH      4
      DIMENSION V(30,50),V1(30,50),V2(30,50)                            CONUH      5
      DIMENSION HL(30,50),HL1(30,50),HL2(30,50)                         CONUH      6
      DIMENSION HAVG(30,50),PX(50),QX(50),RX(50),TX(50)                 CONUH      7
      DIMENSION EEX(50),FFX(50)                                         CONUH      8
      DIMENSION PY(50),QY(50),RY(50),TY(50)                             CONUH      9
      DIMENSION EEY(50),FFY(50)                                         CONUH     10
      DIMENSION S(30,50),S1(30,50),H(30,50),S2(30,50)                   CONUH     11
      COMMON          HJMKM,HL1JK,HJKM1,JM1,KM1,JP1,KP1,HJK,HJM1K,      CONUH     12
     1BX,CX,DCX,E1,E2,E3,EX,HC1A,HC1B,HC1D,HC1,HC2,HC3,HC4A,HC4B,HC4C,  CONUH     13
     1HC4D,HC4,HC5,HC6,HC7,HCX,G,FC,        H,HL1,HL2,U,   U2,V,   V2,S, CONUH     14
     1S1,DX,DY,DX1,DY1,R1,C1,HXB1,HXF1,HYB1,HYF1,C,HXF,HXB,HAVG,V1A,A,  CONUH     15
     1F,L1,L2,L3,L4,WSX,AA1,AA2,AA3,AA4,AAX,BB1,BB2,BBX,CC1,CC2,CC3,CC4, CONUH     16
     1CCX,DD1,DD2,DD3,DDX,C2,HL,S2,TX,EEX,FFX,RX,L,J,K                  CONUH     17
      COMMON BY,CY,DCY,EY,HCY,AAY,BBY,CCY,DDY,HYF,HYB,WSY,U1A,          CONUH     18
     1C1JP,R1JP,DXJM,DY1KH,CJM,C1KM,C1KP,R1KP,DYKM,DX1JM,CKM,C1JM       CONUH     19
      EOUIVALENCE (PX,EEX,PY,EEY)                                       CONUH     20
      EOUIVALENCE (QX,FFX,QY,FFY)                                       CONUH     21
      EQUIVALENCE (RX,RY),(TX,TY)                                       CONUH     22
      EOUIVALENCE (U,U1),(V,V1)                                         CONUH     23
      C1=400.0                                                          ES75001   41
      R1=1.00+(.007945*S1(J,K))                                         CONUH     25
      C1JP=C1                                                           ES75001   42
      R1JP=1.00+(.007945*S1(JP1,K))                                     CONUH     27
      V1A=(V1(JP1,K)+V1(JP1,KM1)+V1(J,KM1)+V1(J,K))                     CONUH     28
      BX=L1*HXF1                                                        CONUH     29
      CX=-(L1*HXB1)                                                     CONUH     30
      DCX=-(((-HL1(J,K))*A)+(L1*(HYF1*V1(J,KM1)-HYB1*V1(J,K))))         ES75001   43
      E1=(A/2)+(L1*(U2(JP1,K)-U2(JM1,K)))                               ES75001   44
      E2=(((U2(J,K))**2)+(.0625)*(V1A**2))**0.5                         CONUH     33
      E3=(HXF1*((C1JP+C1)/2)**2)                                        CONUH     34
      EX=((E2/E3)*G)+E1                                                 CONUH     35
      HC1A=U2(J,KM1)-U2(J,KP1)                                          CONUH     36
      HC1B=HC1A*V1A                                                     CONUH     37
      HC1C=HC1B*L4                                                      CONUH     38
      HC1D=U2(J,K)*(A/2)                                                ES75001   45
      HC1=-HC1D+HC1C                                                    CONUH     40
      HC2=((HL2(JP1,K)-HL2(J,K))*F)+ ((R1JP-                            CONUH     41
     1R1)*HXF1*(1/(R1JP+R1))*F)                                         CONUH     42
      HC3=(FC/4.)*V1A                                                   CONUH     43
      HC4A=2*G*U2(J,K)                                                  CONUH     44
      HC4B=U2(J,K)**2                                                   CONUH     45
      HC4C=HC4B+(0.0625 )*(V1A)**2                                      CONUH     46
      HC4D=HC4C**0.5                                                    CONUH     47
      HC4=HC4A*HC4D                                                     CONUH     48
      HC5=(HXF1*((C1JP+C1)/2)**2)*2                                     CONUH     49
      HC6     = HC4      / HC5                                          CONUH     50
      HC7=4*WSX/((R1JP+R1)*HXF1)                                        CONUH     51
      HCX=-(HC1+HC2-HC3+HC6-HC7)                                        CONUH     52
      RETURN                                                            CONUH     53
      END                                                               CONUH     54
```

```
      SUBROUTINE CONSX                                                  CONSX   2
      REAL L,L1,L2,L3,L4                                                CONSX   3
      DIMENSION U(30,50),U1(30,50),U2(30,50)                            CONSX   4
      DIMENSION V(30,50),V1(30,50),V2(30,50)                            CONSX   5
      DIMENSION HL(30,50),HL1(30,50),HL2(30,50)                         CONSX   6
      DIMENSION HAVG(30,50),PX(50),QX(50),RX(50),TX(50)                 CONSX   7
      DIMENSION EEX(50),FFX(50)                                         CONSX   8
      DIMENSION PY(50),QY(50),RY(50),TY(50)                             CONSX   9
      DIMENSION EEY(50),FFY(50)                                         CONSX  10
      DIMENSION S(30,50),S1(30,50),H(30,50),S2(30,50)                   CONSX  11
      COMMON          HJMKM,HL1JK,HJKM1,JM1,KM1,JP1,KP1,HJK,HJM1K,      CONSX  12
     1BX,CX,DCX,E1,E2,E3,EX,HC1A,HC1B,HC1D,HC1,HC2,HC3,HC4A,HC4B,HC4C,  CONSX  13
     1HC4D,HC4,HC5,HC6,HC7,HCX,G,FC,        H,HL1,HL2,U,   U2,V,   V2,S,CONSX  14
     1S1,DX,DY,DX1,DY1,R1,C1,HXB1,HXF1,HYB1,HYF1,C,HXF,HXB,HAVG,V1A,A,  CONSX  15
     1F,L1,L2,L3,L4,WSX,AA1,AA2,AA3,AA4,AAX,BB1,BB2,BBX,CC1,CC2,CC3,CC4,CONSX  16
     1CCX,DD1,DD2,DD3,DDX,C2,HL,S2,TX,EEX,FFX,RX,L,J,K                  CONSX  17
      COMMON BY,CY,DCY,EY,HCY,AAY,BBY,CCY,DDY,HYF,HYB,WSY,U1A,          CONSX  18
     1C1JP,R1JP,DXJM,DY1KM,CJM,C1KM,C1KP,R1KP,DYKM,DX1JM,CKM,C1JM       CONSX  19
      EQUIVALENCE (PX,EEX,PY,EEY)                                       CONSX  20
      EQUIVALENCE (QX,FFX,QY,FFY)                                       CONSX  21
      EQUIVALENCE (RX,RY),(TX,TY)                                       CONSX  22
      EQUIVALENCE (U,U1),(V,V1)                                         CONSX  23
      HXF=HJK + HJKM1 + HL(JP1,K) + HL(J,K)                             CONSX  24
      HXB=HJM1K + HJMKM + HL(J,K) + HL(JM1,K)                           CONSX  25
      C=491.9                                                           CONSX  26
      DX=(5.93*HJK*U(J,K)*31.3049)/C                                    CONSX  27
      CJM=491.9                                                         CONSX  28
      DXJM=(5.93*H(JM1,K)*U(JM1,K)*31.3049)/CJM                         CONSX  29
      C1=491.9                                                          CONSX  30
      DY1=((5.93*HJK*V1(J,K)*31.3049)/C1 )                              CONSX  31
      C1KM=491.9                                                        CONSX  32
      DY1KM=((5.93*H(J,KM1)*V1(J,KM1)*31.3049)/C1KM)                    CONSX  33
      AA1=HXB1*U(JM1,K)                                                 CONSX  34
      AA2=AA1*L2                                                        CONSX  35
      AA3=HXB*DXJM                                                      CONSX  36
      AA4=AA3*L3                                                        CONSX  37
      AAX=-(AA2+AA4)                                                    CONSX  38
      BB1=(A*(HAVG(J,K)+HL(J,K)))+(((HXF1*U(J,K))-                      CONSX  39
     1(HXB1*U(JM1,K)))*L2)                                              CONSX  40
      BB2=(HXF*DX+HXB*DXJM)*L3                                          CONSX  41
      BBX=BB1+BB2                                                       CONSX  42
      CC1=HXF1*U(J,K)                                                   CONSX  43
      CC2=CC1*L2                                                        CONSX  44
      CC3=HXF*DX                                                        CONSX  45
      CC4=CC3*L3                                                        CONSX  46
      CCX=CC2-CC4                                                       CONSX  47
      DD1A=HAVG(J,K)+HL1(J,K)                                           ES75001 46
      DD1B=DD1A*S1(J,K)                                                 ES75001 47
      DD1=-DD1B*A                                                       CONSX  50
      DD2=((HYF1* V1(J,KM1))*(S1(J,KM1)+S1(J,K)))                       CONSX  51
     1-(HYB1*V1(J,K)*(S1(J,K)+S1(J,KP1))))*L2                           CONSX  52
      DD3=(((HYF1*DY1KM*(S1(J,KM1)-S1(J,K)))                            CONSX  53
     1-(HYB1*DY1*(S1(J,K)-S1(J,KP1))))*L3)                              CONSX  54
      DDX=-(DD1+DD2-DD3)                                                CONSX  55
      RETURN                                                            CONSX  56
      END                                                               CONSX  57
```

```
      SUBROUTINE CONVH                                                  CONVH       2
      REAL L,L1,L2,L3,L4                                                CONVH       3
      DIMENSION U(30,50),U1(30,50),U2(30,50)                            CONVH       4
      DIMENSION V(30,50),V1(30,50),V2(30,50)                            CONVH       5
      DIMENSION HL(30,50),HL1(30,50),HL2(30,50)                         CONVH       6
      DIMENSION HAVG(30,50),PX(50),QX(50),RX(50),TX(50)                 CONVH       7
      DIMENSION EEX(50),FFX(50)                                         CONVH       8
      DIMENSION PY(50),QY(50),RY(50),TY(50)                             CONVH       9
      DIMENSION EEY(50),FFY(50)                                         CONVH      10
      DIMENSION S(30,50),S1(30,50),H(30,50),S2(30,50)                   CONVH      11
      COMMON         HJMK4,HL1JK,HJKM1,JM1,KM1,JP1,KP1,HJK,HJM1K,       CONVH      12
     1BX,CX,DCX,E1,E2,E3,EX,HC1A,HC1B,HC1D,HC1,HC2,HC3,HC4A,HC4B,HC4C,  CONVH      13
     1HC4D,HC4,HC5,HC6,HC7,HCX,G,FC,       H,HL1,HL2,U,   U2,V,   V2,S, CONVH      14
     1S1,DX,DY,DX1,DY1,R1,C1,HXB1,HXF1,HYB1,HYF1,C,HXF,HXB,HAVG,V1A,A,  CONVH      15
     1F,L1,L2,L3,L4,WSX,AA1,AA2,AA3,AA4,AAX,BB1,BB2,BBX,CC1,CC2,CC3,CC4, CONVH      16
     1CCX,DD1,DD2,DD3,DDX,S2,HL,S2,TX,EEX,FFX,RX,L,J,K                  CONVH      17
      COMMON BY,CY,DCY,EY,HCY,AAY,BBY,CCY,DDY,HYF,HYB,WSY,U1A,          CONVH      18
     1C1JP,R1JP,DXJM,DY1KM,CJM,C1KM,C1KP,R1KP,DYKM,DX1JM,CKM,C1JM       CONVH      19
      EQUIVALENCE (PX,EEX,PY,EEY)                                       CONVH      20
      EQUIVALENCE (QX,FFX,QY,FFY)                                       CONVH      21
      EQUIVALENCE (RX,RY),(TX,TY)                                       CONVH      22
      EQUIVALENCE (U,U1),(V,V1)                                         CONVH      23
      C1=400.0                                                          ES75001    48
      C1KP=C1                                                           ES75001    49
      U1A=(U1(JM1,K)+U1(JM1,KP1)+U1(J,KP1)+U1(J,K))                     CONVH      26
      R1=1.00+(.007945*S1(J,K))                                         CONVH      27
      R1KP=1.00+(.007945*S1(J,KP1))                                     CONVH      28
      BY=L1*HYF1                                                        CONVH      29
      CY=-L1*HYB1                                                       CONVH      30
      DCY=-(((-HL1(J,K))*A)+(L1*(HXF1*U1(J,K)-HXB1*U1(JM1,K))))         ES75001    50
      E1=(A/2)+(L1*(V2(J,KM1)-V2(J,KP1)))                               ES75001    51
      E2=(((V2(J,K))**2)+(.0625)*((U1A)**2))**0.5                       CONVH      33
      E3=(HYB1*((C1KP+C1)/2)**2)                                        CONVH      34
      EY=((E2/E3)*G)+E1                                                 CONVH      35
      HC1A=V2(JP1,K)-V2(JM1,K)                                          CONVH      36
      HC1B=HC1A*U1A                                                     CONVH      37
      HC1C=HC1B*L4                                                      CONVH      38
      HC1D=V2(J,K)*(A/2)                                                ES75001    52
      HC1=-HC1D+HC1C                                                    CONVH      40
      HC2=((HL2(J,K)-HL2(J,KP1))*F)+ ((R1-                              CONVH      41
     1R1KP)*HYB1)*F*(1/(R1KP+R1))                                       CONVH      42
      HC3=(FC/4.)*U1A                                                   CONVH      43
      HC4A=2*G*V2(J,K)                                                  CONVH      44
      HC4B=V2(J,K)**2                                                   CONVH      45
      HC4C=HC4B+(0.0625 )*(U1A)**2                                      CONVH      46
      HC4D=HC4C**0.5                                                    CONVH      47
      HC4=HC4A*HC4D                                                     CONVH      48
      HC5=(HYB1*((C1KP+C1)/2)**2)*2                                     CONVH      49
      HC6      = HC4       / HC5                                        CONVH      50
      HC7=4*WSY/((R1KP+R1)*HYB1)                                        CONVH      51
      HCY=-(HC1+HC2+HC3+HC6-HC7)                                        CONVH      52
      RETURN                                                            CONVH      53
      END                                                               CONVH      54
```

```
      SUBROUTINE CONSY                                                  CONSY       2
      REAL L,L1,L2,L3,L4                                                CONSY       3
      DIMENSION U(30,50),U1(30,50),U2(30,50)                            CONSY       4
      DIMENSION V(30,50),V1(30,50),V2(30,50)                            CONSY       5
      DIMENSION HL(30,50),HL1(30,50),HL2(30,50)                         CONSY       6
      DIMENSION HAVG(30,50),PX(50),QX(50),RX(50),TX(50)                 CONSY       7
      DIMENSION EEX(50),FFX(50)                                         CONSY       8
      DIMENSION PY(50),QY(50),RY(50),TY(50)                             CONSY       9
      DIMENSION EEY(50),FFY(50)                                         CONSY      10
      DIMENSION S(30,50),S1(30,50),H(30,50),S2(30,50)                   CONSY      11
      COMMON          HJMKM,HL1JK,HJKM1,JM1,KM1,JP1,KP1,HJK,HJM1K,      CONSY      12
     1BX,CX,DCX,E1,E2,E3,EX,HC1A,HC1B,HC1D,HC1,HC2,HC3,HC4A,HC4B,HC4C,  CONSY      13
     1HC4D,HC4,HC5,HC6,HC7,HCX,G,FC,         H,HL1,HL2,U,    U2,V,    V2,S,  CONSY      14
     1S1,DX,DY,DX1,DY1,R1,C1,HXB1,HXF1,HYB1,HYF1,C,HXF,HXB,HAVG,V1A,A,  CONSY      15
     1F,L1,L2,L3,L4,WSX,AA1,AA2,AA3,AA4,AAX,BB1,BB2,BBX,CC1,CC2,CC3,CC4,  CONSY      16
     1CCX,DD1,DD2,DD3,DDX,C2,HL,S2,TX,EEX,FFX,RX,L,J,K                  CONSY      17
      COMMON BY,CY,DCY,EY,HCY,AAY,BBY,CCY,DDY,HYF,HYB,WSY,U1A,          CONSY      18
     1C1JP,R1JP,DXJM,DY1KM,CJM,C1KM,C1KP,R1KP,DYKM,DX1JM,CKM,C1JM       CONSY      19
      EQUIVALENCE (PX,EEX,PY,EEY)                                       CONSY      20
      EQUIVALENCE (QX,FFX,QY,FFY)                                       CONSY      21
      EQUIVALENCE (RX,RY),(TX,TY)                                       CONSY      22
      EQUIVALENCE (U,U1),(V,V1)                                         CONSY      23
      HYF=HJKM1+HJMKM+HLJK+HL(J,KM1)                                    CONSY      24
      HYB=HJK+HJM1K+HLJK+HL(J,KP1)                                      CONSY      25
      C=491.9                                                           CONSY      26
      DY=((5.93*HJK*V(J,K)*31.3049)/C)                                  CONSY      27
      CKM=491.9                                                         CONSY      28
      DYKM=((5.93*H(J,KM1)*V(J,KM1)*31.3049)/CKM)                       CONSY      29
      C1=491.9                                                          CONSY      30
      DX1=(5.93*H(J,K)*U1(J,K)*31.3049)/C1                              CONSY      31
      C1JM=491.9                                                        CONSY      32
      DX1JM=(5.93*H(JM1,K)*U1(JM1,K)*31.3049)/C1JM                      CONSY      33
      AA1=HYF1*V(J,KM1)                                                 CONSY      34
      AA2=AA1*L2                                                        CONSY      35
      AA3=HYF*DYKM                                                      CONSY      36
      AA4=AA3*L3                                                        CONSY      37
      AAY=-AA4+AA2                                                      CONSY      38
      BB1=(A*(HAVG(J,K)+HL(J,K)))+(((HYF1*V(J,KM1))-                    CONSY      39
     1(HYB1*V(J,K)))*L2)                                                CONSY      40
      BB2=(HYF*DYKM-HYB*DY)*L3                                          CONSY      41
      BBY=BB1+BB2                                                       CONSY      42
      CCY=(((-HYB1*V(J,K))*L2)-((HYB*DY)*L3))                           CONSY      43
      DD1A=HAVG(J,K)+HL1(J,K)                                           ES75001    53
      DD1B=DD1A*S1(J,K)                                                 ES75001    54
      DD1=-DD1B*A                                                       CONSY      46
      DD2=((HXF1*U1(J,K)*(S1(JP1,K)+S1(J,K)))                           CONSY      47
     1-(HXB1*U1(JM1,K)*(S1(J,K)+S1(JM1,K))))*L2                         CONSY      48
      DD3=(((HXF1*DX1*(S1(JP1,K)-S1(J,K)))                              CONSY      49
     1-(HXB1*DX1JM*(S1(J,K)-S1(JM1,K))))*L3)                            CONSY      50
      DDY=-(DD1+DD2-DD3)                                                CONSY      51
      RETURN                                                            CONSY      52
      END                                                               CONSY      53
```

APPENDIX D

BOTTOM STRESS, VERTICAL EDDY VISCOSITY, AND CHÉZY COEFFICIENT RELATIONSHIPS

To determine the relationship between values of the Chézy coefficient and the vertical eddy viscosity, we can use equation 2.33

$$-\frac{gU[U^2+V^2]^{1/2}}{C^2} = -\frac{\tau_x^b}{\rho} . \qquad \text{D.1}$$

Using notation from Dyer (1973), we can set

$$-\frac{\tau_x^b}{\rho} = A_z \frac{\partial u}{\partial z} . \qquad \text{D.2}$$

From D.1 and D.2 we now have

$$A_z \frac{\partial u}{\partial z} = \frac{g\,U[U^2+V^2]^{1/2}}{C^2} . \qquad \text{D.3}$$

Letting $[U^2 + V^2]^{1/2} = U$ for the purpose of calculation and re-arranging D.3, we have

$$A_z = \frac{gU^2}{C^2 \frac{\partial u}{\partial z}} \qquad \text{D.4}$$

If $C = 400\ cm^{1/2}\ sec^{-1}$, $U = 25\ cm\ sec^{-1}$ (an average velocity), and the velocity has a linear variation with depth, then

$$\frac{\partial u}{\partial z} = \frac{50}{1000} = .050$$

and

$$A_z = \frac{980(25)^2}{(400)^2(.050)} = 76.6 .$$

If a vertical distribution of velocity of the form

$$u = U_{max}\left(\frac{z}{H}\right)^{1/7} \qquad \text{D.5}$$

is used (Dronkers (1964)), then $u = U_{max}$ at the surface. From Dronkers (1964) a value of $U = 25\ cm\ sec^{-1}$ gives a

U_{max} = 28.6 cm sec^{-1}. Then $\partial u/\partial z$ = (28.6/1000) = 0.0286 and

$$A_z = \frac{(980)(25)^2}{(400)^2(.0286)} = 133.9 .$$

An alternate check of the bottom stress is given by the term $\gamma = g/C^2$ ($\tau_b = \rho\gamma^2 U^2$) which for g = 980 cm sec^{-1} and C = 400 cm$^{1/2}$ sec^{-1} gives $\gamma = 6.1 \times 10^{-3}$. Dronkers reports values for their coastal work of $\gamma = 2.9 \times 10^{-3}$.

BIBLIOGRAPHY

Abramovich, G. N. (1963) The Theory of Turbulent Jets. MIT Press, Cambridge, Mass., 671 pp.

Albertson, M. L., Y. B. Dai, R. A. Jensen, and H. Rouse (1950) Diffusion of submerged jets. Transactions of the ASCE, 115, 639-697.

Bates, C. C. (1953) Rational theory of delta formation. Bulletin of the American Association of Petroleum Geologists, 37, 2119-2162.

Bickley, W. G. (1937) The plane jet. Philosophical Magazine S., 23, 727-731.

Bigelow, H. B. (1933) Studies in the waters on the continental shelf, Cape Cod to Chesapeake Bay, I. The cycle of temperature. Papers in Physical Oceanography and Meteorology, 2, 1-135.

Bigelow, H. B. and M. Sears (1935) Studies of the waters on the continental shelf, Cape Cod to Chesapeake Bay, II. Salinity. Papers in Physical Oceanography and Meteorology, 4, 1-94.

Birkhoff, G. and E. H. Zarantonello (1957) Jets, Wakes and Cavities. Academic Press, Inc., New York, 353 pp.

Boicourt, W. C. (1973) The circulation of water on the continental shelf from Chesapeake Bay to Cape Hatteras. Johns Hopkins University, PhD dissertation, 183 pp.

Bondar, C. (1970) Considerations théoriques sur la dispersion d'un courant liquide de densité réduite et a niveau libre, dans un bassin contenant un liquide d'une plus grande densité. UNESCO Report, Symposium on the Hydrology of Deltas. 246-256.

Borichansky, L. S. and V. N. Mikhailov (1966) Interaction of river and sea water in the absence of tides. UNESCO Report, Scientific Problems of the Humid, Tropical Zone, Deltas and their Implications, 175-180.

Budinger, T. F., L. K, Coachman, and C. A. Barnes (1964) Columbia River effluent in the Northeast Pacific Ocean, 1961, 1962: Selected aspects of physical oceanography. University of Washington, Department of Oceanography Technical Report 99 (unpublished manuscript).

Bumpus, D. F. (1965) Residual drift along the bottom on the continental shelf in the Middle Atlantic Bight area. Limnology and Oceanography, Supplement to 3, 48-53.

Bumpus, D. F. (1969) Reversals in the surface drift in the Middle Atlantic Bight area. Deep Sea Research, Supplement to 16, 17-23.

Bumpus, D. F. and L. M. Lauzier (1965) Surface circulation on the continental shelf off Eastern North America between Newfoundland and Florida. Serial Atlas of the Marine Environment Folio 7, American Geographical Society, New York, 4 pp.

Bumpus, D. F. and E. L. Pierce (1955) The hydrography and the distribution of chaetognaths over the continental shelf off North Carolina. Deep Sea Research, Supplement to 3, 92-109.

Douglas, J. and J. F. Gunn (1964) A general formulation of alternating direction procedures in the presence of singular operators. Numerical Mathematics, 5, 175-184.

Dronkers, J. J. (1964) Tidal Computations. North-Holland Publishing Company, Amsterdam, 518 pp.

Duxbury, A. C., B. A. Mare, and N. McGary (1966) The Columbia River effluent and its distribution at sea, 1961-1963. University of Washington, Department of Oceanography Technical Report 156 (unpublished manuscript).

Dyer, K. R. (1973) Estuaries: A Physical Introduction. John Wiley and Sons, New York, 140 pp.

Engelund, F. and F. B. Pedersen (1973) Surface jet at small Richardson numbers. Proceedings of the ASCE, HY 3, 405-416.

Fisher, A. (1972) Entrainment of shelf water by the Gulf Stream northeast of Cape Hatteras. Journal of Geophysical Research, 77, 3248-3255.

Ford, W. L. and A. R. Miller (1952) The surface layer of the Gulf Stream and adjacent waters. Journal of Marine Research, 1, 267-280.

Gadgil, S. (1971) Structure of jets in rotating systems. Journal of Fluid Mechanics, 47, 417-436.

Garvine, R. W. (1974) Physical features of the Connecticut River outflow during high discharge. Journal of Geophysical Research, 79, 831-846.

Gibbs, R. J. (1970) Circulation in the Amazon River estuary and adjacent Atlantic Ocean. Journal of Marine Research, 28, 113-123.

Gordon, R. and M. Spaulding (1974) A bibliography of numerical models for tidal rivers, estuaries and coastal rivers. University of Rhode Island, Marine Technical Report 32, 55 pp.

Harrison, W., J. J. Norcross, N. A. Pore, and E. M. Stanley (1967) Circulation of shelf waters off the Chesapeake Bight. U. S. Department of Commerce, ESSA Professional Paper 3, 82 pp.

Howe, M. R. (1962) Some direct measurements of the non-tidal drift on the continental shelf between Cape Cod and Cape Hatteras. Deep Sea Research, 9, 445-455.

Ippen, A. I. (1966) Estuary and Coastal Hydrodynamics. McGraw Hill, New York, 744 pp.

Iselin, C. O'D. (1955) Coastal currents and the fisheries. Deep Sea Research, Supplement to 3, 474-478.

Leendertse, J. J. (1967) Aspects of a computational model for long-period water-wave propagation. The Rand Corporation Technical Report, RM-5294-PR, 164 pp.

Leendertse, J. J. (1970) A water-quality simulation model for well-mixed estuaries and coastal seas: Vol. 1 principles of computation. The Rand Corporation Technical Report, RM-6230-RC, 71 pp.

Leendertse, J. J. and E. C. Gritten (1971) Volume II computation procedures. The Rand Corporation Technical Report, R-708-NYC, 53 pp.

Miller, A. R. (1952) A pattern of surface coastal circulation inferred from surface salinity-temperature data and drift bottle recoveries, Woods Hole Oceanographic Institution Technical Report 52-28, 14 pp.

Neumann, G. and W. J. Pierson, Jr. (1966) Principles of Physical Oceanography. Prentice-Hall, Inc., Englewood Cliffs, N. J., 545 pp.

Park, K. (1966) Columbia River plume identification by specific alkalinity. Limnology and Oceanography, 11, 118-120.

Parr, A. E. (1933) A geographical-ecological analysis of the seasonal changes in temperature conditions in shallow water along the Atlantic Coast of the United States. Bulletin of the Bingham Oceanographic Collection, 4, 1-90.

Peaceman, D. W. and H. H. Rachford, Jr. (1965) The numerical solution of parabolic and elliptic differential equations. Journal Society of Industrial and Applied Mathematics, 3, 28-41.

Redfreld, A. C. (1958) The influence of the continental shelf on the tides of the Atlantic Coast of the United States. Journal of Marine Research, 17, 432-448.

Ryther, J. H., D. W. Menzel, and N. Corwin (1967) Influence of the Amazon River outflow on the ecology of the western tropical Atlantic. I. Hydrography and nutrient chemistry. Journal of Marine Research, 25, 69-83.

Schlichting, H. (1933) Laminare Strahlausbreitung. Z. Angew. Math. Mech., 13, 260-263.

Stefánsson, U. and F. A. Richards (1963) Processes contributing to the nutrient distributions off the Columbia River and Strait of Juan de Fuca. Limnology and Oceanography, 8, 394-410.

Stefánsson, U., L. P. Atkinson, and D. F. Bumpus (1971) Hydrographic properties and circulation of the North Carolina shelf and slope waters. Deep Sea Research, 18, 383-420.

Stommel, H. (1965) The Gulf Stream. University of California Press, Berkeley, 248 pp.

Stommel, H. and A. Leetmaa (1972) Circulation on the continental shelf. Proceedings of the National Academy of Science, U. S. A., 69, 3380-3384.

Sturges, W. (1974) Sea level slope along continental boundaries. Journal of Geophysical Research, 79, 825-830.

Sverdrup, H. V., M. W. Johnson, and R. H. Fleming (1942) The Oceans. Prentice-Hall, Inc., Englewood Cliffs, N. J., 1087 pp.

Takano, K. (1954a) On the velocity distribution off the mouth of a river. Journal of the Oceanographic Society of Japan, 10, 1-5.

Takano, K. (1954b) On the salinity and velocity distributions off the mouth of a river. Journal of the Oceanographic Society of Japan, 10, 92-98.

Takano, K. (1955) A complementary note on the diffusion of the seaward river flow off the mouth. Journal of the Oceanographic Society of Japan, 11, 1-3.

Wright, L. D. and J. M. Coleman (1971) Effluent expansion and interfacial mixing in the presence of a salt wedge, Mississippi River delta. Journal of Geophysical Research, 76, 8649-8661.

VITA

Everett Michael Stanley

Born in Orangeburg, South Carolina, March 7, 1938. Graduated from Fairfax Public School, Fairfax, South Carolina, June 1956; B.S., Physics, The Citadel, June 1960; M.S., Oceanography, Massachusetts Institute of Technology, June 1964. The author is now an Oceanographer employed at the David W. Taylor Naval Ship Research and Development Center, Annapolis, Maryland.

In January 1973, the author entered the School of Marine Science of the College of William and Mary, located at the Virginia Institute of Marine Science, Gloucester Point, Virginia.